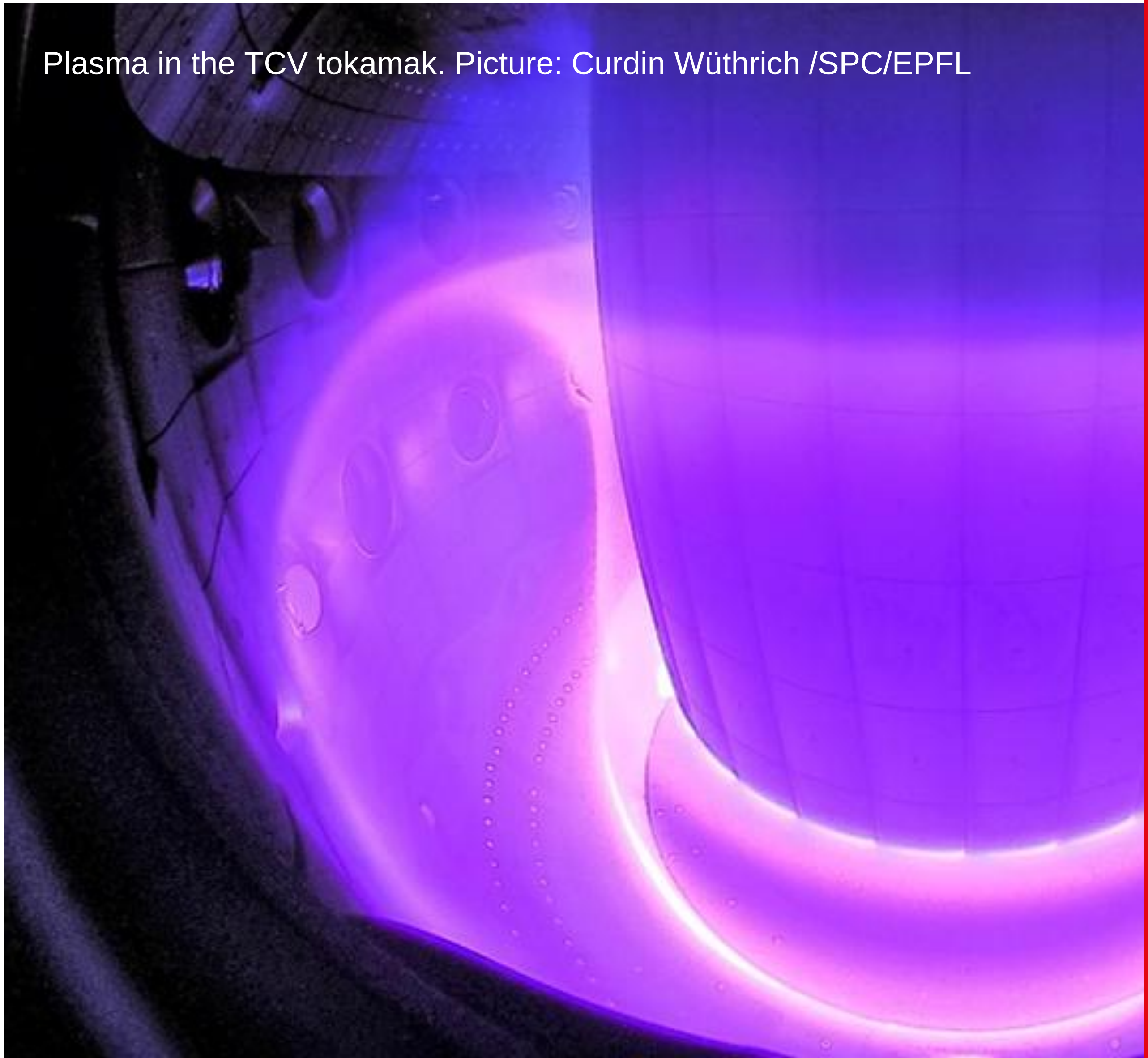
Plasma in the TCV tokamak. Picture: Curdin Wüthrich /SPC/EPFL

State observers: introduction and application to density profile reconstruction and control

F. Pastore, F. Felici, O. Sauter, A. Mele, S. Van Mulders

11th of February 2025
Ecole Polytechnique Fédérale de Lausanne,
Swiss Plasma Center

Outline

- Introduction to state observers
    - Concepts behind observers
    - Observability of a dynamical system
    - Kalman filter: the optimal observer
- Plasma electron density reconstruction and control on TCV
    - Motivation and applications
    - RAPDENS model presentation
    - Multi-rate Extended Kalman Filter
    - Summary and lessons learned

Motivation behind the design of an observer

Given a plant P represented by a generic Multi-Input Multi-Output (MIMO) discrete-time state space representation:

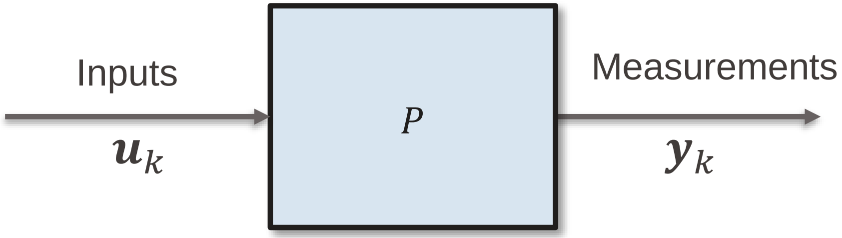

$$\begin{cases} \boldsymbol{x}_{k+1} = \boldsymbol{f}_k(\boldsymbol{x}_k, \boldsymbol{u}_k, t_k) & \text{State evolution equation} \\ \boldsymbol{y}_k = \boldsymbol{g}_k(\boldsymbol{x}_k, \boldsymbol{u}_k, t_k) & \text{Measurement equation} \end{cases}$$

One can be interested in the reconstruction of the internal state $\boldsymbol{x}_k$ of the plant for:

- Full-state feedback control
- Infer $\boldsymbol{x}_k$ not directly measured in $\boldsymbol{y}_k$
  - Example: infer a kinetic profile from integral values of the profiles along the lines of sight of the diagnostic
- Filter out/fuse different diagnostic data, synthetized in $\boldsymbol{x}_k$

Many techniques can be devised for such task:

- Open-loop model-based estimation
- Luenberger observer
- Kalman Filter (or Extended Kalman Filter), …

Motivation behind the design of an observer

☐ How can one compute $\hat{\boldsymbol{x}}_k$ (estimate of $\boldsymbol{x}_k$)?

Known data:

- Input $\boldsymbol{u}_k$
- Measurements $\boldsymbol{y}_k$

Unknown data:

- $\boldsymbol{x}_0$, initial condition of $\boldsymbol{x}_k$

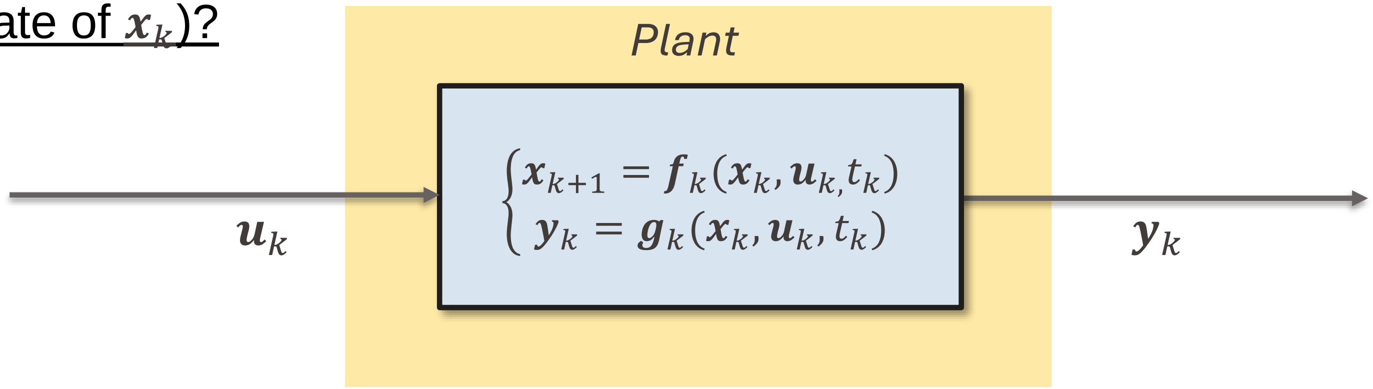

$$\begin{cases} \boldsymbol{x}_{k+1} = \boldsymbol{f}_k(\boldsymbol{x}_k, \boldsymbol{u}_{k,} t_k) \\ \boldsymbol{y}_k = \boldsymbol{g}_k(\boldsymbol{x}_k, \boldsymbol{u}_k, t_k) \end{cases}$$

☐ By adopting a *mathematical model* of the plant P:

- If the dynamics is known, one can directly adopt $(\boldsymbol{f}_k, \boldsymbol{g}_k)$ for the computation of $\hat{\boldsymbol{x}}_k$.

$$\longrightarrow \begin{cases} \hat{\boldsymbol{x}}_{k+1} = \boldsymbol{f}_k(\hat{\boldsymbol{x}}_k, \boldsymbol{u}_k, t_k) \\ \hat{\boldsymbol{y}}_k = \boldsymbol{g}_k(\hat{\boldsymbol{x}}_k, \boldsymbol{u}_k, t_k) \end{cases}$$

- Otherwise, one can model the system P with $(\hat{\boldsymbol{f}}_k, \hat{\boldsymbol{g}}_k)$ where $\hat{\boldsymbol{f}}_k \approx \boldsymbol{f}_k$ and $\hat{\boldsymbol{g}}_k \approx \boldsymbol{g}_k$.

$$\longrightarrow \begin{cases} \hat{\boldsymbol{x}}_{k+1} = \hat{\boldsymbol{f}}_k(\hat{\boldsymbol{x}}_k, \boldsymbol{u}_k, t_k) \\ \hat{\boldsymbol{y}}_k = \hat{\boldsymbol{g}}_k(\hat{\boldsymbol{x}}_k, \boldsymbol{u}_k, t_k) \end{cases}$$

Open-loop model-based state estimation

Before starting with computations, let's make the following hypothesis:

- The dynamics of the plant P is known.

Given $\hat{\boldsymbol{x}}_0$ and $\boldsymbol{u}_k$, one can use the *Observer* block to estimate:

- the state $\hat{\boldsymbol{x}}_k$
- the synthetic measurements $\hat{\boldsymbol{y}}_k$.

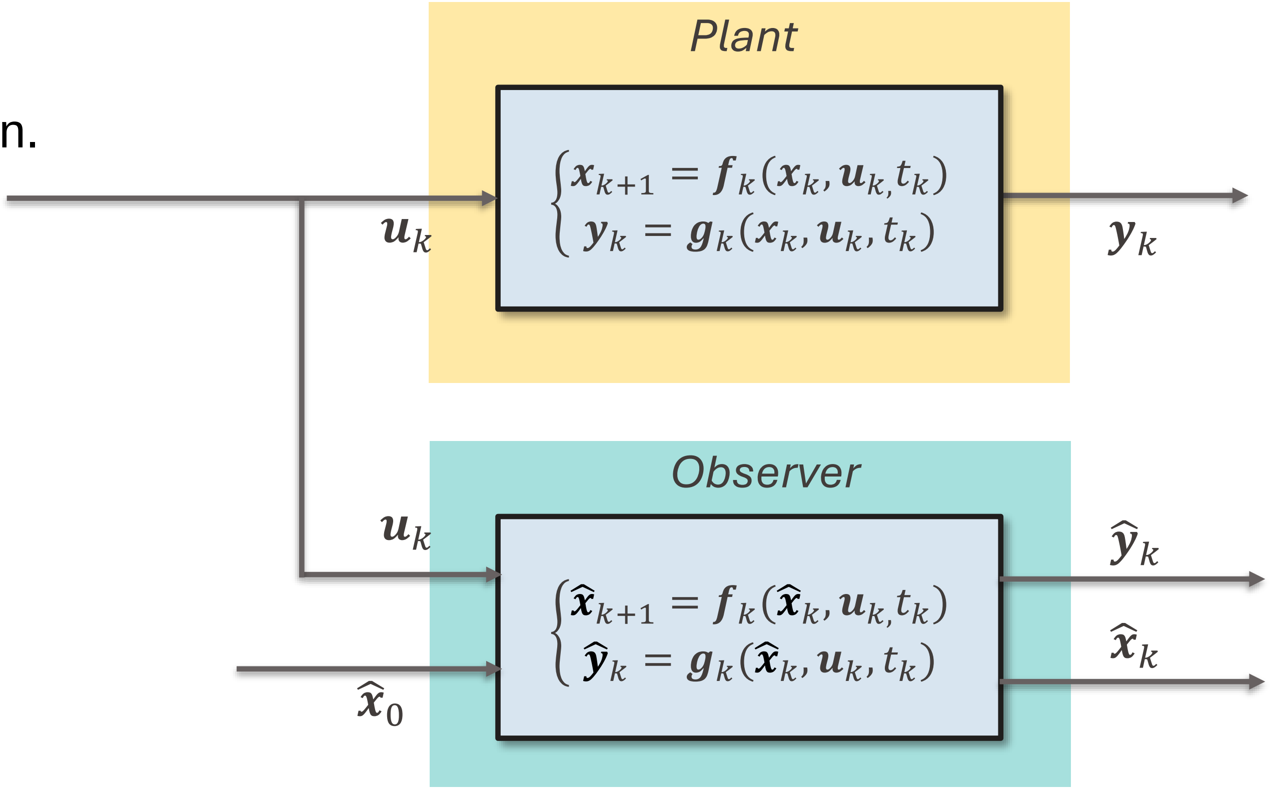

Plant

$$\begin{cases} \boldsymbol{x}_{k+1} = \boldsymbol{f}_k(\boldsymbol{x}_k, \boldsymbol{u}_k, t_k) \\ \boldsymbol{y}_k = \boldsymbol{g}_k(\boldsymbol{x}_k, \boldsymbol{u}_k, t_k) \end{cases}$$

Observer

$$\begin{cases} \hat{\boldsymbol{x}}_{k+1} = \boldsymbol{f}_k(\hat{\boldsymbol{x}}_k, \boldsymbol{u}_k, t_k) \\ \hat{\boldsymbol{y}}_k = \boldsymbol{g}_k(\hat{\boldsymbol{x}}_k, \boldsymbol{u}_k, t_k) \end{cases}$$

Open-loop estimation of the motion of a vehicle

Example: 1D motion of a point-wise vehicle

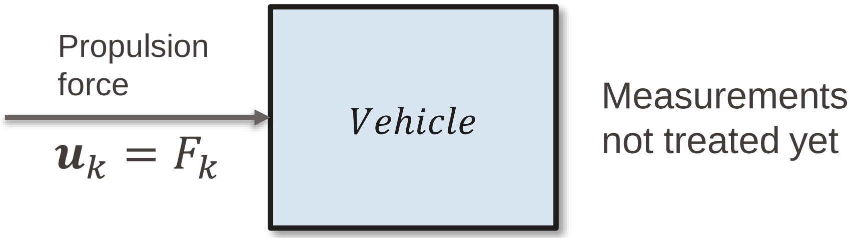

Propulsion force

$\boldsymbol{u}_k = F_k$

$Vehicle$

Measurements not treated yet

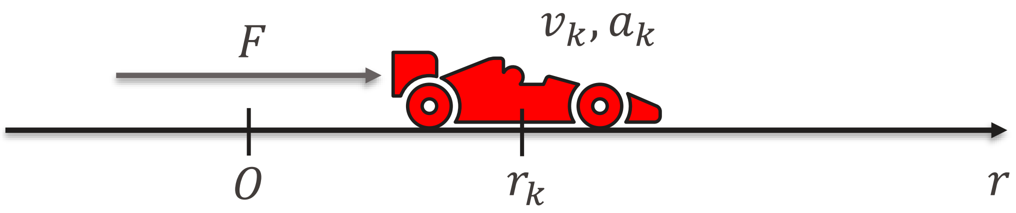

Continuous time state-space representation:

$$\begin{bmatrix}\dot{r}\\ \dot{v}\end{bmatrix} = \begin{bmatrix}0 & 1\\ 0 & 0\end{bmatrix}\begin{bmatrix}r\\ v\end{bmatrix} + \begin{bmatrix}0\\ 1/m\end{bmatrix}F(t)$$

Exponential matrix discretization

Discrete time state-space representation, with sampling time Δt (constant-sampling):

$$\begin{bmatrix}r_{k+1}\\ v_{k+1}\end{bmatrix} = \begin{bmatrix}1 & \Delta t\\ 0 & 1\end{bmatrix}\begin{bmatrix}r_k\\ v_k\end{bmatrix} + \begin{bmatrix}\Delta t^2/2m\\ \Delta t/m\end{bmatrix}F_k$$

Open-loop model-based state estimation: mismatch on initial conditions

Effect of mismatch between $\hat{\boldsymbol{x}}_0$ and $\boldsymbol{x}_0$:

Mismatch on initial condition for the velocity:

- $\boldsymbol{x}_0 = \begin{bmatrix} r_0 \\ v_0 \end{bmatrix} = \begin{bmatrix} 0 \\ 0 \end{bmatrix}$, $\hat{\boldsymbol{x}}_0 = \begin{bmatrix} \hat{r}_0 \\ \hat{v}_0 \end{bmatrix} = \begin{bmatrix} 0 \\ 1 \end{bmatrix}$
- $m = 1, F_k = 1 \cdot step(t).$

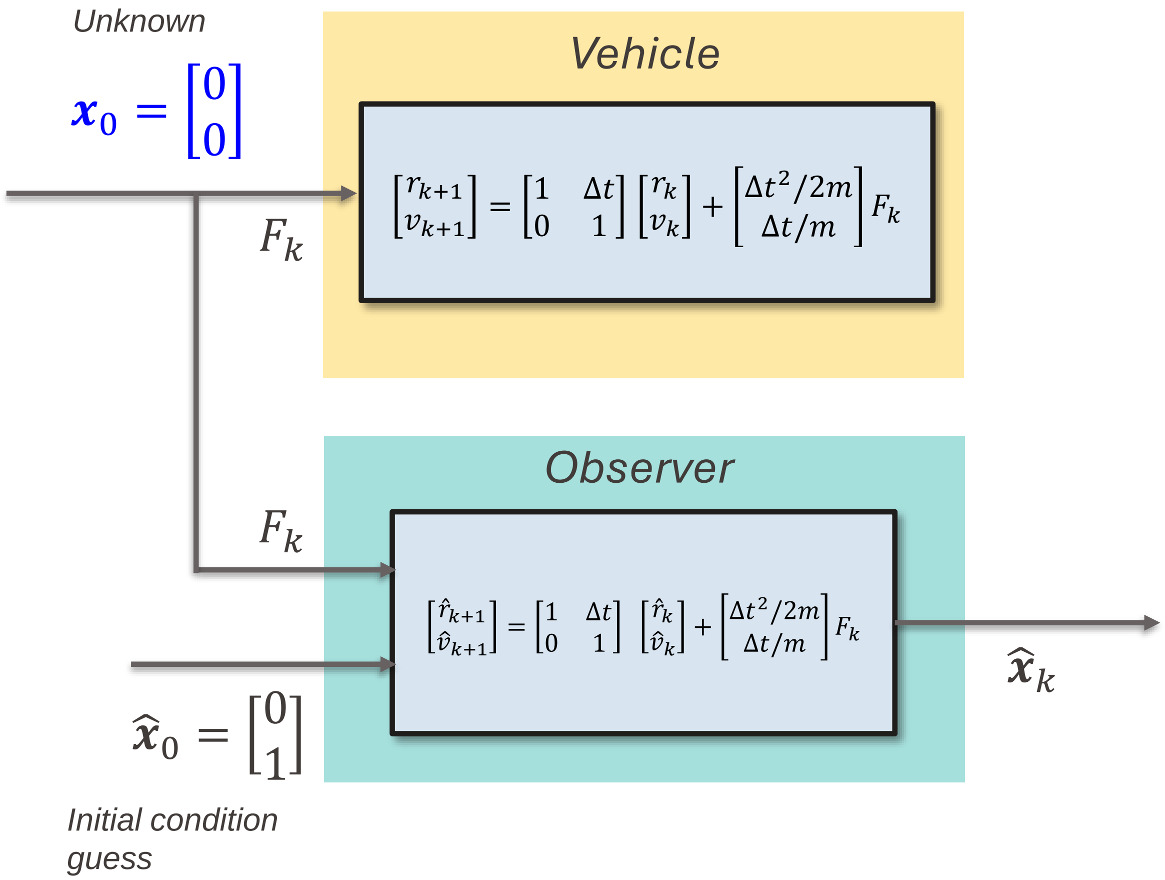

Unknown

$\boldsymbol{x}_0 = \begin{bmatrix} 0 \\ 0 \end{bmatrix}$

Vehicle

F_k

$$\begin{bmatrix} r_{k+1} \\ v_{k+1} \end{bmatrix} = \begin{bmatrix} 1 & \Delta t \\ 0 & 1 \end{bmatrix} \begin{bmatrix} r_k \\ v_k \end{bmatrix} + \begin{bmatrix} \Delta t^2/2m \\ \Delta t/m \end{bmatrix} F_k$$

Observer

F_k

$$\begin{bmatrix} \hat{r}_{k+1} \\ \hat{v}_{k+1} \end{bmatrix} = \begin{bmatrix} 1 & \Delta t \\ 0 & 1 \end{bmatrix} \begin{bmatrix} \hat{r}_k \\ \hat{v}_k \end{bmatrix} + \begin{bmatrix} \Delta t^2/2m \\ \Delta t/m \end{bmatrix} F_k$$

$\hat{\boldsymbol{x}}_k$

$\hat{\boldsymbol{x}}_0 = \begin{bmatrix} 0 \\ 1 \end{bmatrix}$

Initial condition guess

Open-loop model-based state estimation: mismatch on initial conditions

Effect of mismatch between $\hat{\boldsymbol{x}}_0$ and $\boldsymbol{x}_0$:

$$\begin{bmatrix} r_{k+1} \\ v_{k+1} \end{bmatrix} = \begin{bmatrix} 1 & \Delta t \\ 0 & 1 \end{bmatrix} \begin{bmatrix} r_k \\ v_k \end{bmatrix} + \begin{bmatrix} \Delta t^2/2m \\ \Delta t/m \end{bmatrix} F_k$$

Mismatch on initial condition for the velocity:

- $\boldsymbol{x}_0 = \begin{bmatrix} r_0 \\ v_0 \end{bmatrix} = \begin{bmatrix} 0 \\ 0 \end{bmatrix}$, $\hat{\boldsymbol{x}}_0 = \begin{bmatrix} \hat{r}_0 \\ \hat{v}_0 \end{bmatrix} = \begin{bmatrix} 0 \\ 1 \end{bmatrix}$
- $m = 1$, $\boldsymbol{F_k} = \boldsymbol{1} \cdot \boldsymbol{step(t)}.$

- 1) Offset on velocity estimate
- 2) Estimation error on the position drifts over time

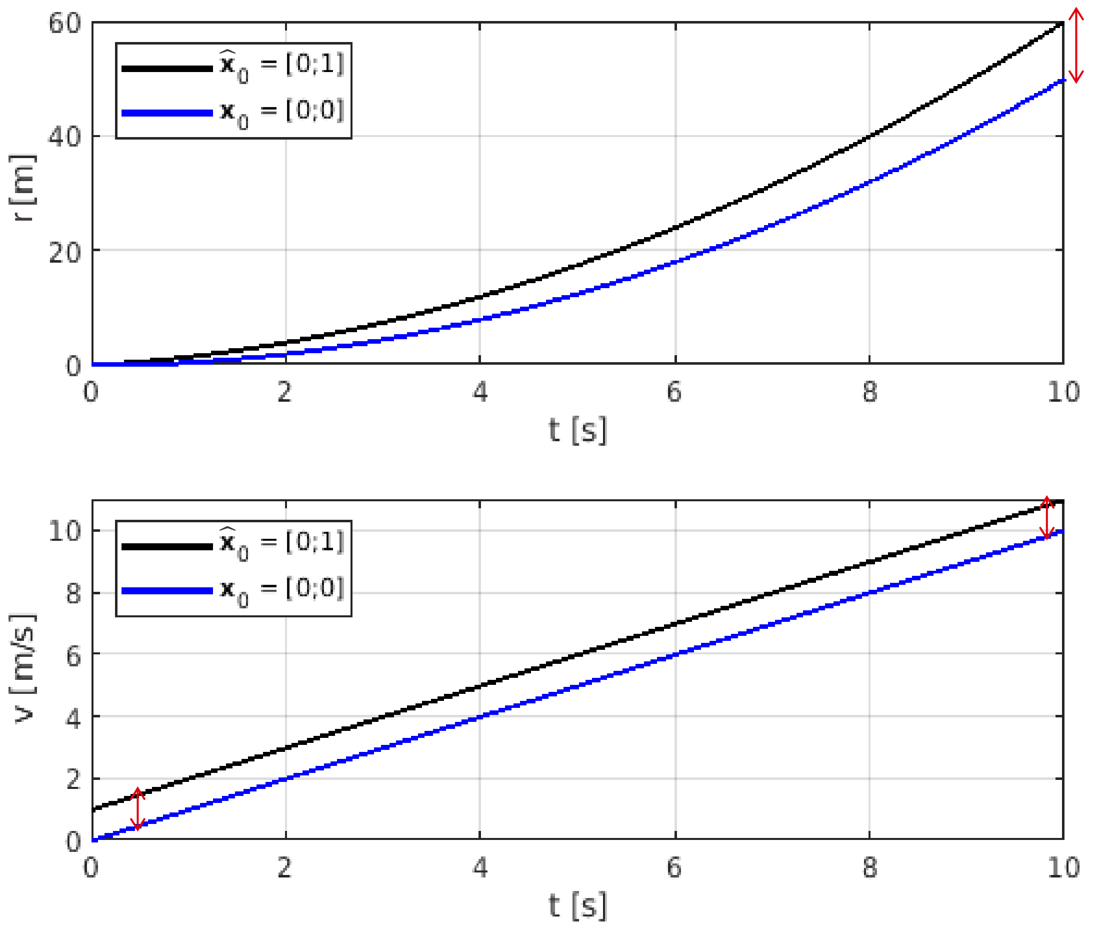

Open-loop model-based state estimation: effect of disturbances on the input

Effect of disturbance on the input, additive standard Gaussian noise $d_k = N(0,1)$ on Force input.

From the observer point of view, the input noise is unknown and doesn't enter in the model inputs.

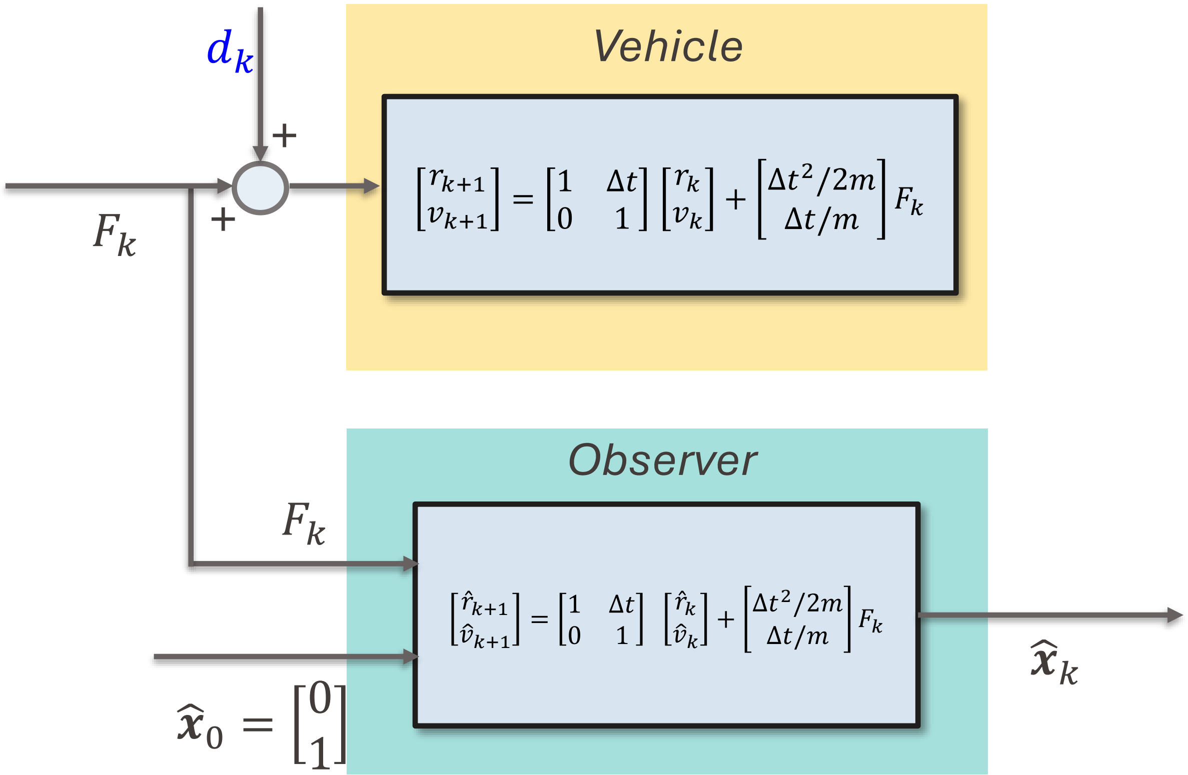

Motivation behind the design of an observer

Effect of disturbance on the input, additive standard Gaussian noise $d_k = N(0,1)$ on Force input:

- Same initial condition $\begin{bmatrix} x_0 \\ v_0 \end{bmatrix} = \begin{bmatrix} 0 \\ 1 \end{bmatrix}$.
- No external forcing term $F_k = 0$.

- State estimation maximum error (in 100 s):
    - $\sim$10% on position.
    - $\sim$20% on velocity.

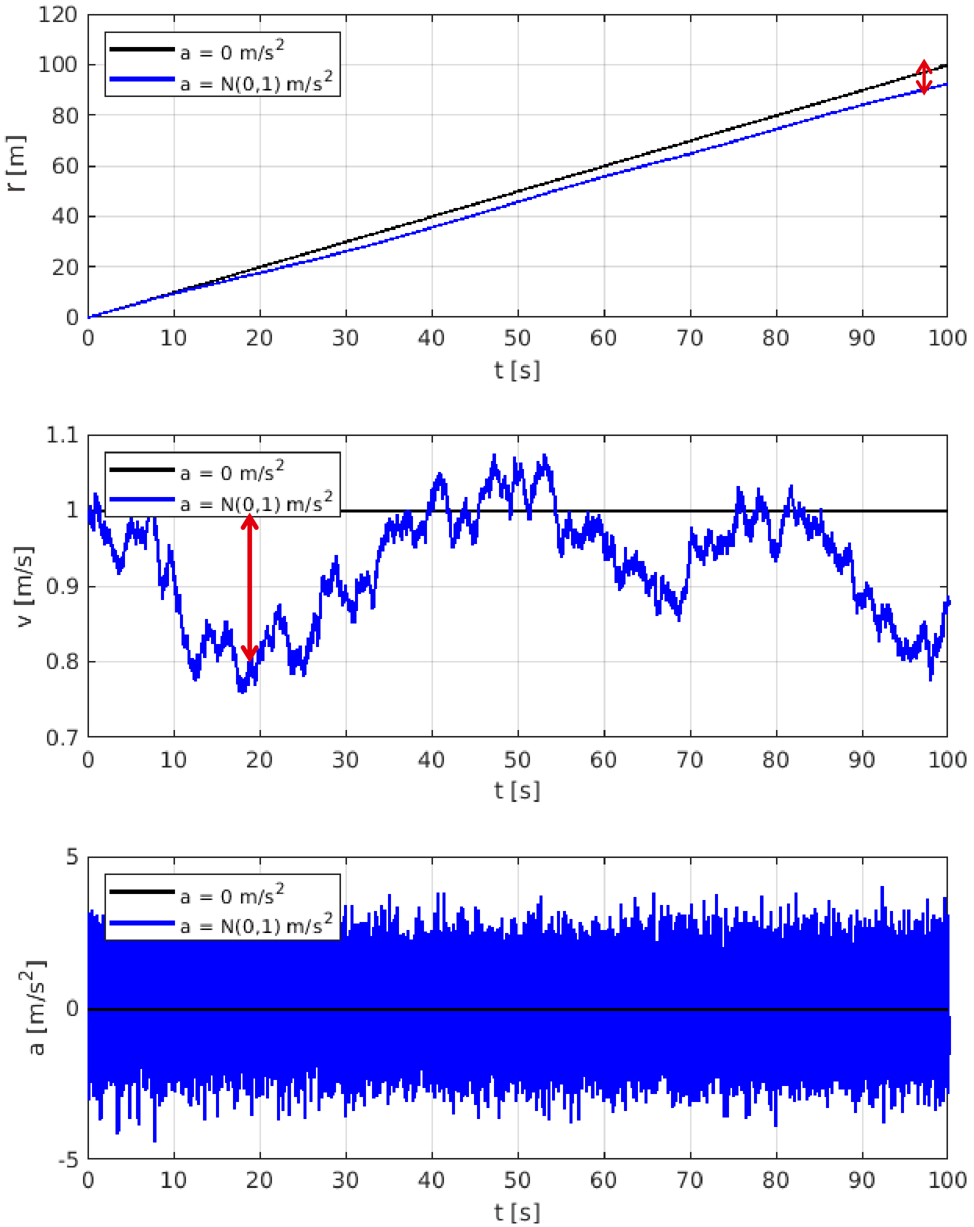

Open-loop state estimation: linear time-independent system

For the next derivations, let's consider the additional hypothesis:

- The plant can be represented by a linear time-independent discrete system (LTI):

$$\begin{cases} \boldsymbol{x}_{k+1} = A\boldsymbol{x}_k + B\boldsymbol{u}_k \\ \boldsymbol{y}_k = C\boldsymbol{x}_k + D\boldsymbol{u}_k \end{cases}$$

$\boldsymbol{x}_k$, *state vector ,*	size [n,1]
$\boldsymbol{u}_k$, *inputs vector,*	size [r,1]
$\boldsymbol{y}_k$, *measurements vector,*	size [m,1]
A, *system/state matrix,*	size [n,n]
B, *input matrix,*	size [n,r]
C, *output matrix,*	size [m,n]
D, *transition matrix,*	size [m,r]

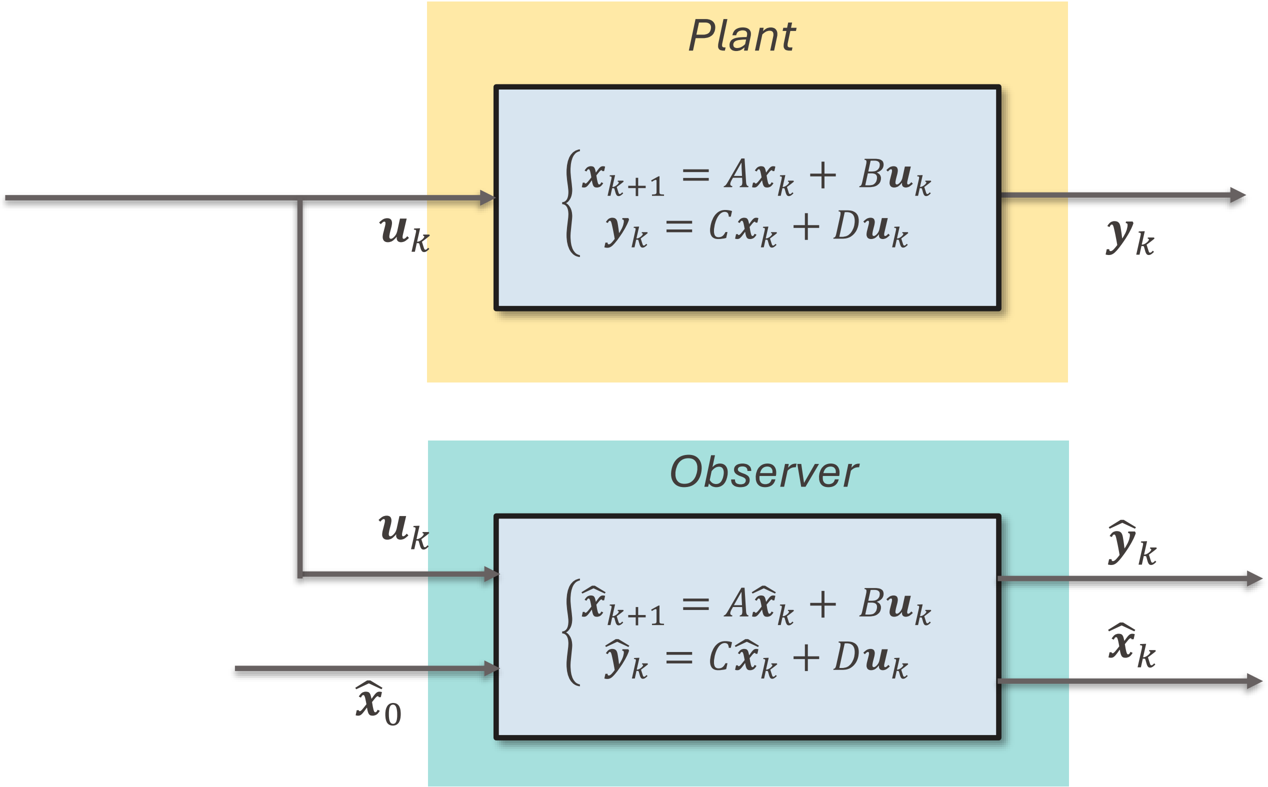

Weaknesses of open-loop state estimation

Study of the estimation error:

$$\hat{\boldsymbol{e}}_k = \boldsymbol{x}_k - \widehat{\boldsymbol{x}}_k$$

Innovation residual:

$$\hat{\boldsymbol{z}}_k = \boldsymbol{y}_k - \widehat{\boldsymbol{y}}_k$$

<u>Plant state system:</u>

① $$\begin{cases} \boldsymbol{x}_{k+1} = A\boldsymbol{x}_k + B\boldsymbol{u}_k \\ \boldsymbol{y}_k = C\boldsymbol{x}_k + D\boldsymbol{u}_k \end{cases}$$

<u>State estimation system:</u>

② $$\begin{cases} \widehat{\boldsymbol{x}}_{k+1} = A\widehat{\boldsymbol{x}}_k + B\boldsymbol{u}_k \\ \widehat{\boldsymbol{y}}_k = C\widehat{\boldsymbol{x}}_k + D\boldsymbol{u}_k \end{cases}$$

① − ②

<u>Estimation error system:</u>

$$\begin{cases} \hat{\boldsymbol{e}}_{k+1} = A\hat{\boldsymbol{e}}_k \\ \hat{\boldsymbol{z}}_k = C\hat{\boldsymbol{e}}_k \end{cases}$$

The state estimation evolves over time solely with the system dynamics represented by A:

- If the <u>plant is unstable</u>, the <u>estimation error will diverge</u> over time.
- Enforce the stability condition by manipulating the poles of the estimation error equation.

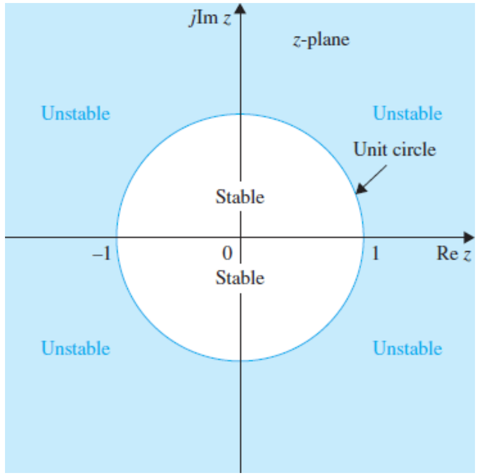

Automatic Control Systems, 10th Edition. Dr. Farid Golnaraghi, Dr. Benjamin, C. Kuo, 2017 McGraw-Hill Education.

Weaknesses of open-loop state estimation

Example: 1D motion of a point-wise vehicle

Estimation error system:

$$\begin{cases} \hat{\boldsymbol{e}}_{k+1} = A\hat{\boldsymbol{e}}_k \\ \hat{\boldsymbol{z}}_k = C\hat{\boldsymbol{e}}_k \end{cases}$$

Discrete state-space representation, with sampling time Δt:

$$\begin{bmatrix} x_{k+1} \\ v_{k+1} \end{bmatrix} = \begin{bmatrix} 1 & \Delta t \\ 0 & 1 \end{bmatrix} \begin{bmatrix} x_k \\ v_k \end{bmatrix} + \begin{bmatrix} \Delta t^2/2m \\ \Delta t/m \end{bmatrix} F_k \longrightarrow A = \begin{bmatrix} 1 & \Delta t \\ 0 & 1 \end{bmatrix}$$

$$\boldsymbol{y}_k = \begin{bmatrix} 1 & 0 \\ 0 & 0 \end{bmatrix} \begin{bmatrix} x_k \\ v_k \end{bmatrix} + \begin{bmatrix} 0 \\ 1/m \end{bmatrix} F_k$$

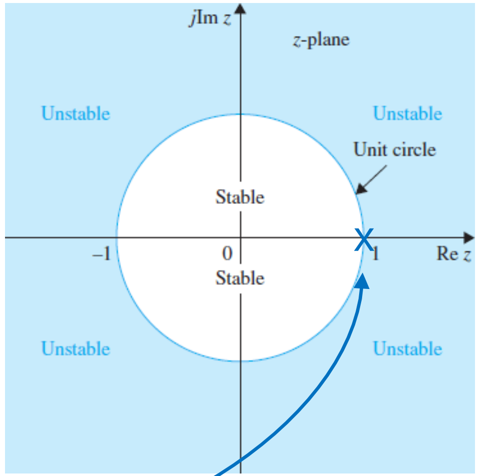

$$\boldsymbol{\lambda}_{1,2} = eig(A) = [1,1]$$

Marginally stable system, open-loop state estimation fails

Closing the loop: state observer and measurements

What are we missing?

- We are just currently using the info contained in the inputs $\boldsymbol{u}_k$…

- **Measurements $\boldsymbol{y}_k$ coming from the plant represent a rich information**!

- Additional input term to the state estimation equation that encorporates the difference between:
  - The plant measurements $\boldsymbol{y}_k$
  - The synthetic measurements $\widehat{\boldsymbol{y}}_k$

$$\begin{cases} \widehat{\boldsymbol{x}}_{k+1} = A\widehat{\boldsymbol{x}}_k + B\boldsymbol{u}_k + L(\boldsymbol{y}_k - \widehat{\boldsymbol{y}}_k) \\ \widehat{\boldsymbol{y}}_k = C\widehat{\boldsymbol{x}}_k + D\boldsymbol{u}_k \end{cases}$$

Closing the loop: state observer and measurements

- Feedback loop to take into account the innovation residual:

$$\hat{\boldsymbol{z}}_k = \boldsymbol{y}_k - \hat{\boldsymbol{y}}_k.$$

- **State observers:** integration of **measurements** with **model prediction** in a self-consistent way.

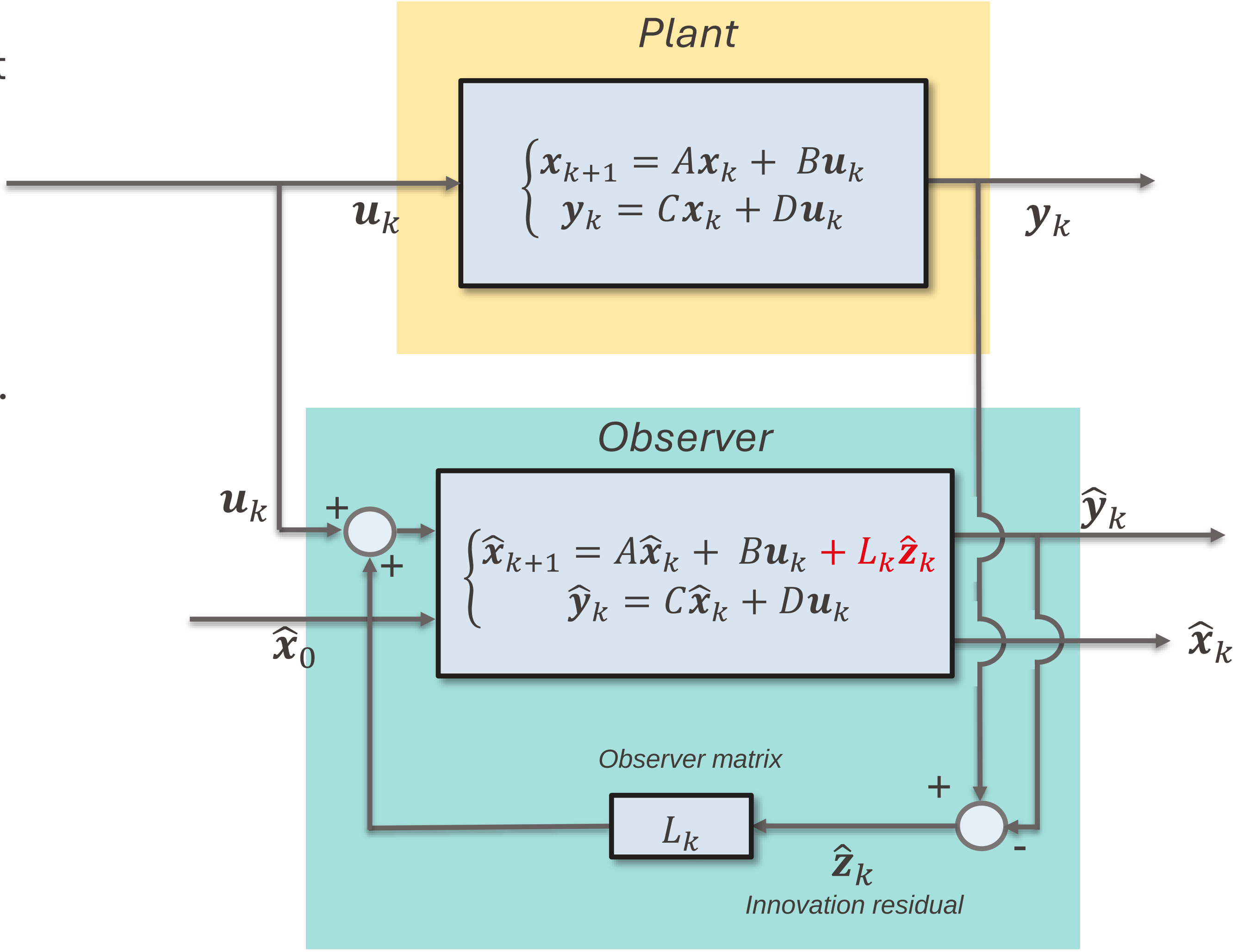

Measurements: example of the 1D motion of a vehicle

Example: 1D motion of a point-wise vehicle

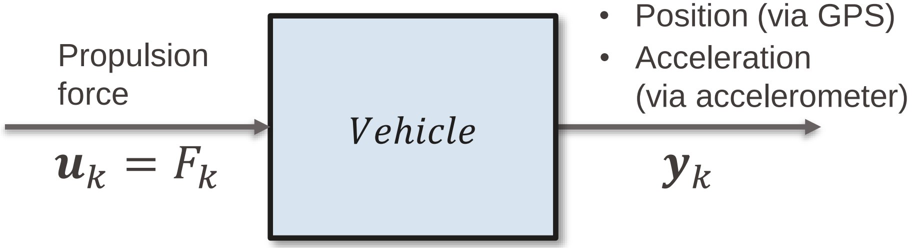

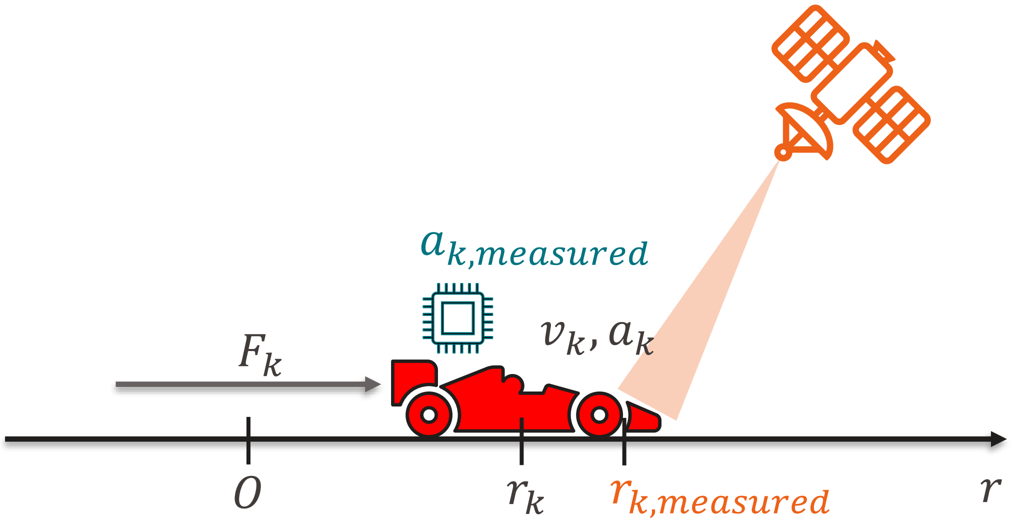

Continuous state-space representation:

$$\begin{bmatrix}\dot{r}\\ \dot{v}\end{bmatrix} = \begin{bmatrix}0 & 1\\ 0 & 0\end{bmatrix}\begin{bmatrix}r\\ v\end{bmatrix} + \begin{bmatrix}0\\ 1/m\end{bmatrix}F$$

$$\boldsymbol{y} = \begin{bmatrix}1 & 0\\ 0 & 0\end{bmatrix}\begin{bmatrix}r\\ v\end{bmatrix} + \begin{bmatrix}0\\ 1/m\end{bmatrix}F$$

- Position (via GPS)
- Acceleration (via accelerometer)

Discrete state-space representation, with sampling time Δt:

$$\begin{bmatrix}r_{k+1}\\ v_{k+1}\end{bmatrix} = \begin{bmatrix}1 & \Delta t\\ 0 & 1\end{bmatrix}\begin{bmatrix}r_k\\ v_k\end{bmatrix} + \begin{bmatrix}\Delta t^2/2m\\ \Delta t/m\end{bmatrix}F_k$$

$$\boldsymbol{y}_k = \begin{bmatrix}1 & 0\\ 0 & 0\end{bmatrix}\begin{bmatrix}r_k\\ v_k\end{bmatrix} + \begin{bmatrix}0\\ 1/m\end{bmatrix}F_k$$

Closed-loop state estimation

Study of the estimation error:

$$\hat{\boldsymbol{e}}_k = \boldsymbol{x}_k - \widehat{\boldsymbol{x}}_k$$

$$\hat{\boldsymbol{z}}_k = \boldsymbol{y}_k - \widehat{\boldsymbol{y}}_k$$

Plant state system:

①
$$\begin{cases} \boldsymbol{x}_{k+1} = A\boldsymbol{x}_k + \ B\boldsymbol{u}_k \\ \boldsymbol{y}_k = C\boldsymbol{x}_k + D\boldsymbol{u}_k \end{cases}$$

State estimation system:

②
$$\begin{cases} \widehat{\boldsymbol{x}}_{k+1} = A\widehat{\boldsymbol{x}}_k + \boldsymbol{B}\boldsymbol{u}_k + L\hat{\boldsymbol{z}}_k \\ \widehat{\boldsymbol{y}}_k = C\widehat{\boldsymbol{x}}_k + D\boldsymbol{u}_k \end{cases}$$

① − ②

Estimation error system:

$$\begin{cases} \hat{\boldsymbol{e}}_{k+1} = (A - LC)\hat{\boldsymbol{e}}_k \\ \hat{\boldsymbol{z}}_k = C\hat{\boldsymbol{e}}_k \end{cases}$$

- Matrix L has size [n,m].
- By tuning the coefficients of L, one can stabilize the *estimation error state equation.*
- The coefficients of L will determine the dynamical response of $\hat{\boldsymbol{e}}_k$.

Important remark:

This procedure only works if the pair (A, C) is ***observable.***

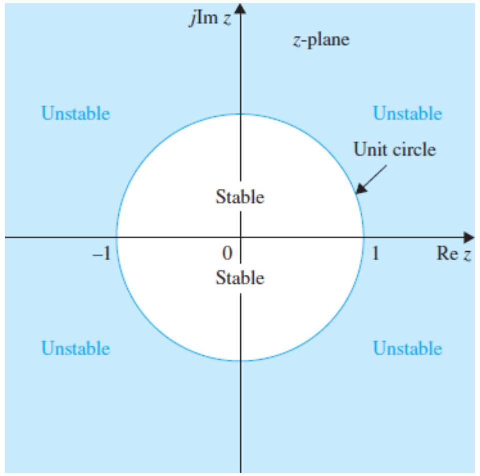

Automatic Control Systems, 10th Edition. Dr. Farid Golnaraghi, Dr. Benjamin, C. Kuo, 2017 McGraw-Hill Education.

Concept of observability

Observability:

- Find the *initial conditions* $\boldsymbol{x}_0$ of a given system P from:
    - measurements $\{\boldsymbol{y}_0, \boldsymbol{y}_1, \dots, \boldsymbol{y}_N\}$
    - inputs $\{\boldsymbol{u}_0, \boldsymbol{u}_1, \dots, \boldsymbol{u}_N\}$
    - system (A, B, C, D) .

- **The manipulation of the poles is not only connected to the values of $\boldsymbol{L}$, but also to the structure of $(\boldsymbol{A}, \boldsymbol{C})$.**

Estimation error equation:

$$\begin{cases} \hat{\boldsymbol{e}}_{k+1} = (A - LC)\hat{\boldsymbol{e}}_k \\ \hat{\boldsymbol{z}}_k = C\hat{\boldsymbol{e}}_k \end{cases}$$

Observability matrix:

$$\mathcal{O} = \begin{bmatrix} C \\ CA \\ \dots \\ CA^{n-1} \end{bmatrix}$$

Where n is the size of the state vector.

- The matrix $\mathcal{O}$ has size [mn,n] (rectangular matrix for MO systems).

- **The system $\boldsymbol{P}$ is *observable* if $\mathbf{rank}(\mathcal{O}) = \boldsymbol{n}$.**

Derivation in backup slides…

Observability: example of the 1D motion of a vehicle

Discrete state-space representation, with sampling time Δt:

$$\begin{bmatrix} r_{k+1} \\ v_{k+1} \end{bmatrix} = \begin{bmatrix} 1 & \Delta t \\ 0 & 1 \end{bmatrix} \begin{bmatrix} r_k \\ v_k \end{bmatrix} + \begin{bmatrix} \Delta t^2/2m \\ \Delta t/m \end{bmatrix} F_k$$

$$\boldsymbol{y} = \begin{bmatrix} 1 & 0 \\ 0 & 0 \end{bmatrix} \begin{bmatrix} r_k \\ v_k \end{bmatrix} + \begin{bmatrix} 0 \\ 1/m \end{bmatrix} F_k$$

- Position (via GPS)
- Acceleration (via accelerometer)

Observability matrix:

$$\mathcal{O} = \begin{bmatrix} C \\ CA \end{bmatrix}$$

if the $rank(\mathcal{O}) = 2$, the system is observable.

$$\mathcal{O} = \begin{bmatrix} C \\ CA \end{bmatrix} = \begin{bmatrix} 1 & 0 \\ 0 & 0 \\ 1 & \Delta t \\ 0 & 0 \end{bmatrix}$$

Since $\Delta t \neq 0$, the matrix $\mathcal{O}$ has rank 2, thus the system is observable.

Remark:

- The acceleration measurement doesn't contribute to the observability of the system!

Conclusion:

- Well-thought design of the measuring system (C matrix) enables the reconstruction of the state $\boldsymbol{x}_k$.
- Many measurements can ensure redundancy in the state observation, in case of failure.

Let's try to apply the previous concepts to design a closed-loop observer matrix L_k for the vehicle example.

Tuning of the observer coefficients

What determines the choice in the selection of the matrix coefficients L?

- Dynamical performances of the observer
- Trust in the model/measurements

There are many techniques to tune the observer gains:

- Luenberger observer:
    - Pole placement of $A - LC$ in the complex plane (deterministic approach).
    - Good performances only for low-noise systems (no noise statistics).
    - Static gain for L.
- Kalman Filter:
    - Noise modeling contained in the formulation of the problem (stochastic approach).
    - Optimal state estimate in the least-squares sense for linear systems.
    - Kalman gain L_k is time-dependent, to be computed at each time step.
    - Can be easily extended for nonlinear systems (Extended Kalman Filter)

Kalman filter: the optimal estimator for linear systems

Kalman filter: the optimal estimator for linear systems

- **Bayesian filter** used as a systematic statistical framework to assimilate experimental data into simulations/RT models.
- First practical use in the aerospace applications, during the **Apollo program**.
- It enabled real-time spacecraft navigation by **optimally fusing noisy sensor data** (e.g., from radar and inertial systems) to estimate *position* and *velocity*.

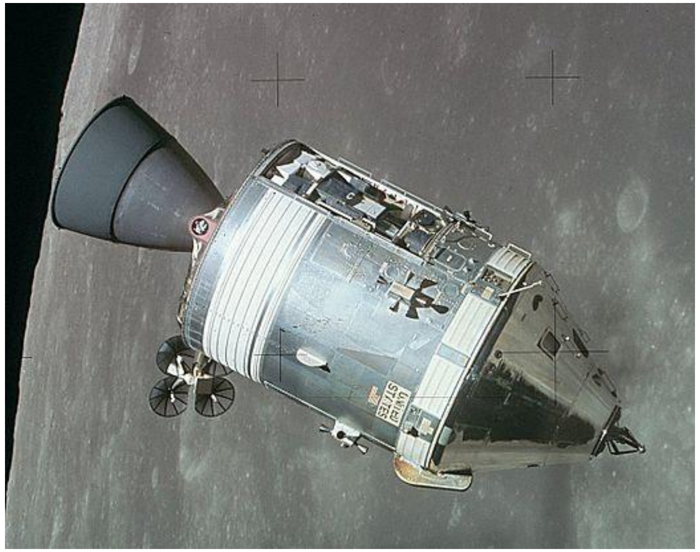

Apollo CSM Endeavour in lunar orbit during Apollo 15

Kalman filter: the optimal estimator for linear systems

Definition: covariance matrix entry for two elements i and j of a stochastic vector $\boldsymbol{x}$ is defined as:

$$cov\left(x_i, x_j\right) = E\left(\left(x_i - E(x_i)\right)\left(x_j - E\left(x_j\right)\right)\right) \qquad E(\boldsymbol{x}\boldsymbol{x}^T) = \begin{bmatrix} var(x_1) & \cdots & cov(x_1, x_N) \\ \vdots & \ddots & \vdots \\ cov(x_1, x_N) & \cdots & var(x_N) \end{bmatrix}$$

- The idea: associate a zero-mean Gaussian white noise to
  - Predictive model equations: $\boldsymbol{w}_k$, $N(0, \boldsymbol{\sigma}_{\mathrm{w}})$
  - Measurements equations: $\boldsymbol{v}_k$, $N(0, \boldsymbol{\sigma}_{\upsilon})$

- Plant state equation:

$$\begin{cases} \boldsymbol{x}_{k+1} = A\boldsymbol{x}_k + \ B\boldsymbol{u}_k + \boldsymbol{w}_k \\ \boldsymbol{y}_k = C\boldsymbol{x}_k + D\boldsymbol{u}_k + \boldsymbol{v}_k \end{cases}$$

- Associate covariance matrices to $\boldsymbol{w}_k$ and $\boldsymbol{v}_k$:
  - Process covariance matrix: $Q_k = E\left(\boldsymbol{w}_k\boldsymbol{w}_k^T\right)$
  - Measurement covariance matrix: $R_k = E(\boldsymbol{v}_k\boldsymbol{v}_k^T)$

Kalman filter: the optimal estimator for linear systems

Algorithm formulation (formulation extended for time-varying systems):

- Predictive/Prior step:

$$\hat{\boldsymbol{x}}_{k+1|k} = A_k\hat{\boldsymbol{x}}_{k|k} + B_k\boldsymbol{u}_k \qquad \text{Prior error: } \hat{\boldsymbol{e}}_{k+1|k} = \hat{\boldsymbol{x}}_{k+1|k} - \boldsymbol{x}_k$$

$$\hat{\boldsymbol{y}}_k = C_k\hat{\boldsymbol{x}}_{k|k} + D_k\boldsymbol{u}_k$$

- Correction/Posterior step:

$$\hat{\boldsymbol{x}}_{k+1|k+1} = \hat{\boldsymbol{x}}_{k+1|k} + L_k(\boldsymbol{y}_k - \hat{\boldsymbol{y}}_k) \qquad \text{Posterior error: } \hat{\boldsymbol{e}}_{k+1|k+1} = \hat{\boldsymbol{x}}_{k+1|k+1} - \boldsymbol{x}_k$$

Computation of the Kalman filter gain:

- Concept behind: find L_k that minimizes the trace of the posterior covariance matrix

$$P_{k+1|k+1} = E(\hat{\boldsymbol{e}}_{k+1|k+1}\hat{\boldsymbol{e}}_{k+1|k+1}^T)$$

- This process naturally incorporates the covariance matrices Q_k and R_k
- L_k retains how much weight has to be put between model and measures:
  - Low $||Q_k||/\ ||R_k||$: more trust in the model
  - High $||Q_k||/\ ||R_k||$: more trust in the measurements

Computation of the Kalman filter gain

- 1) Prediction error covariance matrix $E(\hat{\boldsymbol{e}}_{k+1|k}\hat{\boldsymbol{e}}_{k+1|k}^T)$:

$$P_{k+1|k} = A_k P_{k|k} A_k^T + Q_\mathrm{k}$$

- 2) Innovation residual covariance matrix $E(\hat{\boldsymbol{z}}_k\hat{\boldsymbol{z}}_k^T)$:

$$S_k = C_k P_{k+1|k} C_k^T + R_k$$

- **3) Extended Kalman filter gain** $\min_{L_k} tr(P_{k+1|k+1})$**:**

$$L_k = P_{k+1|k} C_k^T S_k^{-1}$$

- 4) Posterior error covariance matrix $E(\hat{\boldsymbol{e}}_{k+1|k+1}\hat{\boldsymbol{e}}_{k+1|k+1}^T)$:

$$P_{k+1|k+1} = (I - L_k C_k) P_{k+1|k}$$

- 5) Repeat steps 1) to 4) before the **correction step**, setting:

$$P_{k+1|k+1} \xrightarrow{z^{-1}} P_{k|k}$$

Kalman filter: example of the 1D motion of a vehicle

Let’s adopt the Kalman filter to tackle the issues related with:
- The mismatching initial condition
- The disturbance in the input force

Graphical representation of the Gaussian distributions for:
- Measurement position $r_{k,measured}$, covariance R_k
- Predicted position estimate $\hat{r}_{k+1|k}$, covariance $P_{k+1|k}$
- Posterior position estimate $\hat{r}_{k+1|k+1}$, covariance $P_{k+1|k+1}$

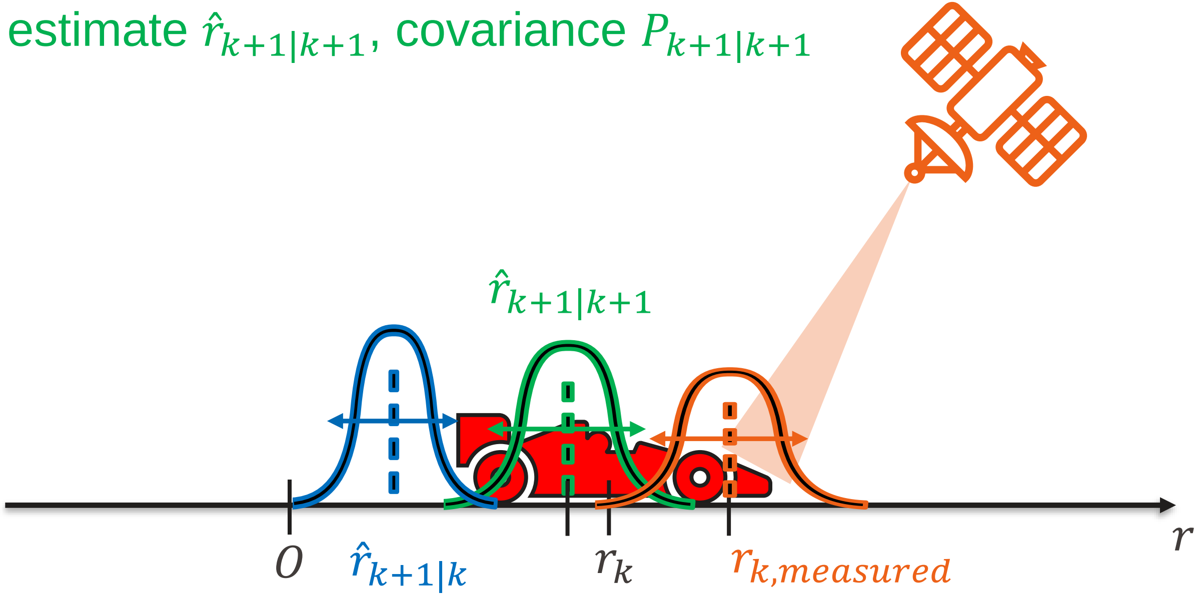

Closed-loop model-based state estimation: mismatch on initial conditions

Effect of mismatch between $\hat{\boldsymbol{x}}_0$ and $\boldsymbol{x}_0$:

Mismatch on initial condition for the velocity:

- $\boldsymbol{x}_0 = \begin{bmatrix} r_0 \\ v_0 \end{bmatrix} = \begin{bmatrix} 0 \\ 0 \end{bmatrix}$, $\hat{\boldsymbol{x}}_0 = \begin{bmatrix} \hat{r}_0 \\ \hat{v}_0 \end{bmatrix} = \begin{bmatrix} 0 \\ 1 \end{bmatrix}$
- $m = 1, F_k = 1 \cdot step(t).$
- Introduction of noisy measurement on position: $y_r = r_{plant} + N(0,1)$
- *Let's start with **zero gain** to the observer matrix:* $L_k = 0$
- *Exactly same behavior recovered, Observer behaves as the open loop Model*

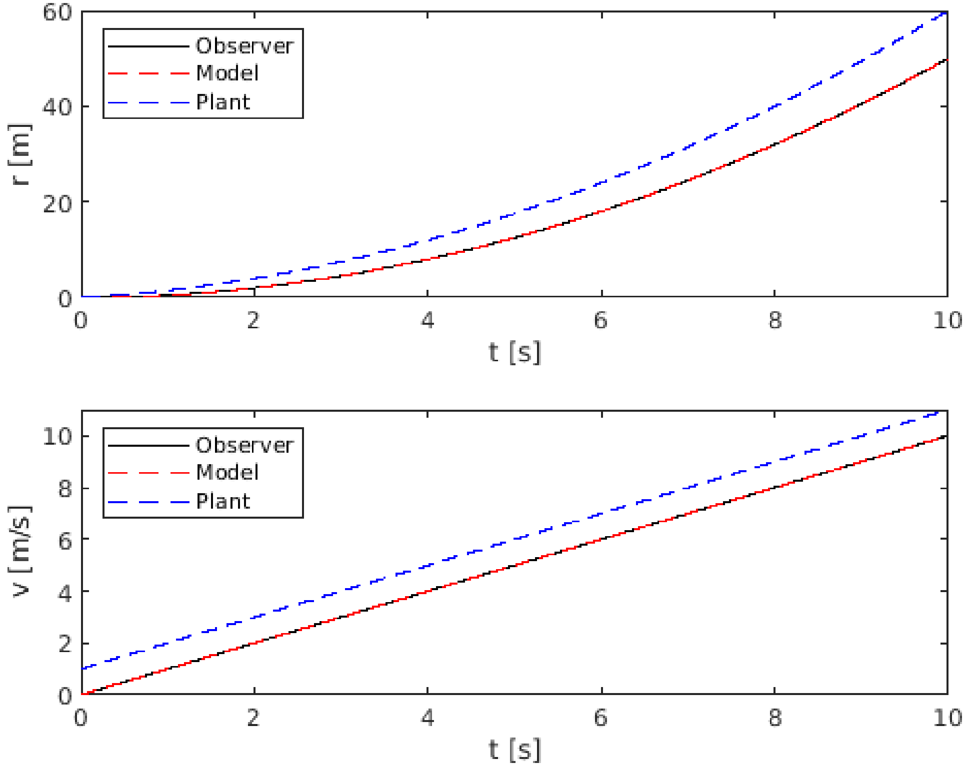

Closed-loop model-based state estimation: mismatch on initial conditions

Effect of mismatch between $\hat{\boldsymbol{x}}_0$ and $\boldsymbol{x}_0$:

- $R_k = \sigma_R^2 \begin{bmatrix} 1 & 0 \\ 0 & 1 \end{bmatrix}$, $\sigma_R^2 = 1$
- $Q_k = \sigma_Q^2 \begin{bmatrix} 1 & 0 \\ 0 & 1 \end{bmatrix}$, $\sigma_Q^2 = 10^{-2}$
- Successful convergence of the posterior error estimate to zero
- Still a bit noisy, let's try to filter it out by playing with σ_Q^2

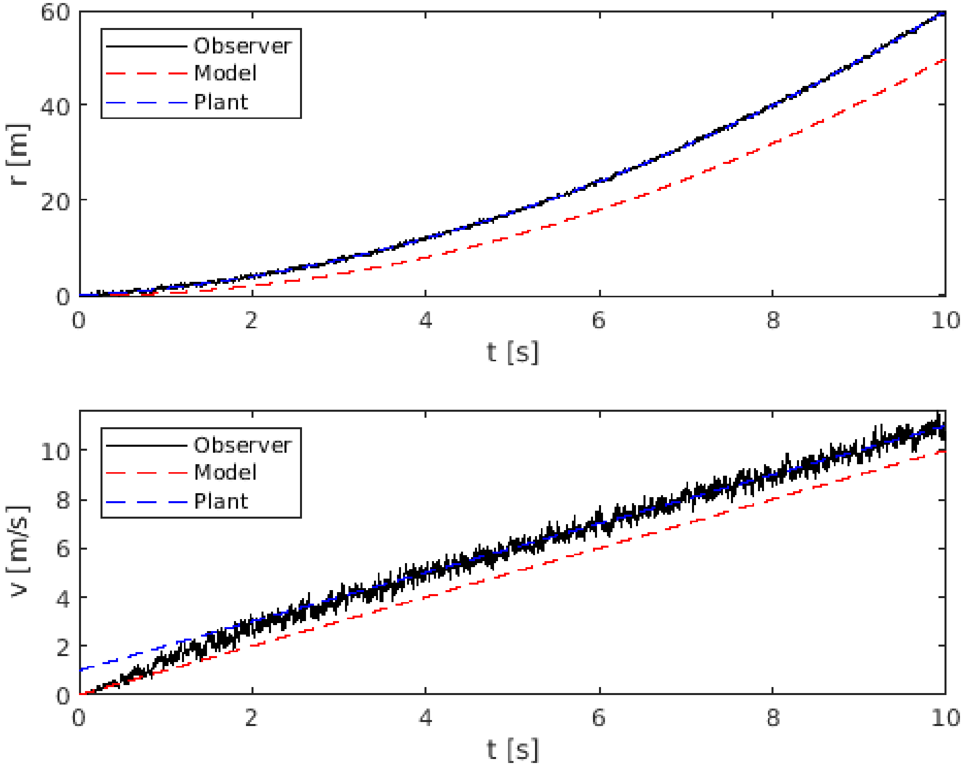

Closed-loop model-based state estimation: mismatch on initial conditions

Effect of mismatch between $\hat{\boldsymbol{x}}_0$ and $\boldsymbol{x}_0$:

- $R_k = \sigma_R^2 \begin{bmatrix} 1 & 0 \\ 0 & 1 \end{bmatrix}, \qquad \sigma_R^2 = 1$
- $Q_k = \sigma_Q^2 \begin{bmatrix} 1 & 0 \\ 0 & 1 \end{bmatrix}, \qquad \sigma_Q^2 = 10^{-6}$
- Successful convergence of the posterior error estimate to zero
- Noise completely filtered out!

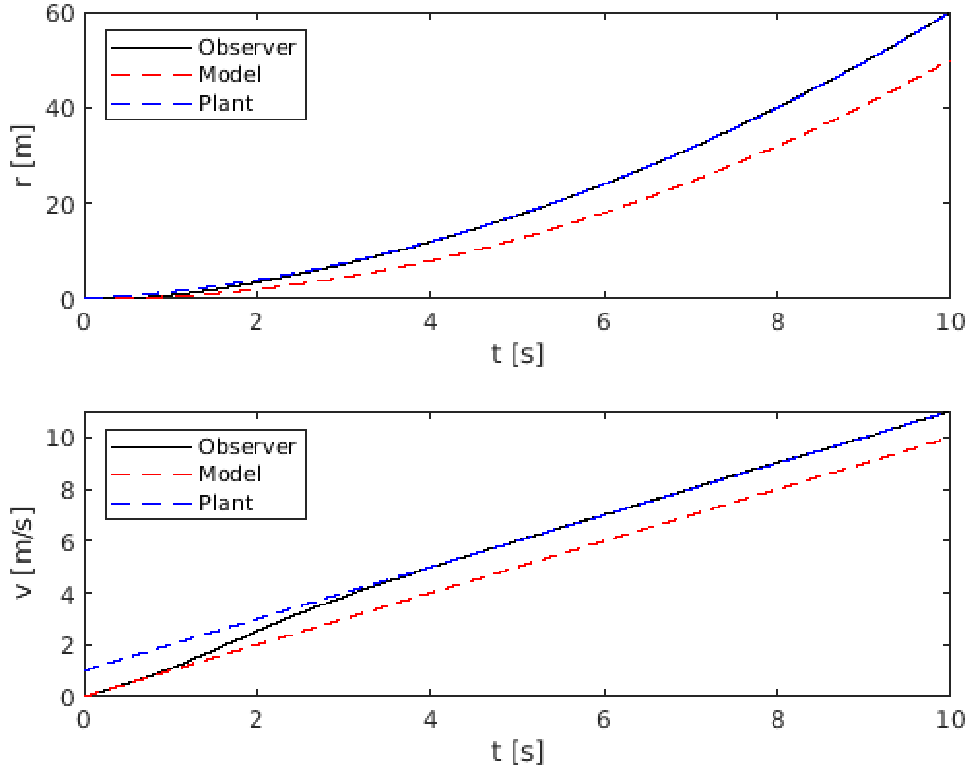

Closed-loop model-based state estimation: mismatch on initial conditions

Effect of mismatch between $\hat{\boldsymbol{x}}_0$ and $\boldsymbol{x}_0$:

- $R_k = \sigma_R^2 \begin{bmatrix} 1 & 0 \\ 0 & 1 \end{bmatrix}, \qquad \sigma_R^2 = 1$
- $Q_k = \sigma_Q^2 \begin{bmatrix} 1 & 0 \\ 0 & 1 \end{bmatrix}, \qquad \sigma_Q^2 = 10^{-6}$
- Successful convergence of the posterior error estimate to zero
- Noise completely filtered out!

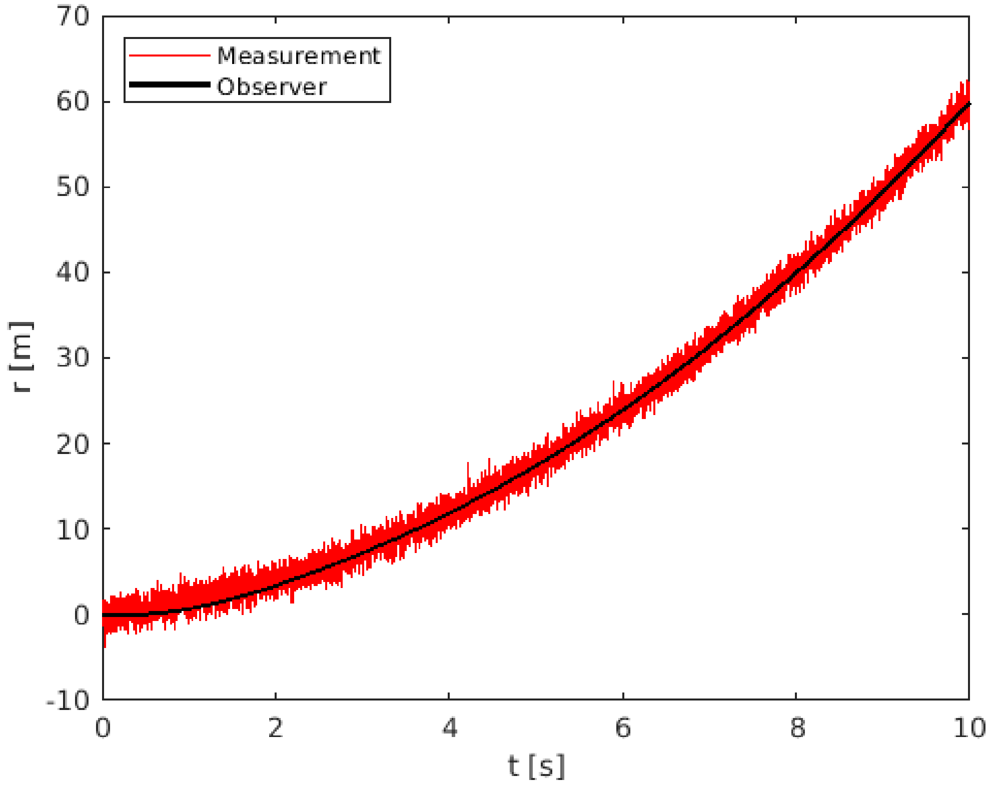

Closed-loop model-based state estimation: mismatch on initial conditions + input disturbance

Effect of mismatch between $\hat{\boldsymbol{x}}_0$ and $\boldsymbol{x}_0$+ white noise input disturbance:

- $R_k = \sigma_R^2 \begin{bmatrix} 1 & 0 \\ 0 & 1 \end{bmatrix}, \qquad \sigma_R^2 = 1$
- $Q_k = \sigma_Q^2 \begin{bmatrix} 1 & 0 \\ 0 & 1 \end{bmatrix}, \qquad \sigma_Q^2 = 10^{-6}$

Mismatch on initial condition for the velocity:

- $\boldsymbol{x}_0 = \begin{bmatrix} r_0 \\ v_0 \end{bmatrix} = \begin{bmatrix} 0 \\ 0 \end{bmatrix}, \ \hat{\boldsymbol{x}}_0 = \begin{bmatrix} \hat{r}_0 \\ \hat{v}_0 \end{bmatrix} = \begin{bmatrix} 0 \\ 1 \end{bmatrix}$
- $m = 1, F_k + d_k = 0 + 3N(0,1).$
- Noisy measurement on position: $y_r = r_{plant} + N(0,1)$

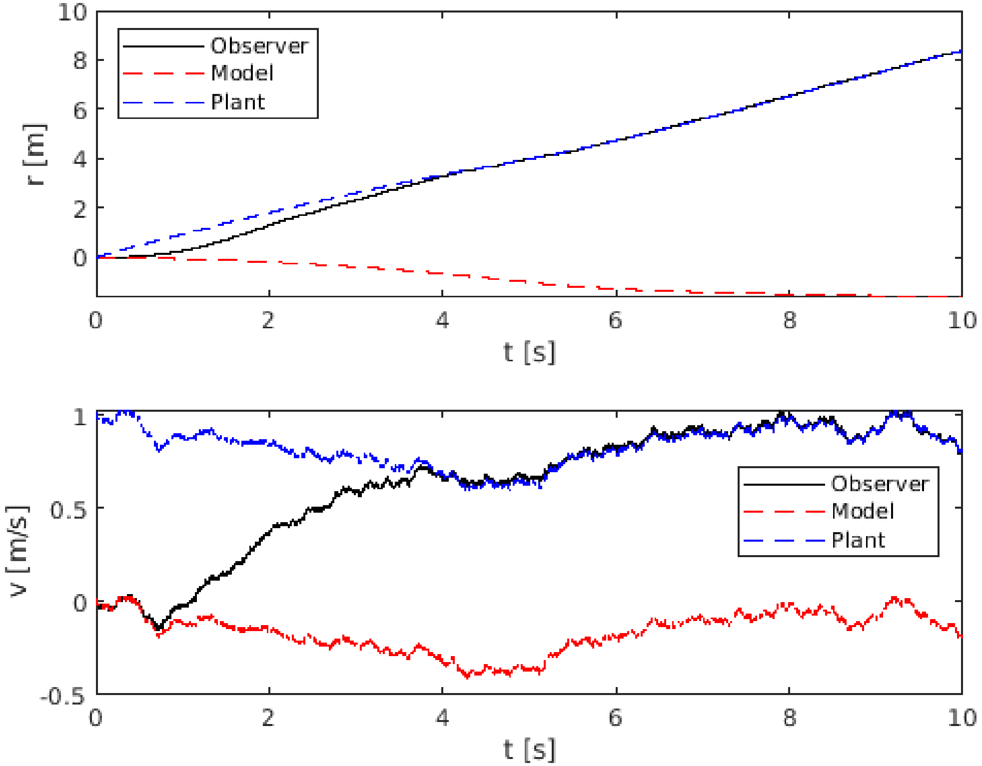

Closed-loop model-based state estimation: mismatch on initial conditions + input disturbance

Effect of mismatch between $\hat{\boldsymbol{x}}_0$ and $\boldsymbol{x}_0$+ white noise input disturbance:

- $R_k = \sigma_R^2 \begin{bmatrix} 1 & 0 \\ 0 & 1 \end{bmatrix}, \qquad \sigma_R^2 = 1$
- $Q_k = \sigma_Q^2 \begin{bmatrix} 1 & 0 \\ 0 & 1 \end{bmatrix}, \qquad \sigma_Q^2 = 10^{-6}$
- Very good tracking of the plant dynamics, even if affected by noises.
- Faster response enabled by tuning the values of R_k and Q_k.

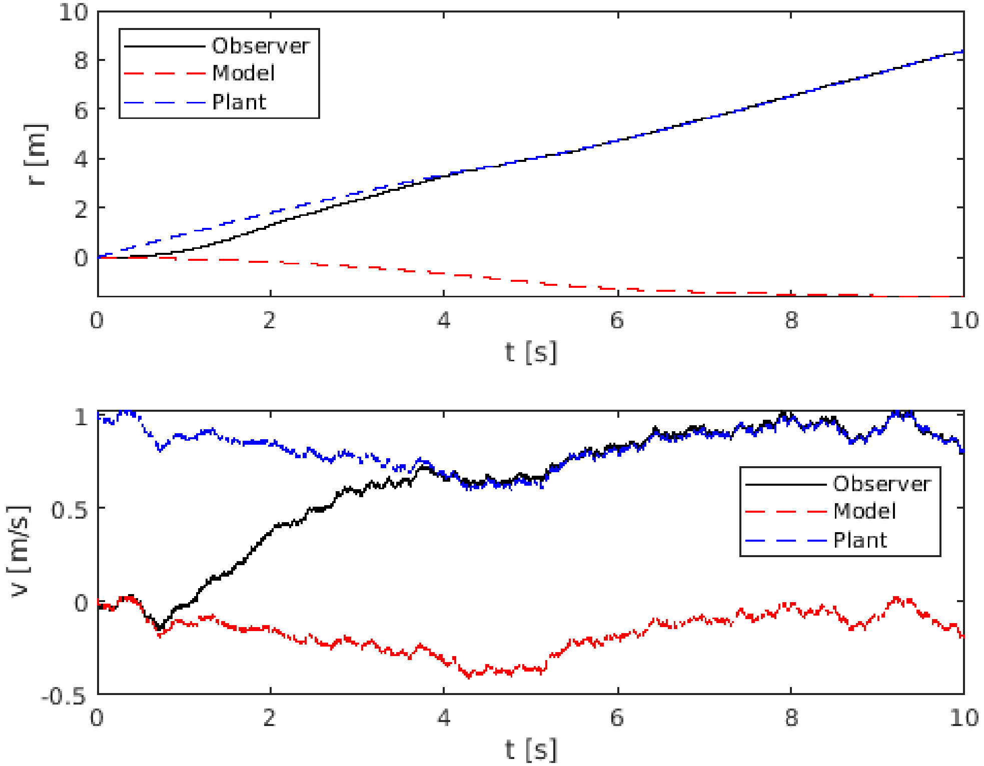

Plasma electron density reconstruction and control on TCV

- Motivation and applications
- RAPDENS model presentation
- Results on local density control

TCV diagnostics for RT density measurement: FIR

- Composed of 14 laser chords (λ = 184.3 μm) at different radial positions, f_{sample} = 20 kHz.
- Phase delay of the 14 FIRs w.r.t. a reference laser outside the plasma:

$$\Delta\phi_k^c = c_{FIR} \int_{L_c} n_e(\rho(z), t_k)dz$$

- $\Delta\phi$ can span different 2π radians, called **fringes**.
- Central chord used routinely used for density feedback

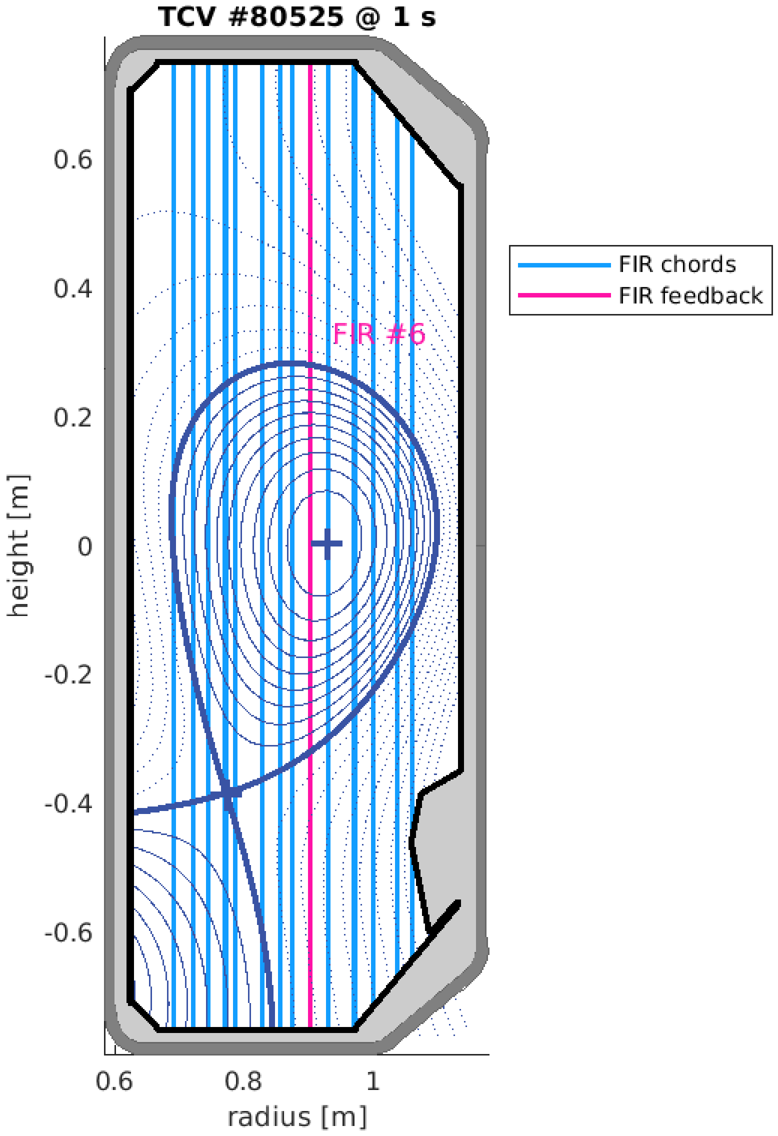

TCV diagnostics for RT density measurement: FIR

- Phase delay of the 14 FIRs w.r.t. a reference laser outside the plasma: $\Delta\phi_k^c = c_{FIR} \int_{L_c} n_e(\rho(z), t_k)dz$
- $\Delta\phi$ can span different 2π radians, called **fringes**.
- Various issues (high density plasmas and/or low SNR) lead to counting errors: ***fringe jumps***.
- Integer errors of 2π lead to density errors of magnitude $\delta \approx 10^{19}\, m^{-2}$

FIR signal normalized and shifted:

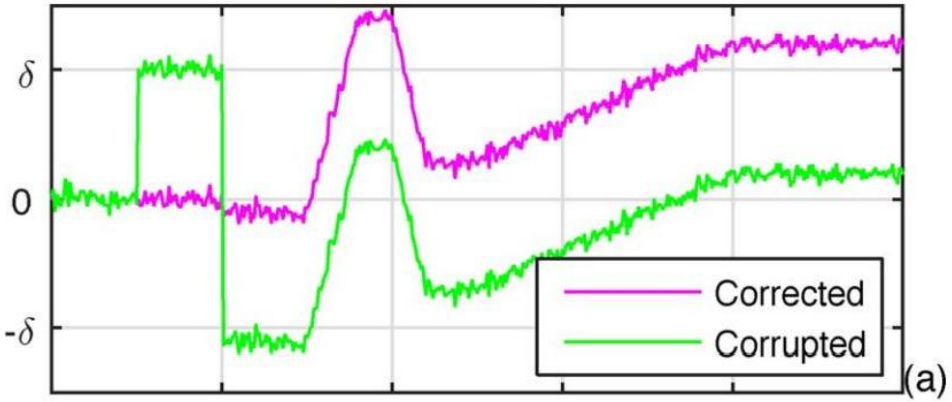

T. C. Blanken et al., Fusion Engineering and Design 126, doi:10.1016/j.fusengdes.2017.11.006., 2018

TCV diagnostics for RT density measurement: Thomson Scattering (TS)

- Main diagnostic for the estimation of the spatial profiles of n_e and T_e on TCV.
- Measurements at **117 positions along a vertical laser beam** (R=0.9 m), covering also divertor region.
- Three lasers firing at a frequency of 20 Hz, independent fire mode:
    - Equispaced in time: **60 Hz**
    - Burst-mode: interleave of 1 ms for three lasers, for fast phenomena in plasma core or SOL.

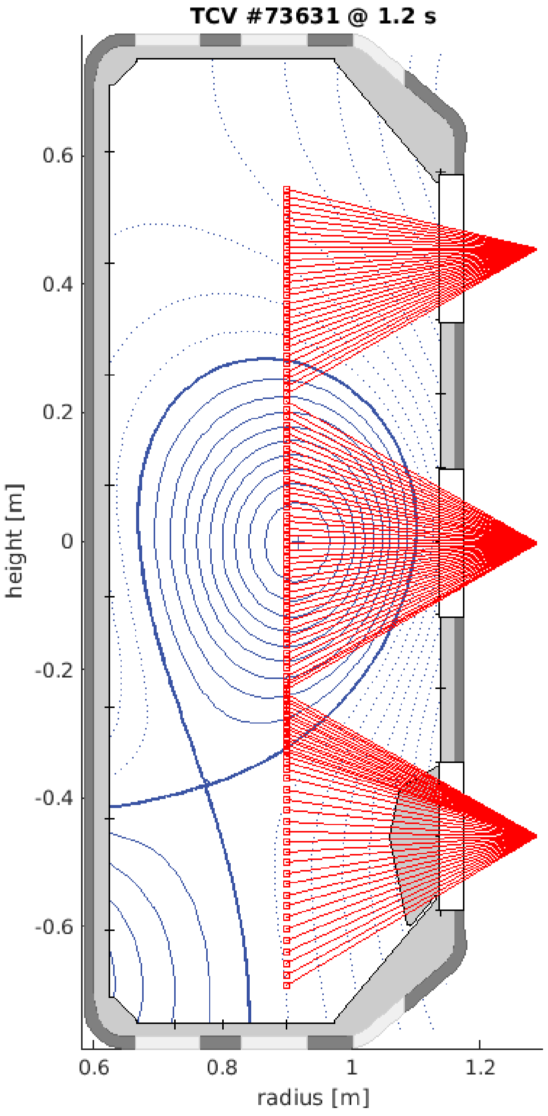

Lines of sight of TS diagnostic

TCV diagnostics for RT density measurement: Thomson Scattering (TS)

- Combining TS data with the real time equilibrium reconstruction enables to:
  - Distinguish between **core plasma** and **SOL** density
  - Provide detailed spatial info of density

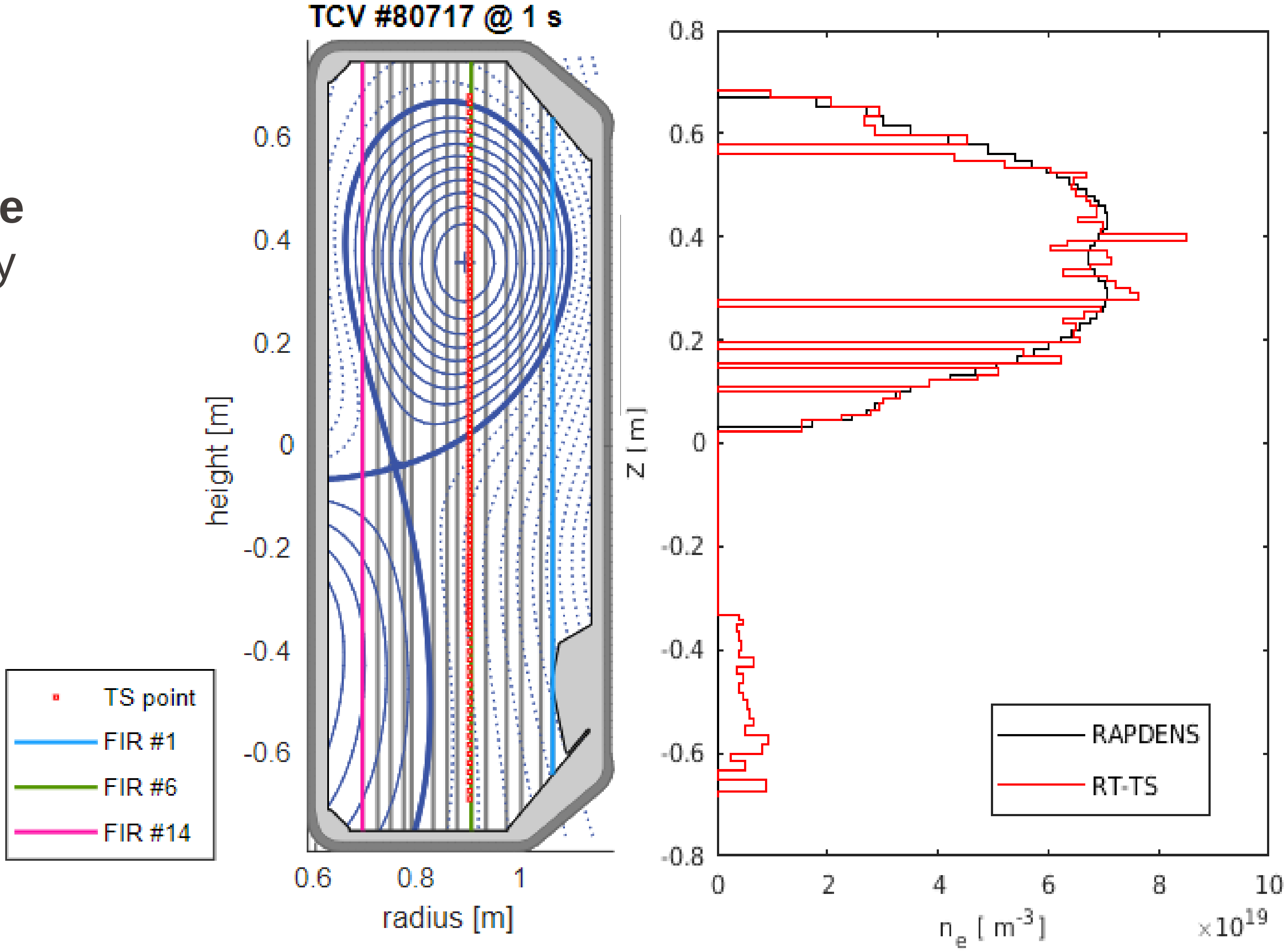

Motivation: real-time estimation and control of ne profile

- **Real-time estimation of plasma electron density profile** enables:
  - Monitoring of plasma density limits in real time for disruption avoidance and integrated control [1].
  - Local control of the density at $\rho = \rho_{target}$, e.g. on rational surfaces below cutoff for suppression of NTMs [2].
  - Real-time Kinetic Equilibrium Reconstruction [3] for self-consistent kinetic profiles + equilibrium.

[1] A. Pau et al., IAEA TM on Disruptions, Cadarache ITER, 2020.

[2] M. Kong et al., Plasma Phys. Control. Fusion 64 044008, doi: 10.1088/1361-6587/ac48be, 2022.

[3] F. Carpanese et al., Nucl. Fusion 60 066020, doi:10.1088/1741-4326/ab81ac, 2020.

Motivation: real-time estimation and control of ne profile

- Adoption of **model-based observers**:
    - Merge different diagnostics for improved reconstruction of n_e.
    - Decoupling between the diagnostics and the controllers.
    - Avoiding propagation of diagnostic faults

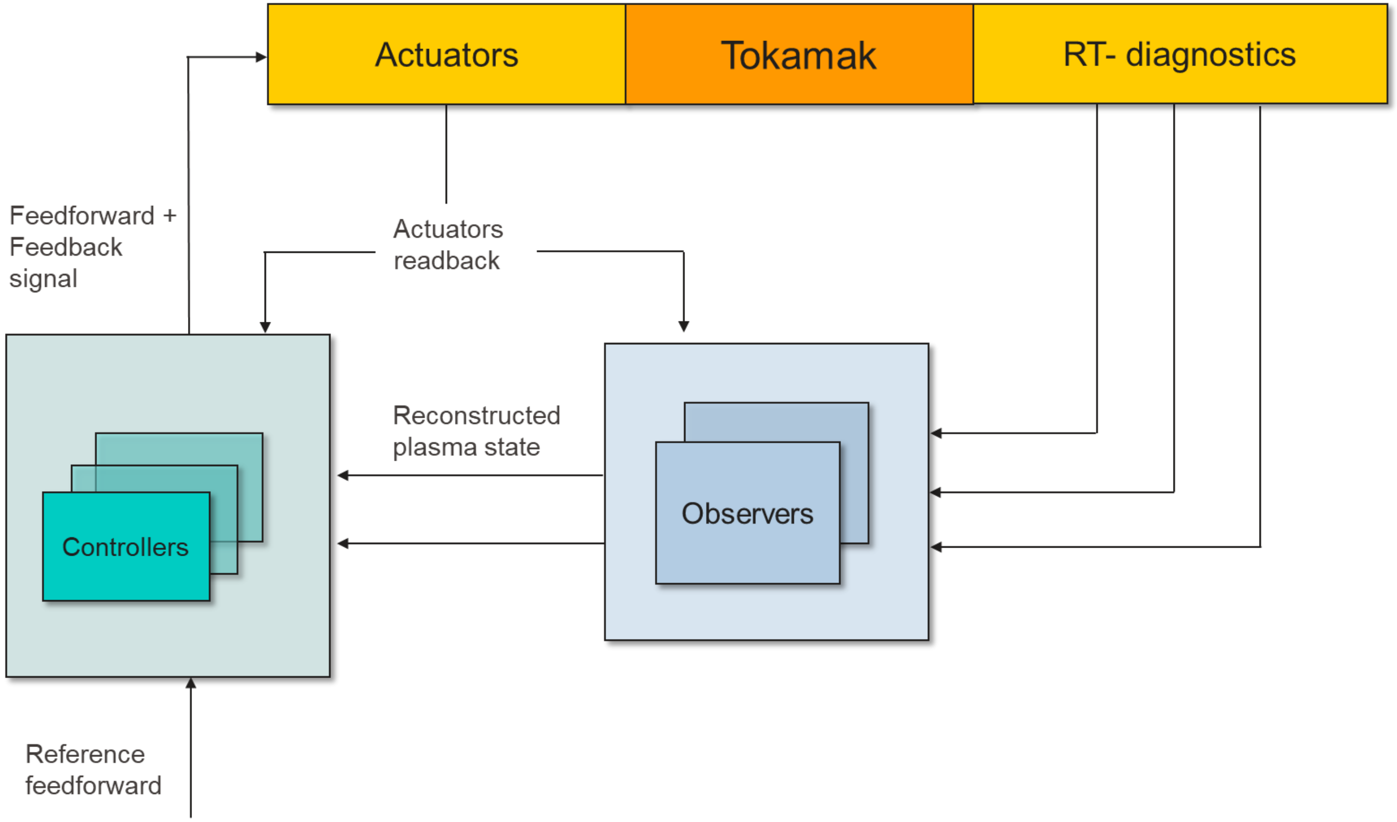

Motivation: real-time estimation and control of ne profile

- Adoption of **model-based observers**:
  - Merge different diagnostics for improved reconstruction of n_e.
  - Decoupling between the diagnostics and the controllers.
  - Avoiding propagation of diagnostic faults

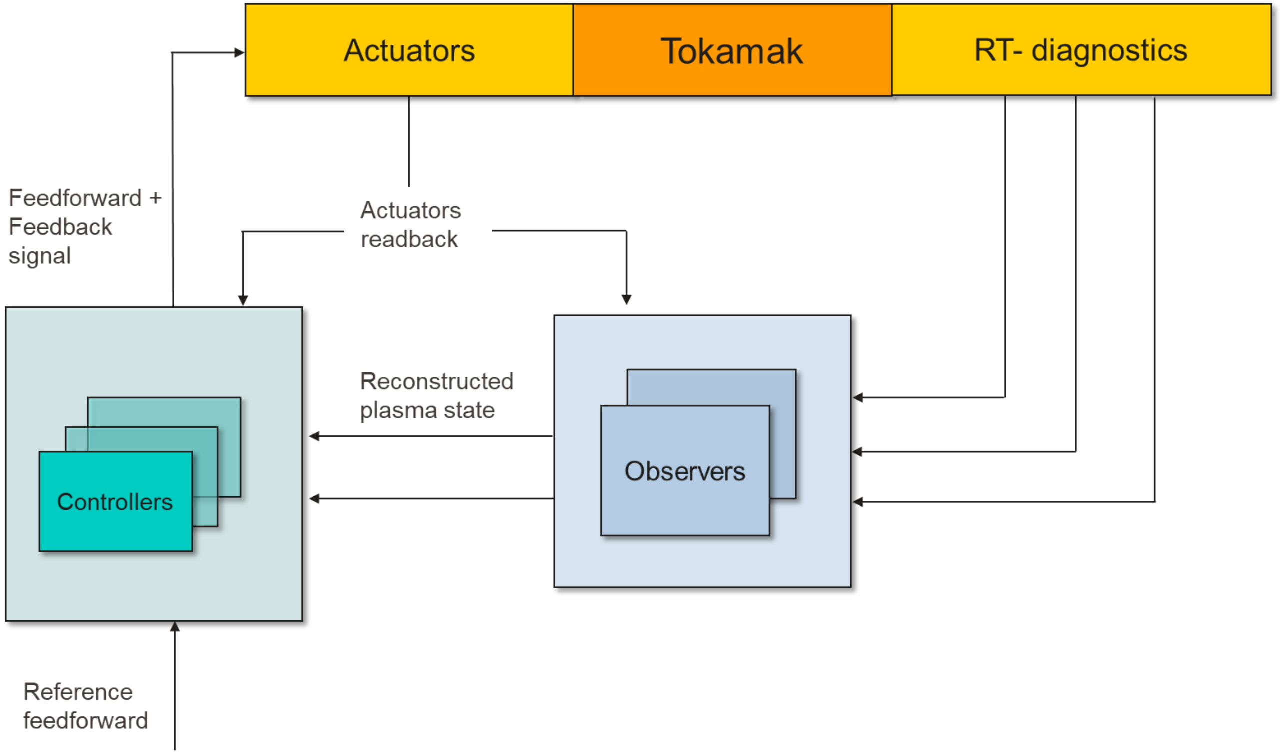

Shot 83394:

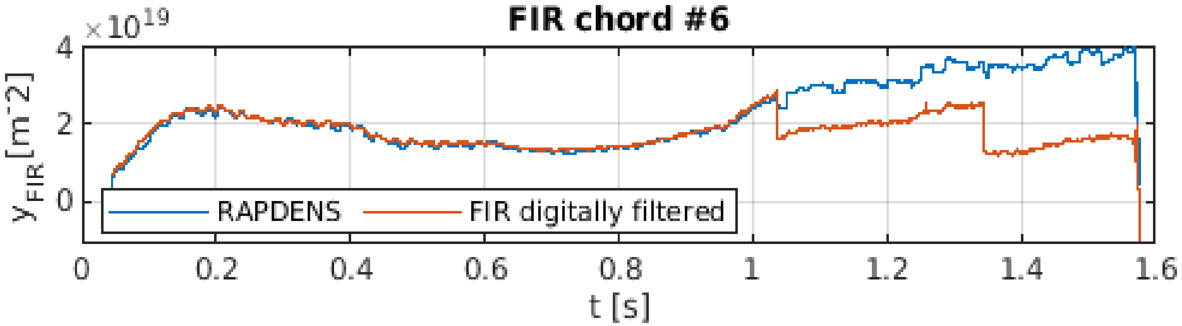

RAPDENS control-oriented model
Plasma electron density

RAPDENS multirate ne profile observer (RT-FIR + RT-TS)

- Multirate electron density observer [9] at 1 kHz, based on Extended Kalman Filter algorithm.

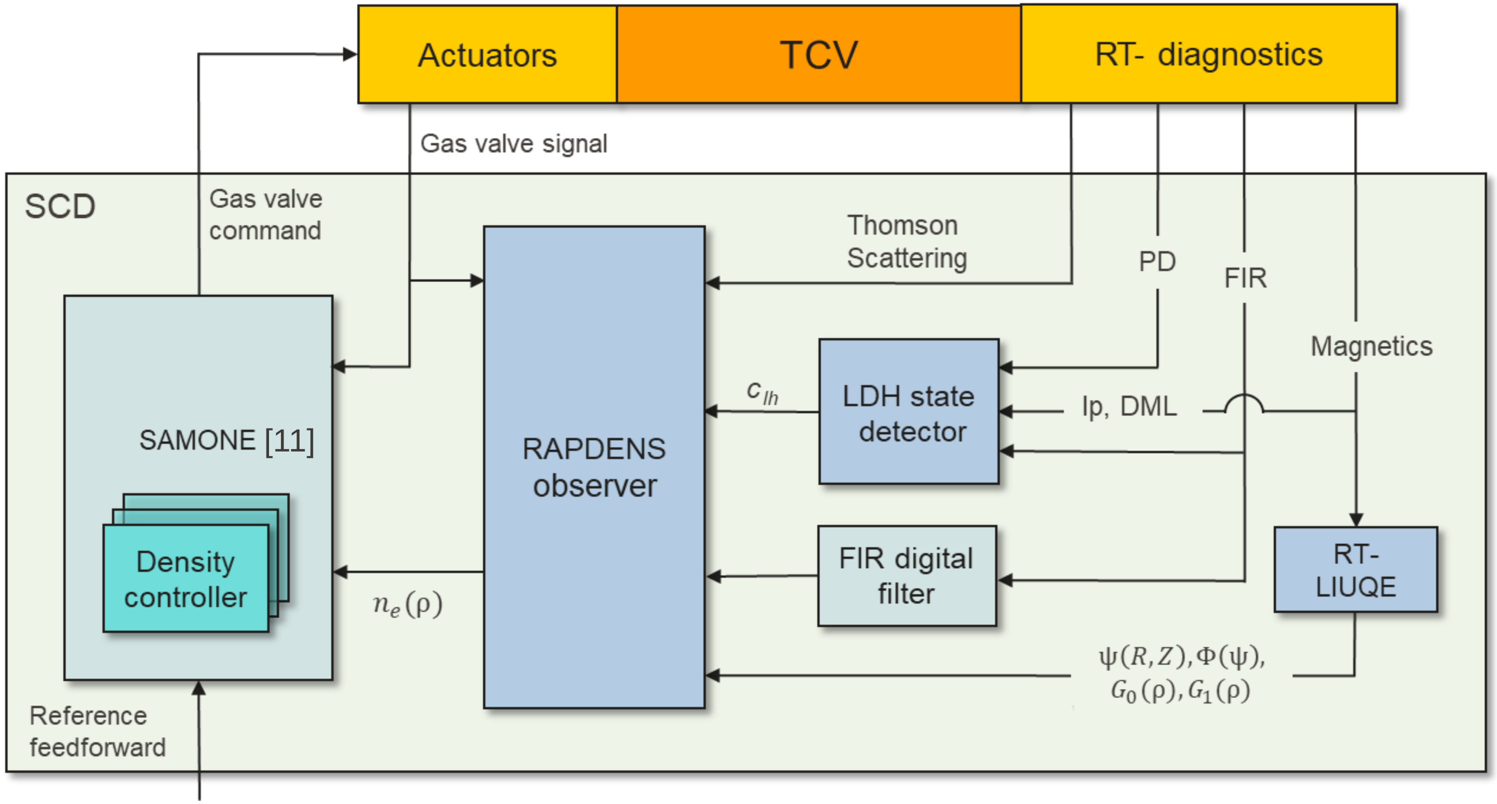

- **Inputs to the observer:**
  - RT-TS: 60 Hz.
  - RT-FIR digitally filtered: 10 kHz.
  - Plasma confinement state [10] (L/H-mode), 1 kHz.
  - Magnetic equilibrium RT-LIUQE, 1 kHz.
- **SAMONE actuator manager [11]**
  - PI density controller, feedback to gas valve.

[9] F. Pastore et al., Fus.Eng.Des vol.192, p.113615, doi:10.1016/j.fusengdes.2023.113615, 2023.
[10] G. Marceca et al., 47th EPS Conference on Plasma Physics: virtual conference, June 21-25.
[11] N.M.T. Vu et al., IEEE Transactions On Nuclear Science 68, doi:10.1109/TNS.2021.3084410, 2021.

RAPDENS multirate observer scheme

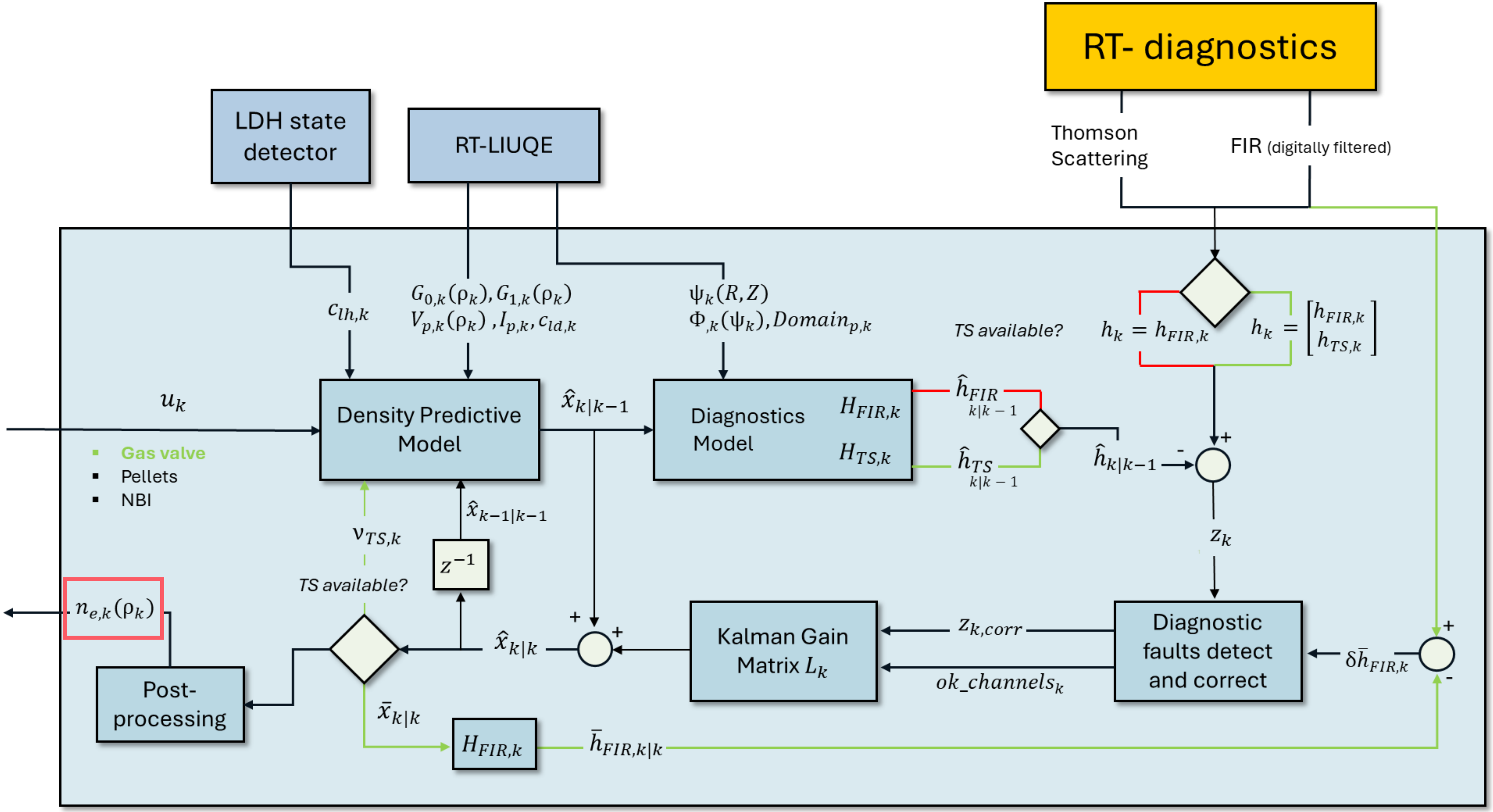

RAPDENS control-oriented model
Plasma electron density

Francesco Pastore

Example: H-to-L back transition for a TCV shot

- Transient H-mode plasma with strong off-axis ECCD + NBI-1.
- Back-transition of n_e reconstructed in detail at 1 kHz.

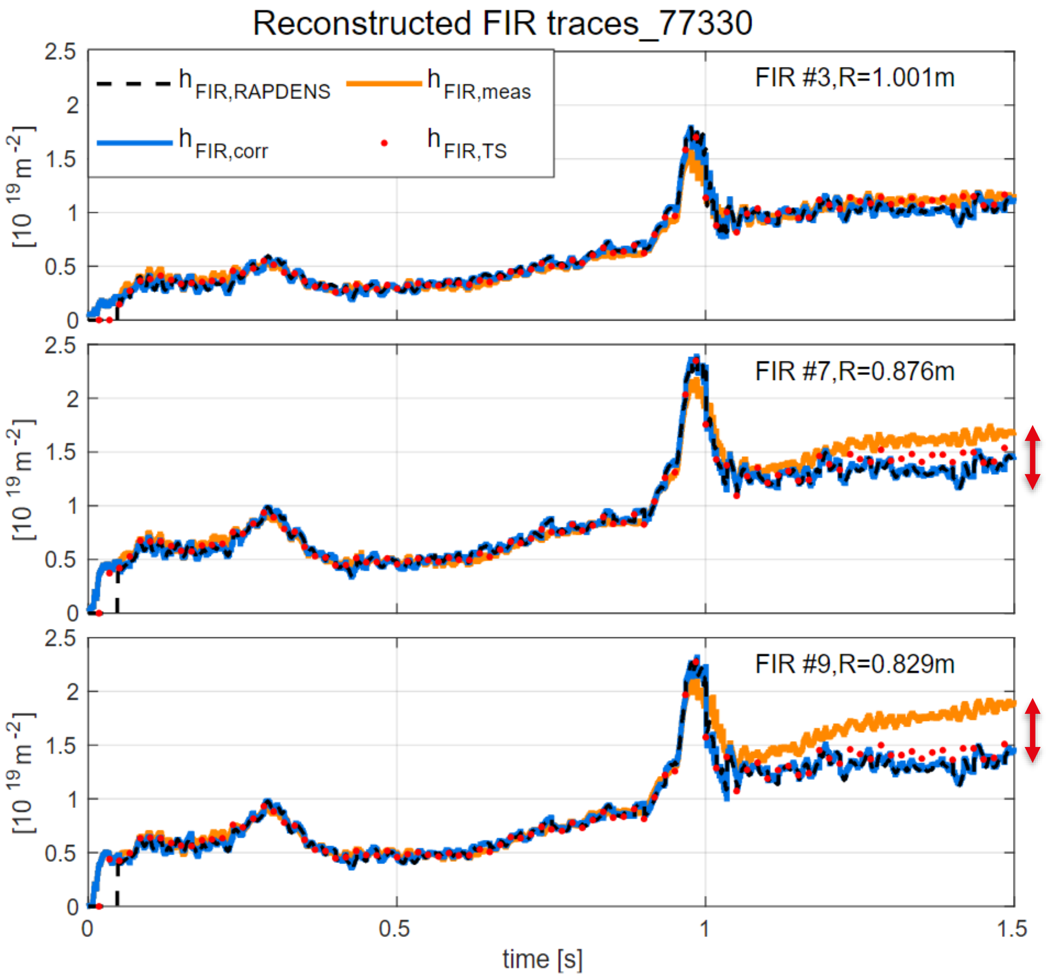

SOL density non-negligible after back-transition

Example: H-to-L back transition for a TCV shot

- Transient H-mode plasma with strong off-axis ECCD + NBI-1.
- Back-transition from H-to-L reconstructed at 1 kHz.

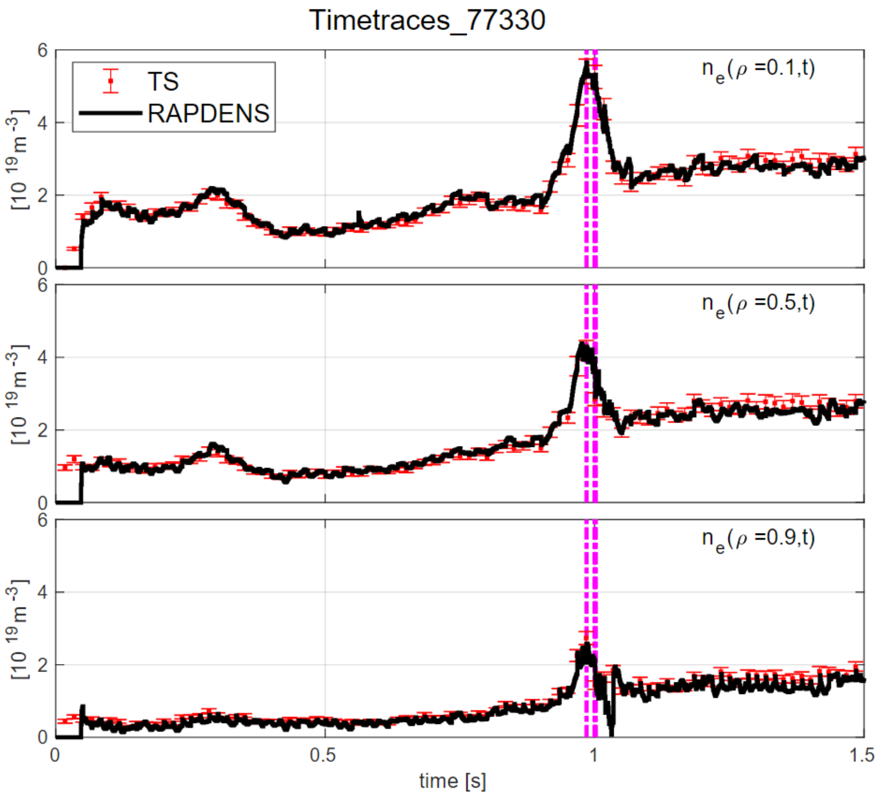

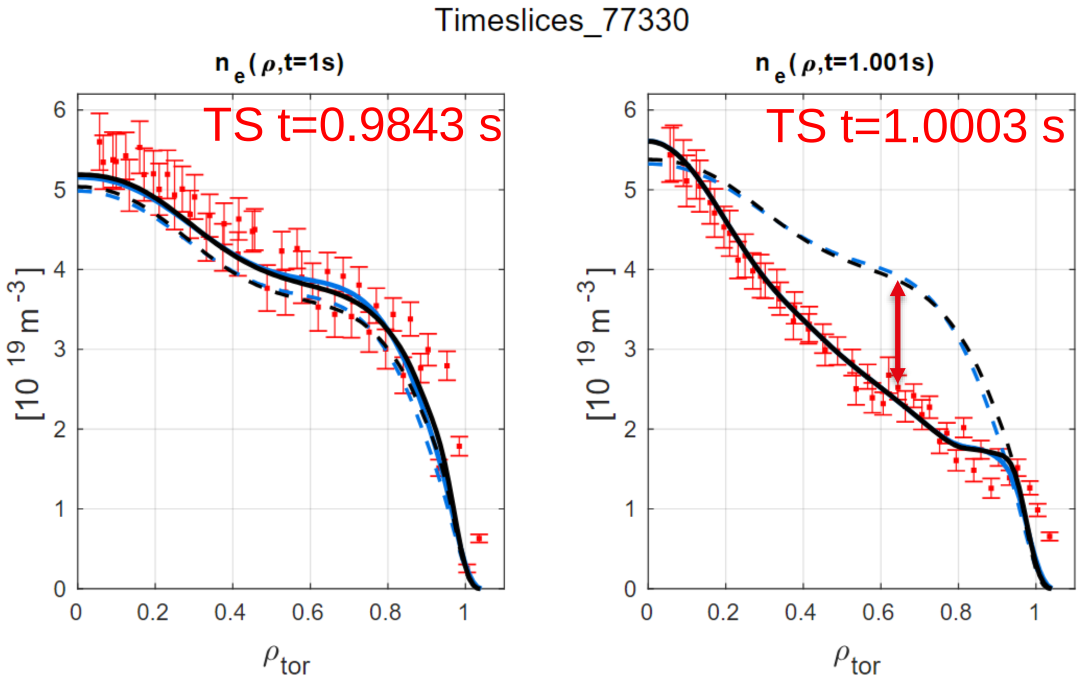

Example: H-to-L back transition for a TCV shot

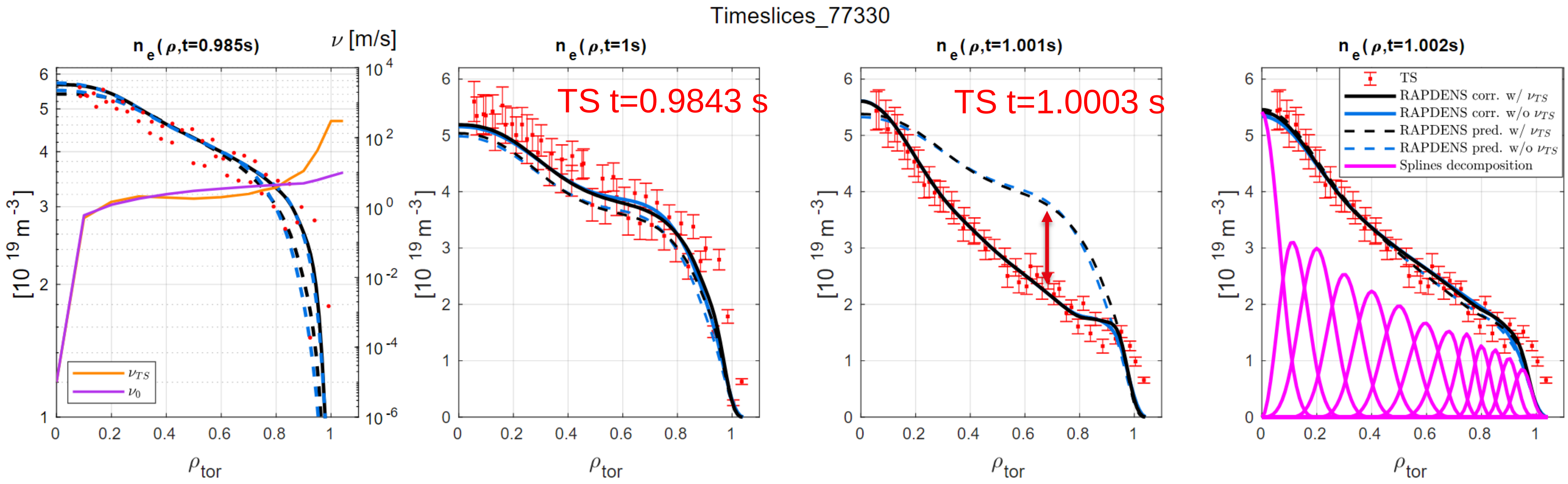

TS t=0.9843 s

TS t=1.0003 s

- Estimated υ_{TS} exhibits stronger gradient at the edge, improving its reconstruction in the predictive step (black dashed profile).
- The EKF deployed algorithm relies on low $R_{k,TS}$ covariance, strong correction step (solid profile).
- $n_e(\rho, t = 1.001\ s)$ coherent with TS profile, degradation of the density gradient captured correctly.
- Profile shape propagated for the time t=1.002 s with only FIR data.

Local density control for ECH discharges

- ECH directed in the plasma core, **control of ne(rho=0)** to ensure stable operation **below cut-off** (X2, 4e19 m^-3).
- Lack of the **pump-out effect** noticeable as ECH is turned off at t=1.50 s.
- Full absorption of ECH power achieved (post-shot TORAY).

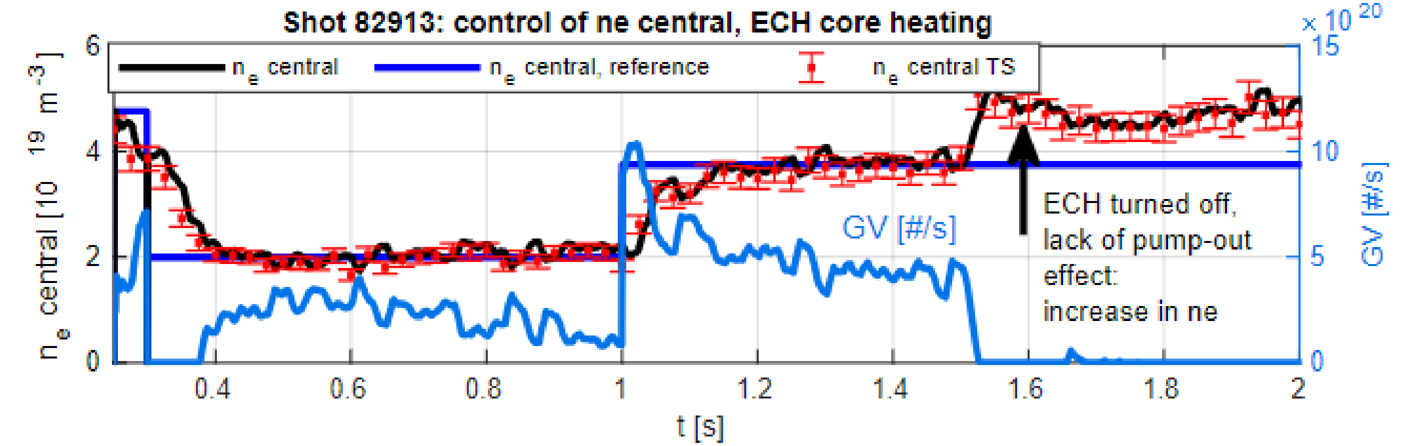
Shot 82913: control of ne central, ECH core heating

ECH turned off, lack of pump-out effect: increase in ne

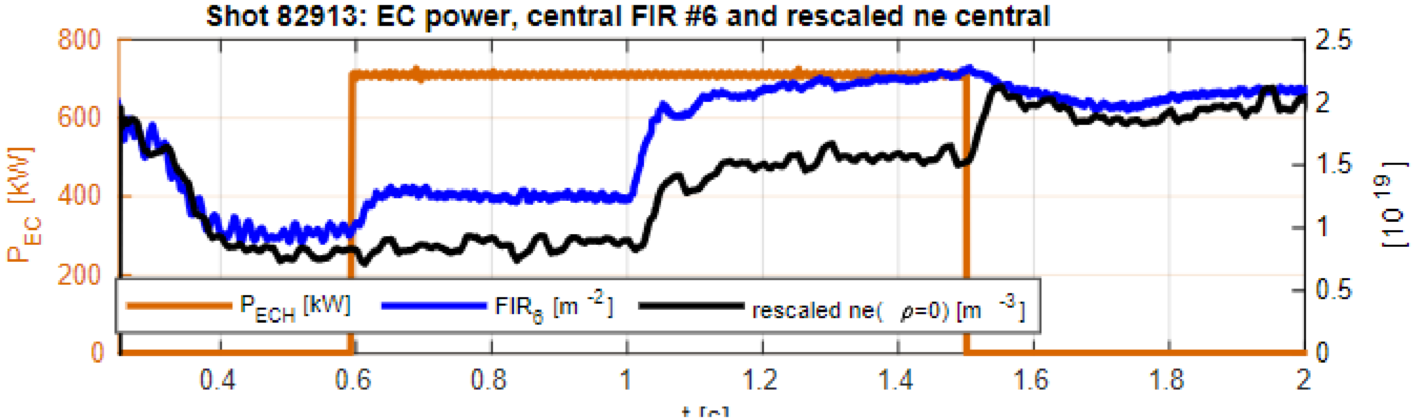
Shot 82913: EC power, central FIR #6 and rescaled ne central

Outlook and conclusion

Summary and lessons learned

- Model-based observers provide a valuable contribution in the reconstruction of the dynamical states.
- Many techniques can be adopted for the tuning of the observer gains:
  - Kalman Filter/ Extended Kalman Filter
- RAPDENS multirate observer integrated in TCV plasma control system, reconstruction comparable with post-shot TS.
- Local density control for ECH discharges, staying below cutoff
  - Improved reliability of density control with fringe jumps filtering.

Summary and lessons learned

- Model-based observers provide a valuable contribution in the reconstruction of the dynamical states.
- Many techniques can be adopted for the tuning of the observer gains:
  - Kalman Filter/ Extended Kalman Filter
- RAPDENS multirate observer integrated in TCV plasma control system, reconstruction comparable with post-shot TS.
- Local density control for ECH discharges, staying below cutoff
  - Improved reliability of density control with fringe jumps filtering.

THANKS FOR YOUR ATTENTION!
Questions?

Bibliography

- Lecture notes of “Multivariable control and coordination systems”, EPFL, EE-477, Denis Gillet, http://react.epfl.ch
- Optimal filtering, B. Anderson and J. Moore.
- T. C. Blanken et al., Fusion Engineering and Design 126, doi:10.1016/j.fusengdes.2017.11.006., 2018.
- T. O.S.J. Bosman et al., Fusion Engineering and Design 170, doi:10.1016/j.fusengdes.2021.112510., 2021.
- T. Ravensbergen, Phd Thesis (Research TU/e / Graduation TU/e), Mechanical Engineering., 2021.
- T.O.S.J Bosman et al., J. Phys. Commun. vol.5, p.115015, doi:10.1088/2399-6528/ac3547, 2021.
- F. Pastore et al., "Integration of a multi-rate electron density profile observer in the plasma control system of TCV", 49th EPS, July 2023.
- F. Pastore et al., “Model-based electron density estimation using multiple diagnostics on TCV”, doi: 10.1016/j.fusengdes.2023.113615, 2023.
- D. Kropackova et al., “Real-time density profile simulations on ASDEX Upgrade and the impact of the edge boundary condition ”, submitted to Fusion Engineering and Design
- S. Van Mulders “Combining measurements and dynamic models to improve estimation of plasma profiles and model parameters for ITER, by using an adaptive Extended Kalman Filter”, submitted to Nuclear Fusion.
- A. Pau et al., IAEA TM on Disruptions, Cadarache ITER, 2020.
- M. Kong et al., Plasma Phys. Control. Fusion 64 044008, doi: 10.1088/1361-6587/ac48be, 2022.
- F. Carpanese et al., Nucl. Fusion 60 066020, doi:10.1088/1741-4326/ab81ac, 2020.
- G. Marceca et al., 47th EPS Conference on Plasma Physics: virtual conference, June 21-25.
- N.M.T. Vu et al., IEEE Transactions On Nuclear Science 68, doi:10.1109/TNS.2021.3084410, 2021.

Backup

Concept of observability: derivation

Objective:
Compute $\boldsymbol{x}_0$ with:

- a set of measurements $\{\boldsymbol{y}_0, \boldsymbol{y}_1, \dots, \boldsymbol{y}_{k-1}\}$
- a set of inputs $\{\boldsymbol{u}_0, \boldsymbol{u}_1, \dots, \boldsymbol{u}_{k-1}\}$
- knowledge of the system (A, B, C, D)

Starting point: solution of the discrete state-space representation of:

$$\begin{cases} \boldsymbol{x}_{k+1} = A\boldsymbol{x}_k + B\boldsymbol{u}_k \\ \boldsymbol{y}_k = C\boldsymbol{x}_k + D\boldsymbol{u}_k \end{cases}$$

$$\boldsymbol{x}_1 = A\boldsymbol{x}_0 + B\boldsymbol{u}_0$$

$$\boldsymbol{x}_2 = A\boldsymbol{x}_1 + B\boldsymbol{u}_1$$

$$\boldsymbol{x}_2 = A[A\boldsymbol{x}_0 + B\boldsymbol{u}_0] + B\boldsymbol{u}_1$$

$$\boldsymbol{x}_2 = A^2\boldsymbol{x}_0 + AB\boldsymbol{u}_0 + B\boldsymbol{u}_1$$

$$\dots$$

$$\boxed{\boldsymbol{x}_k = A^k\boldsymbol{x}_0 + \sum_{i=0}^{k-1} A^{k-1-i}B\boldsymbol{u}_i}$$

Closed solution of discrete difference equations:

$$\boldsymbol{x}_k = A^k\boldsymbol{x}_0 + \sum_{i=0}^{k-1} A^{k-1-i}B\boldsymbol{u}_i$$

- Dependence on initial condition $\boldsymbol{x}_0$
- Inputs $\{\boldsymbol{u}_0, \boldsymbol{u}_1, \dots, \boldsymbol{u}_{k-1}\}$

Measurements equation applied to the closed solution:

$$\boldsymbol{y}_k = C\boldsymbol{x}_k + D\boldsymbol{u}_k$$

$$\boldsymbol{y}_k = CA^k\boldsymbol{x}_0 + \sum_{i=0}^{k-1} CA^{k-1-i}B\boldsymbol{u}_i + D\boldsymbol{u}_k$$

Definition: modified measurement $\boldsymbol{Y}_k$:

$$\boldsymbol{Y}_k = \boldsymbol{y}_k - \sum_{i=0}^{k-1} CA^{k-1-i}B\boldsymbol{u}_i - D\boldsymbol{u}_k$$

Concept of observability: derivation

- One ends up with the following relation:

$$\boldsymbol{Y}_k = CA^k \boldsymbol{x}_0 \qquad [1]$$

- $\boldsymbol{x}_0$ has n elements, so one has to write n equations using [1].

- $$\begin{cases} \boldsymbol{Y}_0 = C\boldsymbol{x}_0 \\ \boldsymbol{Y}_1 = CA\boldsymbol{x}_0 \\ \dots \\ \boldsymbol{Y}_{n-1} = CA^{n-1}\boldsymbol{x}_0 \end{cases} \Rightarrow \begin{bmatrix} \boldsymbol{Y}_0 \\ \boldsymbol{Y}_1 \\ \dots \\ \boldsymbol{Y}_{n-1} \end{bmatrix} = \begin{bmatrix} C \\ CA \\ \dots \\ CA^{n-1} \end{bmatrix} \boldsymbol{x}_0$$

<ins>Observability matrix:</ins>

$$\mathcal{O} = \begin{bmatrix} C \\ CA \\ \dots \\ CA^{n-1} \end{bmatrix}$$

if the $rank(\mathcal{O}) = n$, we ensure uniqueness of the solution for $\boldsymbol{x}_0$.

q.e.d.

Remark: Adding a number of equations to $\mathcal{O}$ s.t. $\mathrm{N} > n$ doesn't change the rank of $\mathcal{O}$.
(Cayley–Hamilton theorem, $A^m = \alpha_0 I + \alpha_1 A + \alpha_2 A^2 + \dots + \alpha_{n-1} A^{n-1}, m > n$, size of matrix A: $[n, n]$).

Observability: example of the 1D motion of a vehicle

Discrete state-space representation, with sampling time Δt:

$$\begin{bmatrix} r_{k+1} \\ v_{k+1} \end{bmatrix} = \begin{bmatrix} 1 & \Delta t \\ 0 & 1 \end{bmatrix} \begin{bmatrix} r_k \\ v_k \end{bmatrix} + \begin{bmatrix} \Delta t^2/2m \\ \Delta t/m \end{bmatrix} F_k$$

$$\boldsymbol{y}_k = \begin{bmatrix} 0 & 1 \\ 0 & 0 \end{bmatrix} \begin{bmatrix} r_k \\ v_k \end{bmatrix} + \begin{bmatrix} 0 \\ 1/m \end{bmatrix} F_k$$

- Velocity (via GPS)
- Acceleration (via accelerometer)

Observability matrix:

$$\mathcal{O} = \begin{bmatrix} C \\ CA \end{bmatrix}$$

$$\mathcal{O} = \begin{bmatrix} C \\ CA \end{bmatrix} = \begin{bmatrix} 0 & 1 \\ 0 & 0 \\ 0 & 1 \\ 0 & 0 \end{bmatrix}$$

The system is **not observable**…

… this makes sense, since with velocity or acceleration information one cannot reconstruct the position initial condition.

Vice-versa, the position measurements are sufficient to reconstruct the position and velocity states.

Conclusion:

- Well-thought design of the measuring system (C matrix) enables the reconstruction of the state $\boldsymbol{x}_k$.
- Many measurements can ensure redundancy in the state observation, in case of failure.

Let's try to apply the previous concepts to design a closed-loop observer for the vehicle example.

Kalman filter: example of the 1D motion of a vehicle

Let's adopt the Kalman filter to tackle the issues related with:

- The mismatching initial condition
- The disturbance in the input force

Tuning of the observer gains:

$$L = \begin{bmatrix} L_1 & L_2 \\ L_3 & L_4 \end{bmatrix} \qquad C = \begin{bmatrix} 1 & 0 \\ 0 & 0 \end{bmatrix} \qquad LC = \begin{bmatrix} L_1 & 0 \\ L_3 & 0 \end{bmatrix}$$

Only the coefficients L_1 and L_3 play a role in modifying the poles of the estimation equation response.

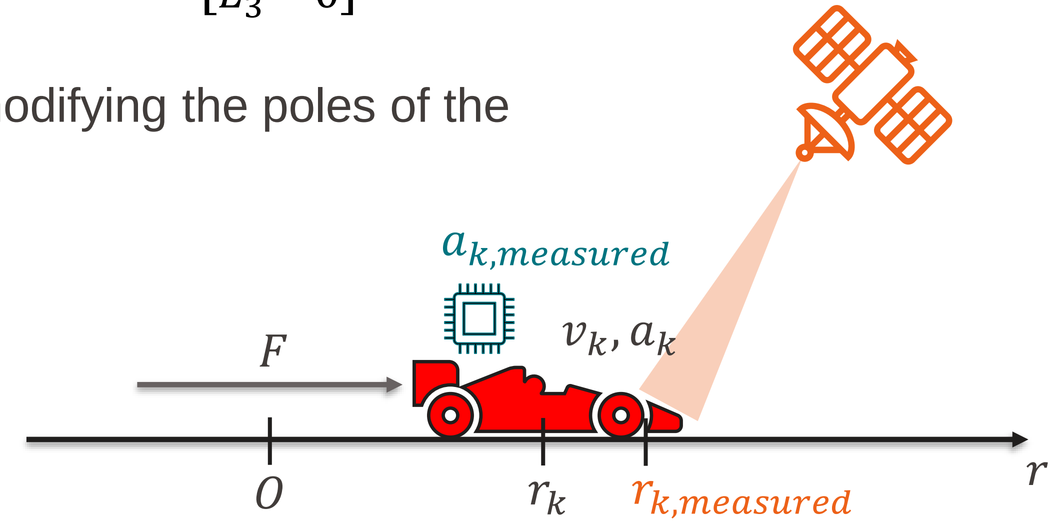

RAPDENS code

- **RAPDENS: Rapid Plasma DENsity Simulator**
  - Computation of 1D flux-surface averaged electron plasma density profile.
  - Coupled with 0D time evolution of:
    - Vacuum neutrals inventory.
    - Wall neutrals inventory.
  - Observer based on Extended Kalman Filter algorithm (EKF)

- Coded in Matlab/Simulink for RT application in Plasma Control Systems.
  - First applications on TCV and AUG [4].
  - Currently deployed on AUG for electron density reconstruction and control via gas valve and pellet-fuelling [5]
  - ITER-based scenario controllers and simulations [6, 7]
  - Integration and employment on TCV [8,9], integrating FIR and TS in the Kalman filter procedure.

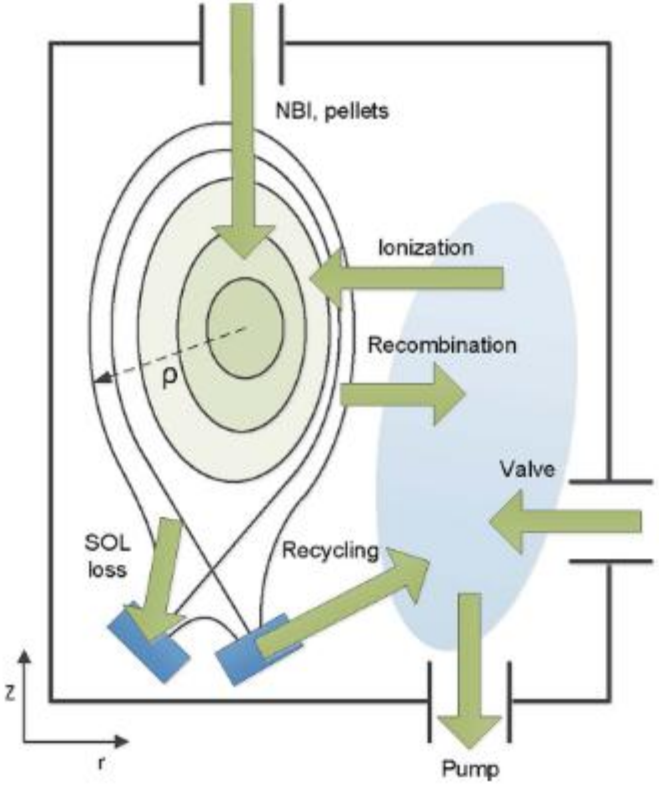

T. C. Blanken et al., Fusion Engineering and Design 126, doi:10.1016/j.fusengdes.2017.11.006., 2018.

[4] T. C. Blanken et al., Fusion Engineering and Design 126, doi:10.1016/j.fusengdes.2017.11.006., 2018.
[5] T. O.S.J. Bosman et al., Fusion Engineering and Design 170, doi:10.1016/j.fusengdes.2021.112510., 2021.
[6] T. Ravensbergen, Phd Thesis (Research TU/e / Graduation TU/e), Mechanical Engineering., 2021.
[7] T.O.S.J Bosman et al., J. Phys. Commun. vol.5, p.115015, doi:10.1088/2399-6528/ac3547, 2021.
[8] F. Pastore et al., "Integration of a multi-rate electron density profile observer in the plasma control system of TCV", 49th EPS, July 2023.
[9] F. Pastore et al., "Model-based electron density estimation using multiple diagnostics on TCV", doi: 10.1016/j.fusengdes.2023.113615, 2023.

RAPDENS predictive model

- **RAPDENS model equations**

Flux-surface averaged n_e equation:

$$\frac{\partial}{\partial t}(n_e V') - \frac{\partial}{\partial \rho}\left[V'\left(G_1 D \frac{\partial n_e}{\partial \rho} + G_0 \nu n_e\right)\right] = SV' \qquad (1)$$

Diffusion coeff. Drift velocity

Vacuum inventory equation:

$$\frac{dN_v}{dt} = \Gamma_{rec} - \Gamma_{iz} + \Gamma|_{\rho=\rho_e} + \Gamma_{recy.} + \Gamma_{valve} - \Gamma_{pump} \qquad (2)$$

Wall inventory equation:

$$\frac{dN_w}{dt} = \Gamma_{SOL\rightarrow wall} - \Gamma_{recy.} \qquad (3)$$

Sources/sinks of electrons:

$$S = S_{iz} - S_{rec} - S_{SOL\rightarrow wall} + S_{NB} + S_{pellets} \qquad (4)$$

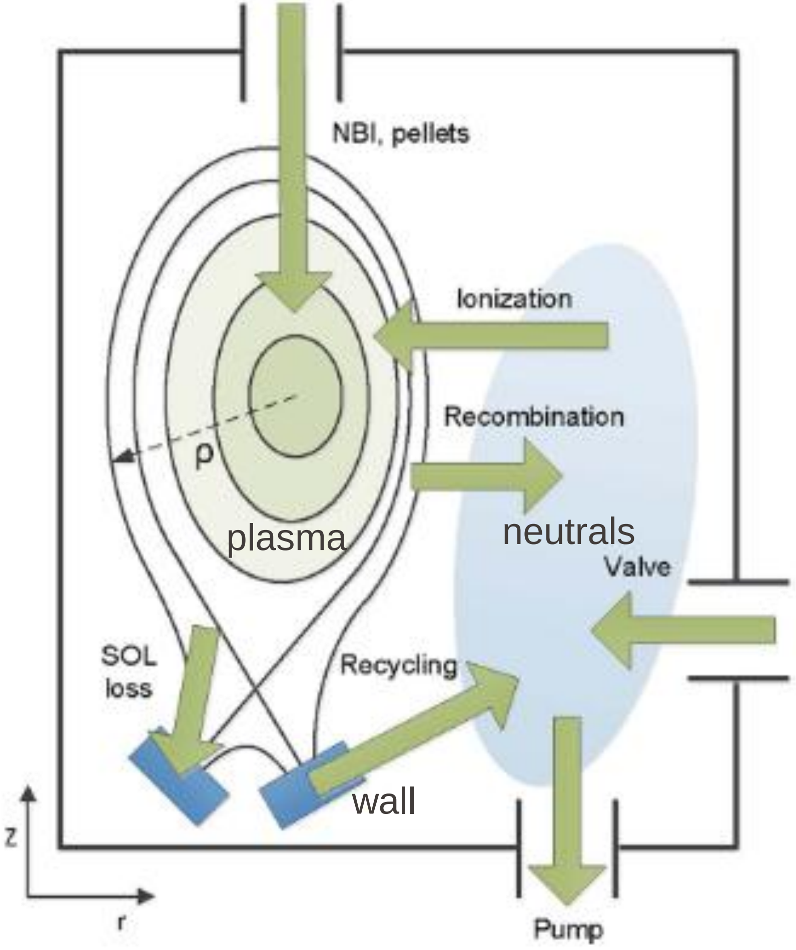

T. C. Blanken et al., Fusion Engineering and Design 126, doi:10.1016/j.fusengdes.2017.11.006., 2018.

Local density control for ECH discharges

- Traditional control using central FIR chord #6?
- Comparison between:
  - FIR signal #6
  - n_e(ρ=0) rescaled (at t=0.20 s)

- **Lack of proportionality in the ECH phase**, due to:
  - profile flattening
  - pick-up of density in the SOL

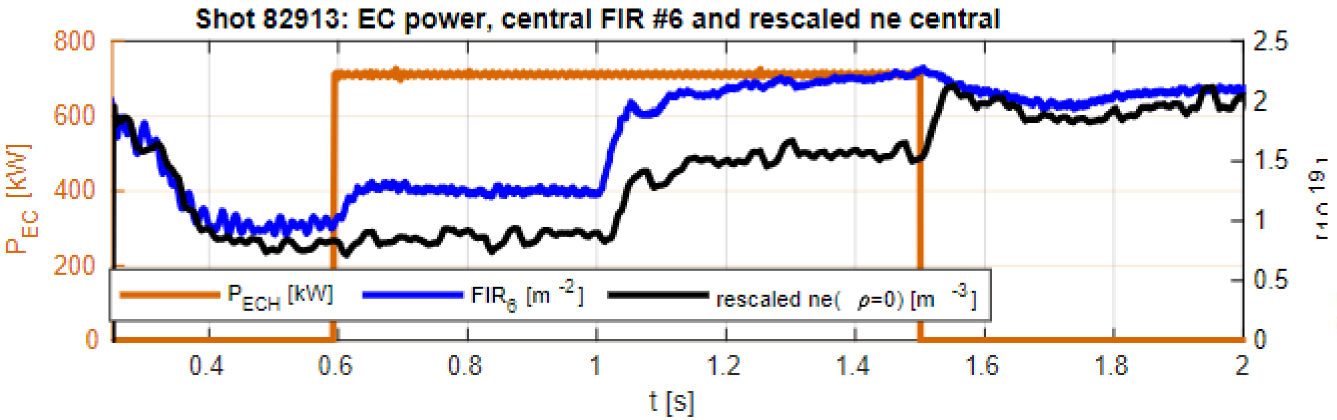

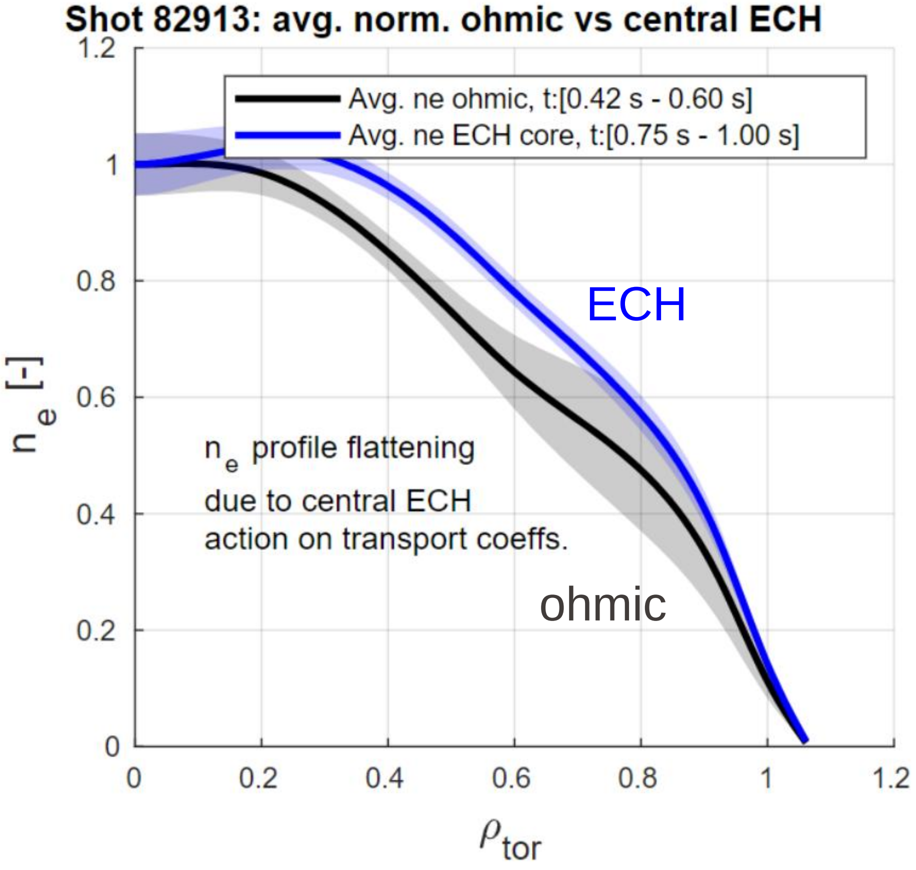

Luenberger observer: example of the 1D motion of a vehicle

Let’s adopt the Luenberger observer to tackle the issues related with:

- The mismatching initial condition

Tuning of the observer gains:

$$L = \begin{bmatrix} L_1 & L_2 \\ L_3 & L_4 \end{bmatrix} \qquad C = \begin{bmatrix} 1 & 0 \\ 0 & 0 \end{bmatrix} \qquad LC = \begin{bmatrix} L_1 & 0 \\ L_3 & 0 \end{bmatrix}$$

Only the coefficients L_1 and L_3 play a role in modifying the poles of the estimation equation response.

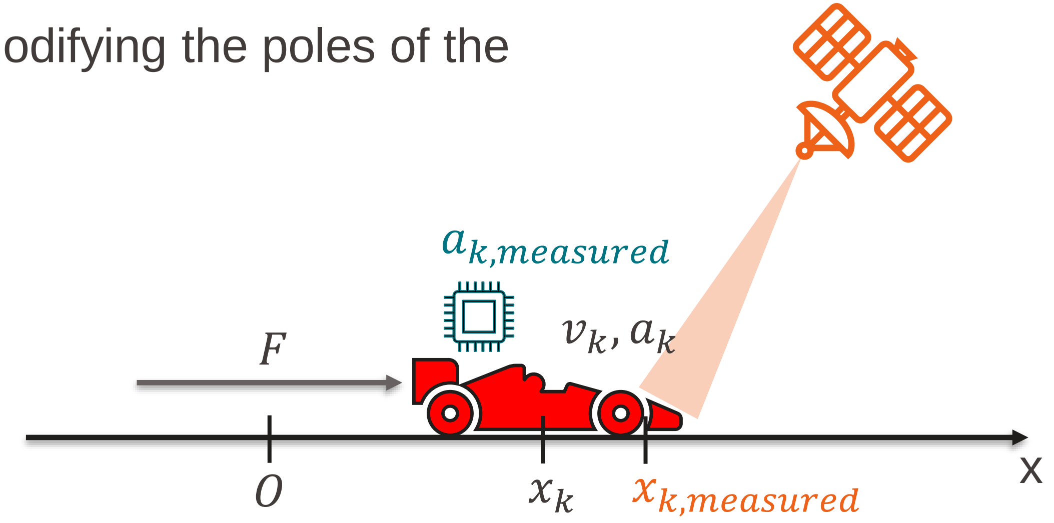

Luenberger observer: example of the 1D motion of a vehicle

Let's study the impact of L_1 and L_3 on the eigenvalues of $A - LC$:

$$\lambda_{1,2} = \frac{(2-L_1)\pm L_1\sqrt{1-4L_3/L_1^2}}{2}$$

$$L_1 = 0.01$$
$$L_3 = 0.02\ s^{-1}$$

System stabilized!

$$\lambda_1 = 0.9928\ s^{-1}$$
$$\lambda_2 = 0.9972\ s^{-1}$$

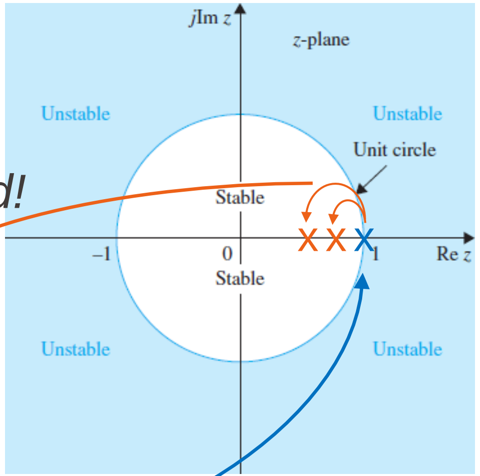

$$\lambda_{1,2} = eig(A) = [1,1]$$

Unstable open loop system

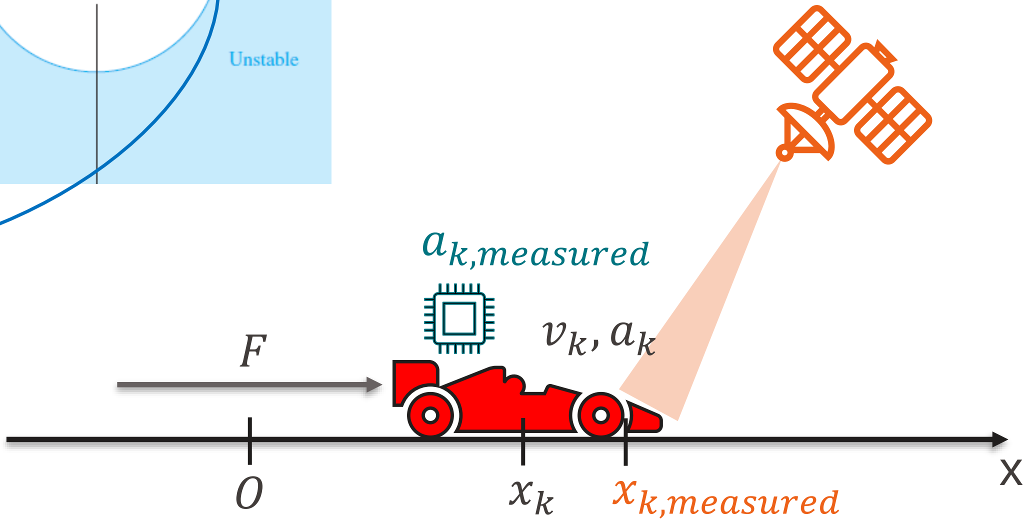

Closed-loop model-based state estimation: mismatch on initial conditions

Effect of mismatch between $\hat{\boldsymbol{x}}_0$ and $\boldsymbol{x}_0$:

Mismatch on initial condition for the velocity:

- $\boldsymbol{x}_0 = \begin{bmatrix} r_0 \\ v_0 \end{bmatrix} = \begin{bmatrix} 0 \\ 0 \end{bmatrix}$, $\hat{\boldsymbol{x}}_0 = \begin{bmatrix} \hat{r}_0 \\ \hat{v}_0 \end{bmatrix} = \begin{bmatrix} 0 \\ 1 \end{bmatrix}$
- $m = 1, F_k = 1 \cdot step(t).$
- Introduction of noisy measurement on position: $y_r = r_{plant} + N(0,1)$
- *Let's start with zero gain to the observer matrix…*
- *Exactly same behavior recovered, Observer behaves as the open loop* *Model*

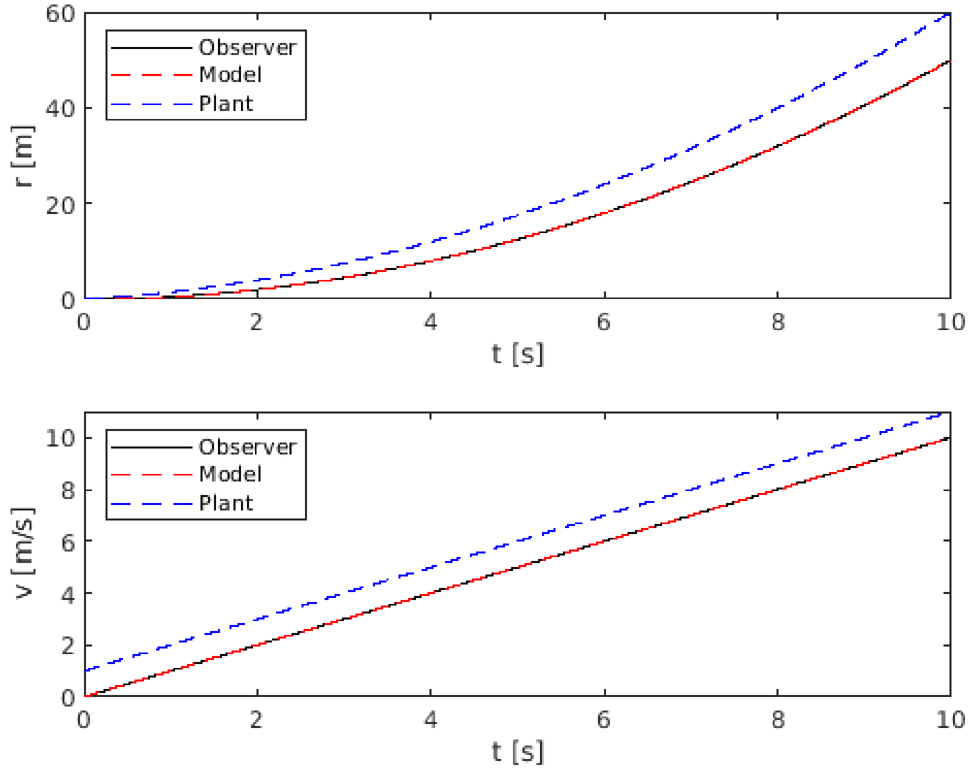

Closed-loop model-based state estimation: mismatch on initial conditions

Effect of mismatch between $\hat{\boldsymbol{x}}_0$ and $\boldsymbol{x}_0$:

Mismatch on initial condition for the velocity:

- $\boldsymbol{x}_0 = \begin{bmatrix} r_0 \\ v_0 \end{bmatrix} = \begin{bmatrix} 0 \\ 0 \end{bmatrix}, \ \hat{\boldsymbol{x}}_0 = \begin{bmatrix} \hat{r}_0 \\ \hat{v}_0 \end{bmatrix} = \begin{bmatrix} 0 \\ 1 \end{bmatrix}$
- $m = 1, F_k = 1 \cdot step(t).$
- Introduction of noisy measurement on position: $y_r = r_{plant} + N(0{,}1)$
- Selection of the Observer gains:

$$L_1 = 0.01$$
$$L_3 = 0.02\ s^{-1}$$

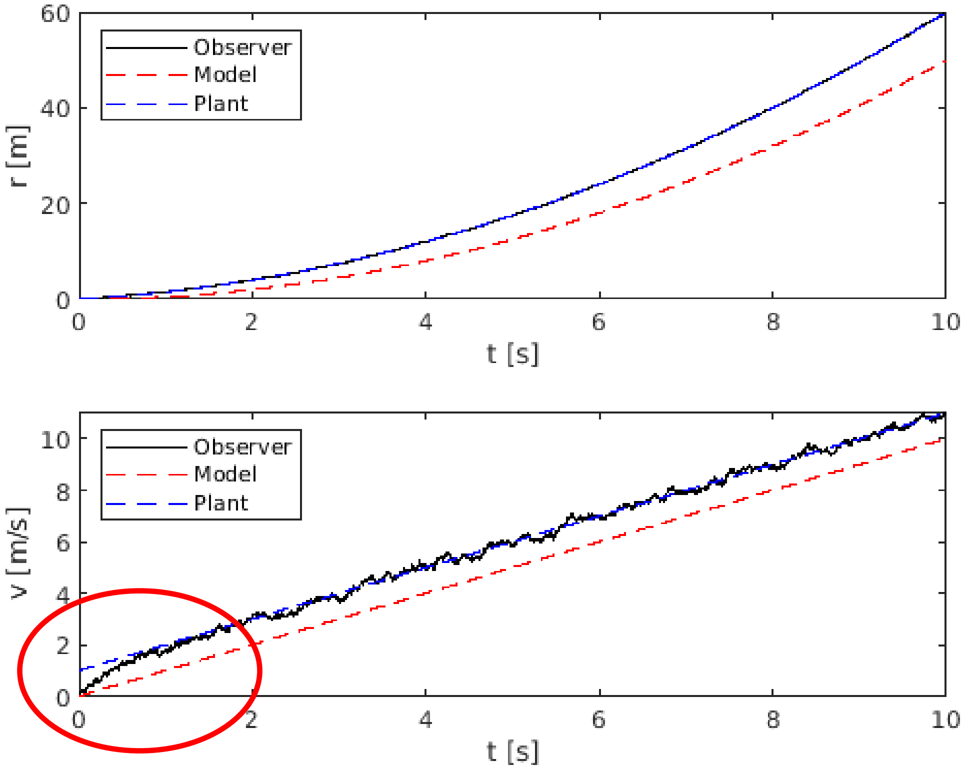

Closed-loop model-based state estimation: mismatch on initial conditions

Effect of mismatch between $\hat{\boldsymbol{x}}_0$ and $\boldsymbol{x}_0$:

- The observer effectively brings the estimation error $\boldsymbol{e}_k$ to zero!
- It also effectively filter measurement noise in the estimation of the position r.

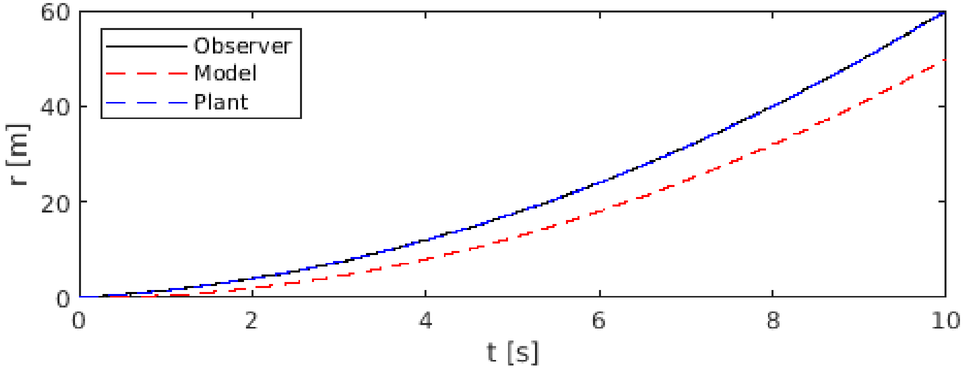

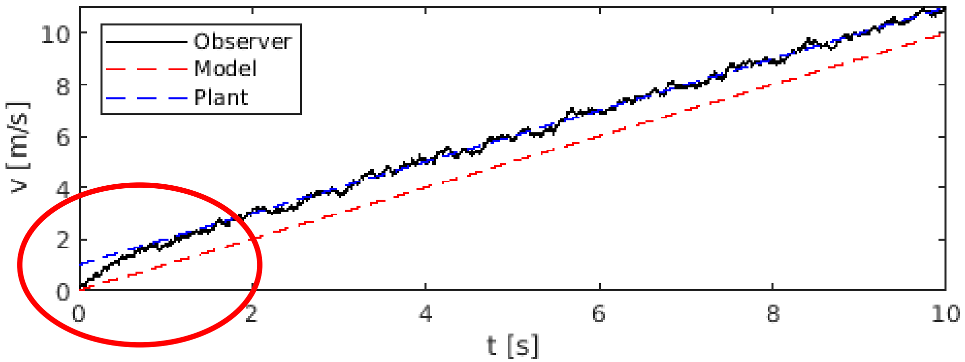

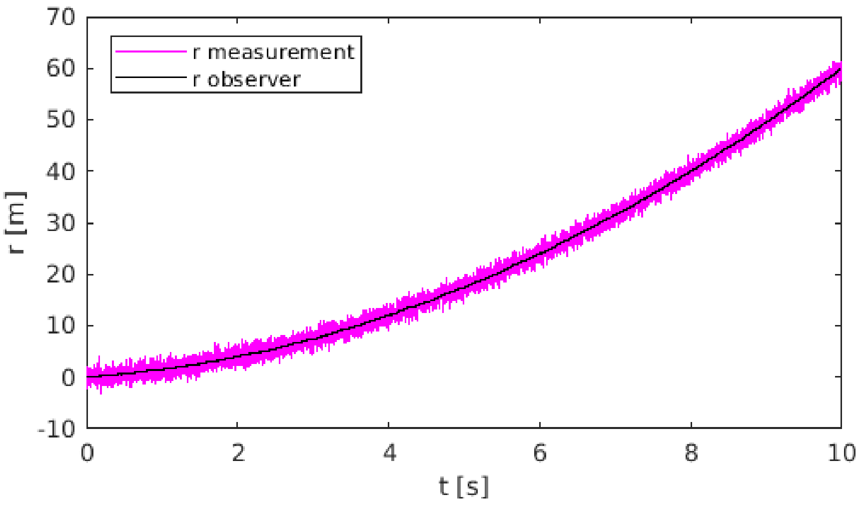

Closed-loop model-based state estimation

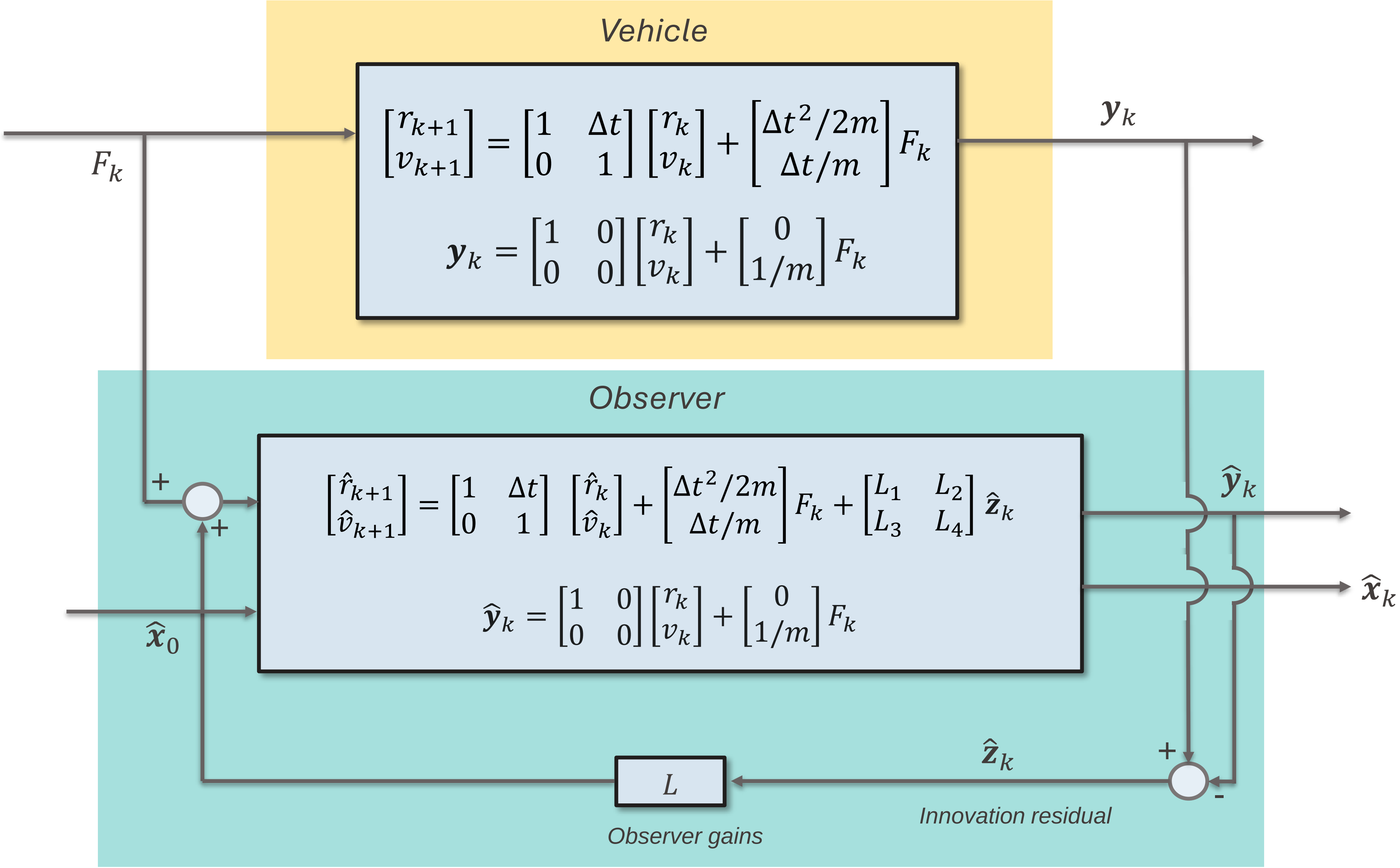

Vehicle

$$\begin{bmatrix} r_{k+1} \\ v_{k+1} \end{bmatrix} = \begin{bmatrix} 1 & \Delta t \\ 0 & 1 \end{bmatrix} \begin{bmatrix} r_k \\ v_k \end{bmatrix} + \begin{bmatrix} \Delta t^2/2m \\ \Delta t/m \end{bmatrix} F_k$$

$$\boldsymbol{y}_k = \begin{bmatrix} 1 & 0 \\ 0 & 0 \end{bmatrix} \begin{bmatrix} r_k \\ v_k \end{bmatrix} + \begin{bmatrix} 0 \\ 1/m \end{bmatrix} F_k$$

F_k

$\boldsymbol{y}_k$

Observer

$$\begin{bmatrix} \hat{r}_{k+1} \\ \hat{v}_{k+1} \end{bmatrix} = \begin{bmatrix} 1 & \Delta t \\ 0 & 1 \end{bmatrix} \begin{bmatrix} \hat{r}_k \\ \hat{v}_k \end{bmatrix} + \begin{bmatrix} \Delta t^2/2m \\ \Delta t/m \end{bmatrix} F_k + \begin{bmatrix} L_1 & L_2 \\ L_3 & L_4 \end{bmatrix} \hat{\boldsymbol{z}}_k$$

$$\hat{\boldsymbol{y}}_k = \begin{bmatrix} 1 & 0 \\ 0 & 0 \end{bmatrix} \begin{bmatrix} r_k \\ v_k \end{bmatrix} + \begin{bmatrix} 0 \\ 1/m \end{bmatrix} F_k$$

+

+

$\hat{\boldsymbol{x}}_0$

$\hat{\boldsymbol{y}}_k$

$\hat{\boldsymbol{x}}_k$

$\hat{\boldsymbol{z}}_k$

+

-

L

Observer gains

Innovation residual

State space representation of RAPDENS model

- **Space discret.**: cubic B-splines with finite support
- **FEM weak formulation**

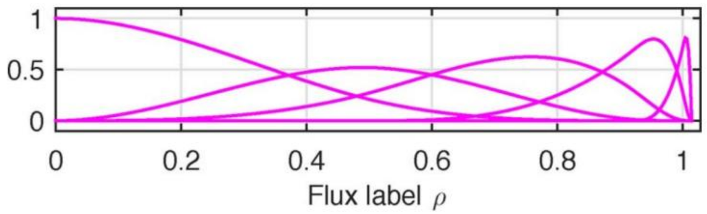

$$n_e(\rho,\, t) = \sum_{\alpha=1}^{m} \Lambda_\alpha(\rho) b_\alpha(t)$$

$$x(t) = \begin{bmatrix} b(t) \\ N_\mathrm{w}(t) \\ N_\mathrm{v}(t) \end{bmatrix} \qquad u(t) = \begin{bmatrix} \Gamma_\mathrm{valve}(t) \\ \Gamma_\mathrm{NBI}(t) \\ \Gamma_\mathrm{pellet}(t) \end{bmatrix}$$

- **Time discret.**: trapezoidal method

$$\frac{x_{k+1} - x_k}{T_s} = (1 - \Theta)(A(p_k) + f(p_k, x_k) + Bu_k) + \Theta(A(p_{k+1}) + f(p_{k+1}, x_{k+1}) + Bu_{k+1})$$

$$\Rightarrow \boxed{x_k = f_\mathrm{d}(p_{k-1},\, x_{k-1}) + B_\mathrm{d}(p_{k-1})u_{k-1}}$$

Discrete state space representation of the predictive model

$$p = [\underbrace{c_\mathrm{D}}_{\text{Limited/ diverted}} \quad \underbrace{c_\mathrm{H}}_{\text{L/H mode}} \quad T_\mathrm{e,b} \quad I_\mathrm{p} \quad \underbrace{V' \quad G_1 \quad G_0 \quad \Omega}_{\text{Geom. quantities}}]$$

Observer for electron density reconstruction

- Definition of the augmented state-space representation:

$$\boldsymbol{x}_{k+1|k} = \boxed{\boldsymbol{f}_d\left(\boldsymbol{x}_{k|k}, \boldsymbol{p}_k\right)} + \mathrm{B}_\varsigma \varsigma_k + \boxed{\mathrm{B}_d \boldsymbol{u}_k} + \boldsymbol{w}_k^x$$

Predictive model

$$\varsigma_{k+1|k} = \varsigma_{k|k} + \boldsymbol{w}_k^\varsigma$$

$$y_k = C(p_k)\boldsymbol{x}_{k+1|k} + \boldsymbol{v}_k$$

Observer for electron density reconstruction

- Definition of the augmented state-space representation:

$$\boldsymbol{x}_{k+1|k} = \boldsymbol{f}_d(\boldsymbol{x}_{k|k}, \boldsymbol{p}_k) + \boxed{\mathrm{B}_\varsigma \varsigma_k} + \mathrm{B}_d \boldsymbol{u}_k + \boldsymbol{w}_k^x$$

$$\boxed{\varsigma_{k+1|k}} = \varsigma_{k|k} + \boldsymbol{w}_k^\varsigma$$

$$y_k = C(p_k)\boldsymbol{x}_{k+1|k} + \boldsymbol{v}_k$$

Disturbances:
Actuators and/or modeling errors.
It acts as an integral term,
compensating for offsets

Observer for electron density reconstruction

- Definition of the augmented state-space representation:

$$\boldsymbol{x}_{k+1|k} = \boldsymbol{f}_d(\boldsymbol{x}_{k|k}, \boldsymbol{p}_k) + \mathrm{B}_\varsigma \varsigma_k + \mathrm{B}_d \boldsymbol{u}_k + \boldsymbol{w}_k^x$$

$$\varsigma_{k+1|k} = \varsigma_{k|k} + \boldsymbol{w}_k^\varsigma$$

$$\boxed{y_k = C(p_k)\boldsymbol{x}_{k+1|k} + \boldsymbol{v}_k}$$

Measurements equation

Observer for electron density reconstruction

- Zero-mean white noise added to prediction and measurement equation:

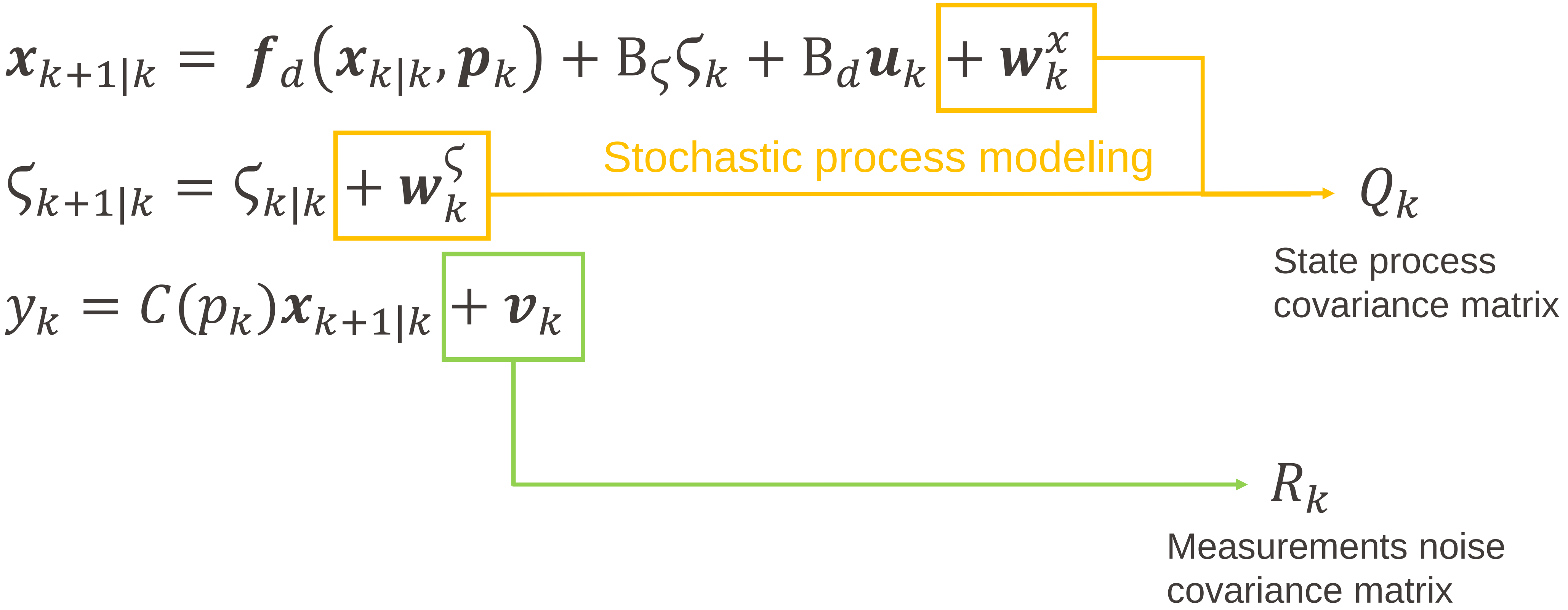

$$\boldsymbol{x}_{k+1|k} = \boldsymbol{f}_d(\boldsymbol{x}_{k|k}, \boldsymbol{p}_k) + \mathrm{B}_\varsigma \varsigma_k + \mathrm{B}_d \boldsymbol{u}_k \boxed{+ \boldsymbol{w}_k^x}$$

$$\varsigma_{k+1|k} = \varsigma_{k|k} \boxed{+ \boldsymbol{w}_k^\varsigma}$$

$$y_k = C(p_k)\boldsymbol{x}_{k+1|k} \boxed{+ \boldsymbol{v}_k}$$

Stochastic process modeling

Q_k

State process covariance matrix

R_k

Measurements noise covariance matrix

Estimation of the augmented state via EKF

- Predictive step: $\hat{\boldsymbol{x}}_{k+1|k} = \begin{bmatrix} \boldsymbol{f}_d\left(\boldsymbol{x}_{k|k}, \boldsymbol{p}_k\right) + \mathrm{B}_{\varsigma}\varsigma_{k|k} \\ \hat{\varsigma}_{k|k} \end{bmatrix} + G\boldsymbol{u}_k$ $\quad G = \begin{bmatrix} B_d \\ 0 \end{bmatrix}$

- Correction step: $\hat{\boldsymbol{x}}_{k+1|k+1} = \hat{\boldsymbol{x}}_{k+1|k} + L_k z_k$

Where L_k is the Extended Kalman Filter gain

Observer for electron density reconstruction

- Linearized dynamics for the state equation:

$$F_k = \begin{bmatrix} \left.\frac{\partial f_\mathrm{d}}{\partial x_k}\right|_{p_k, \hat{x}_{k|k}} & B_\zeta \\ 0 & I^{m\times m} \end{bmatrix} \quad G = \begin{bmatrix} B_\mathrm{d} \\ 0 \end{bmatrix}$$

$$H_k = [C(p_k) \;\; 0] \quad Q_k = \begin{bmatrix} Q_k^x & 0 \\ 0 & Q_k^\zeta \end{bmatrix}$$

- Covariance matrix for the prediction error of augmented state $\mathrm{E}((\mathrm{x}-))$:

$$P_{k+1|k} = F_k P_{k|k} F_k^T + Q_\mathrm{k}$$

- Innovation residual covariance matrix:

$$S_k = R_k + H_k P_{k+1|k} H_k^T$$

Extended Kalman filter gain:

$$L_k = P_{k+1|k} H_k^T S_k^{-1}$$

- Covariance matrix for the posterior error of augmented state:

$$P_{k+1|k+1} = (I - L_k H_k) P_{k+1|k}$$

RAPDENS observer scheme

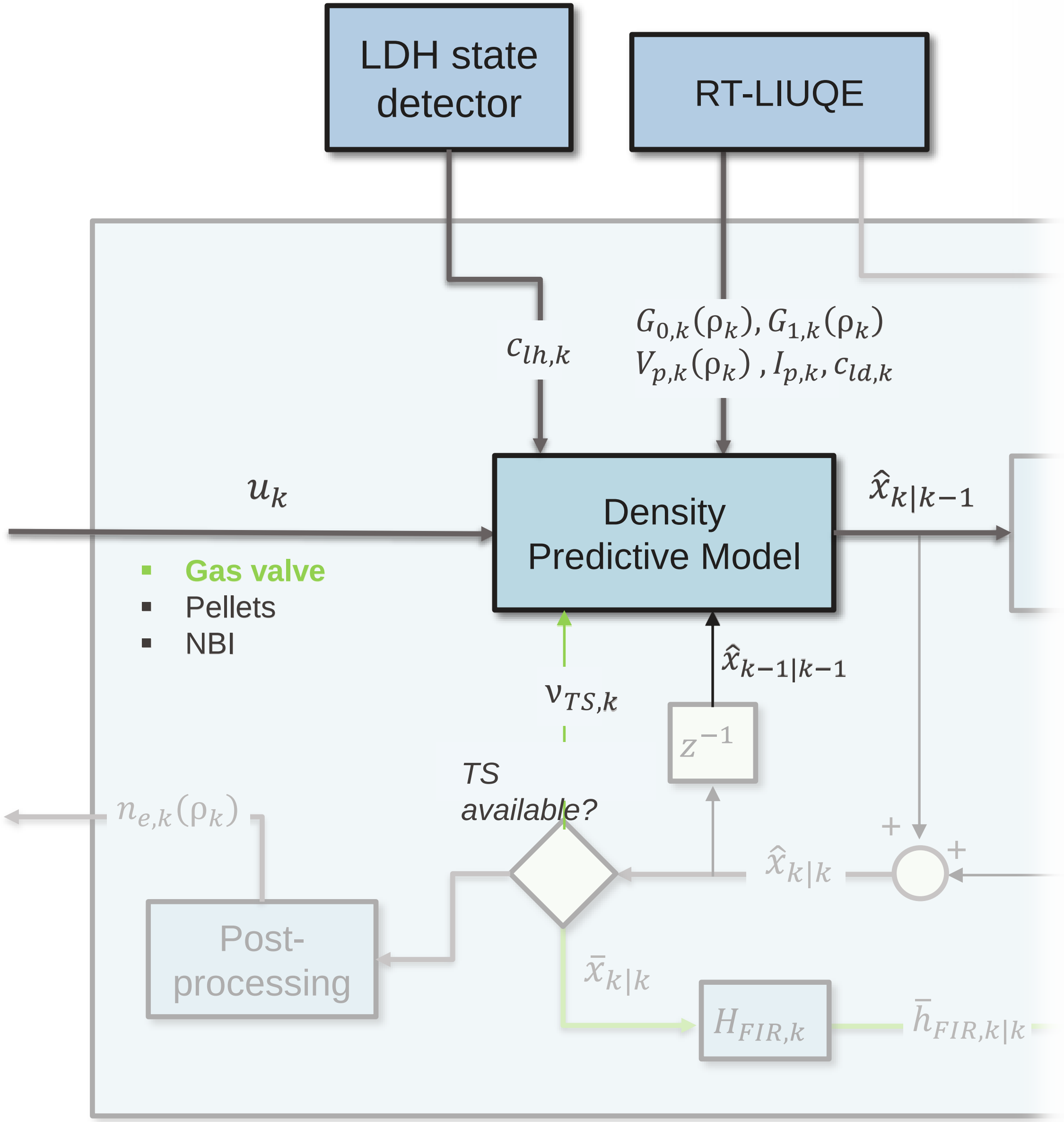

Prediction step:

- Gas valve fuelling u_k from valve controller readback.
- Confinement state L/H-mode boolean c_{lh}
  - Transport coefficient $D_{l/h}$
  - Penetration depth of neutrals $\lambda_{iz,l/h}$(ionization process)
- Magnetic plasma equilibrium from RT-LIUQE:
  - Geometrical quantities $G_0 = \langle|\nabla\rho|\rangle$ and $G_1 = \langle|\nabla\rho|^2\rangle$
  - Plasma volume $V_{p,k}$ and current $I_{p,k}$
- $\upsilon_{TS,k}$ estimated from last RT-TS profile
- Previous time step state $\hat{x}_{k-1|k-1}$

Output from prediction step:

Predicted state $\hat{x}_{k|k-1}$

RAPDENS observer scheme

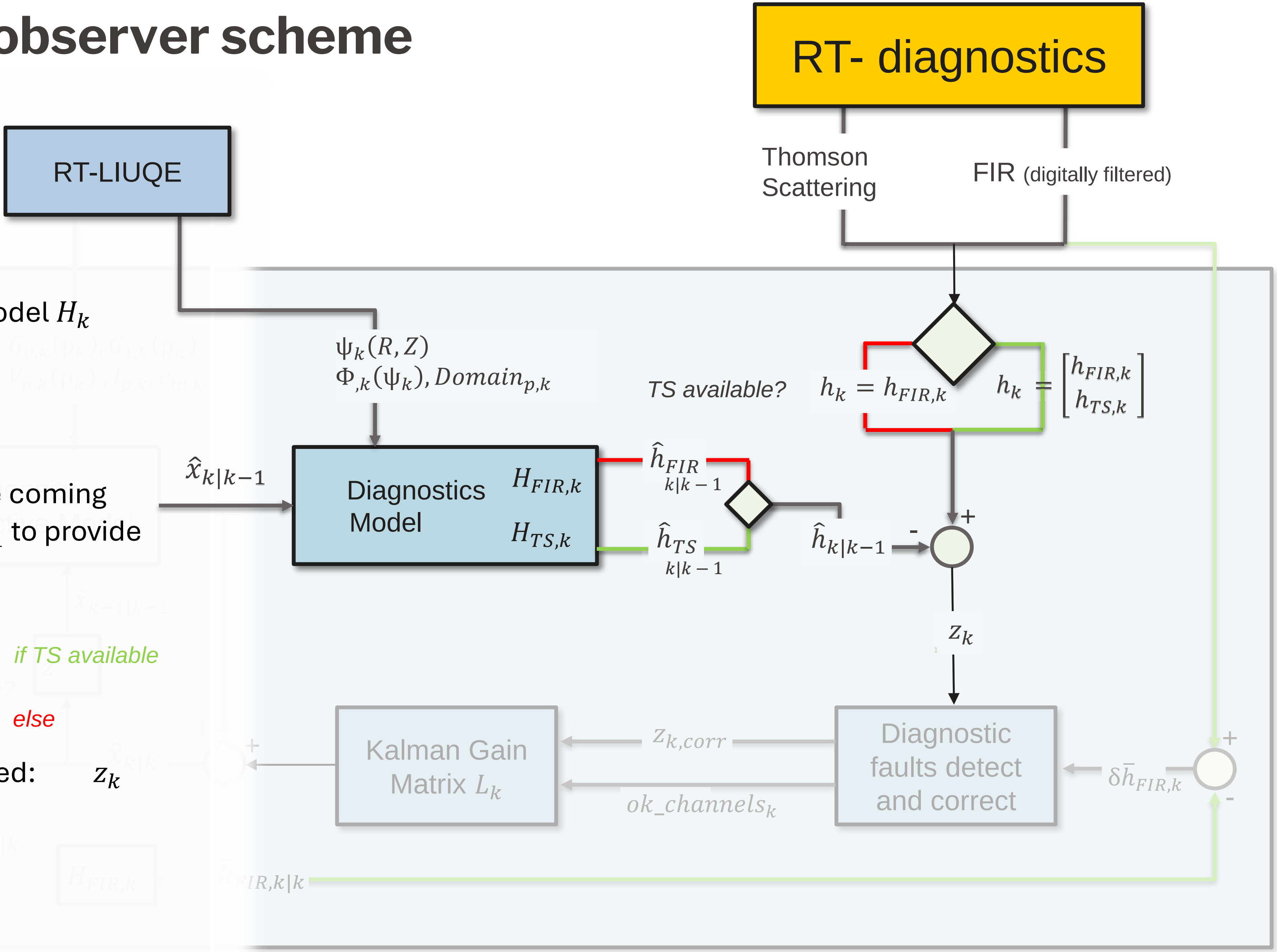

Synthetic measurement step:

- Assembly of the diagnostic model H_k using RT-LIUQE info:
  - Plasma domain
  - Poloidal + toroidal flux
- H_k maps linearly the n_e profile coming from the predictive step $\hat{x}_{k|k-1}$ to provide synth. measurements $\hat{h}_{k|k-1}$.
- $$\begin{cases} \hat{h}_{k|k-1} = \begin{bmatrix} H_{k,FIR} \\ H_{k,TS} \end{bmatrix} \hat{x}_{k|k-1} & \text{if TS available} \\ \hat{h}_{k|k-1} = H_{k,FIR} \quad \hat{x}_{k|k-1} & \text{else} \end{cases}$$
- Innovation residual is computed: $z_k = \hat{h}_{k|k-1} - h_k$

RAPDENS observer scheme

Detection of diagnostic faults and its correction:

- Innovation residual can be used to isolate diagnostic faults (e.g. fringe jumps)
- Model-based prediction doesn't exibit step-wise variation of line-integrated density of $10^{19}m^{-2}$ in 1 ms.
- $z_{k,corr} = Correction\_algo(z_k)$
- Corrupted channels are flagged and suppressed for the upcoming correction step.

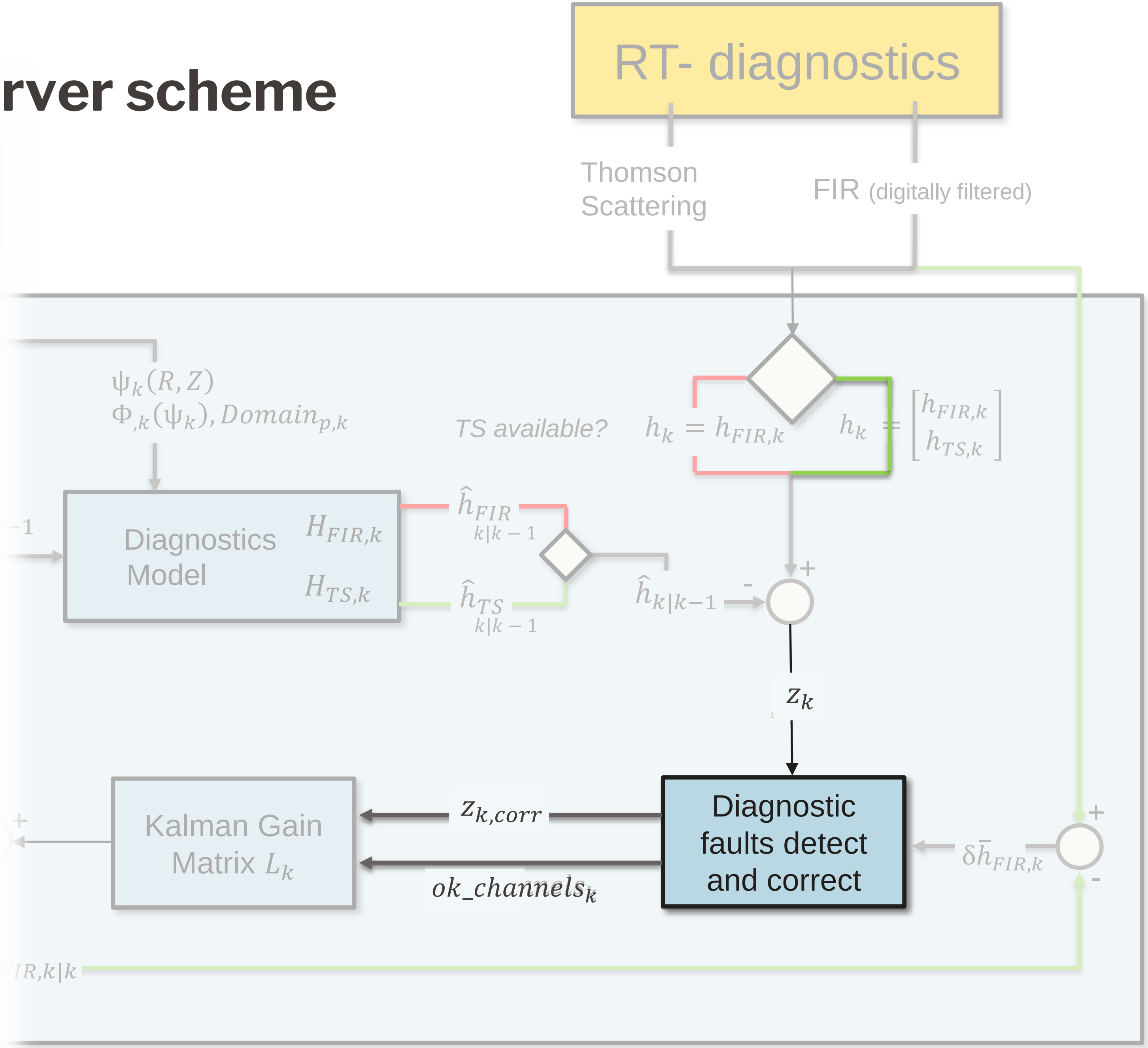

RAPDENS observer scheme

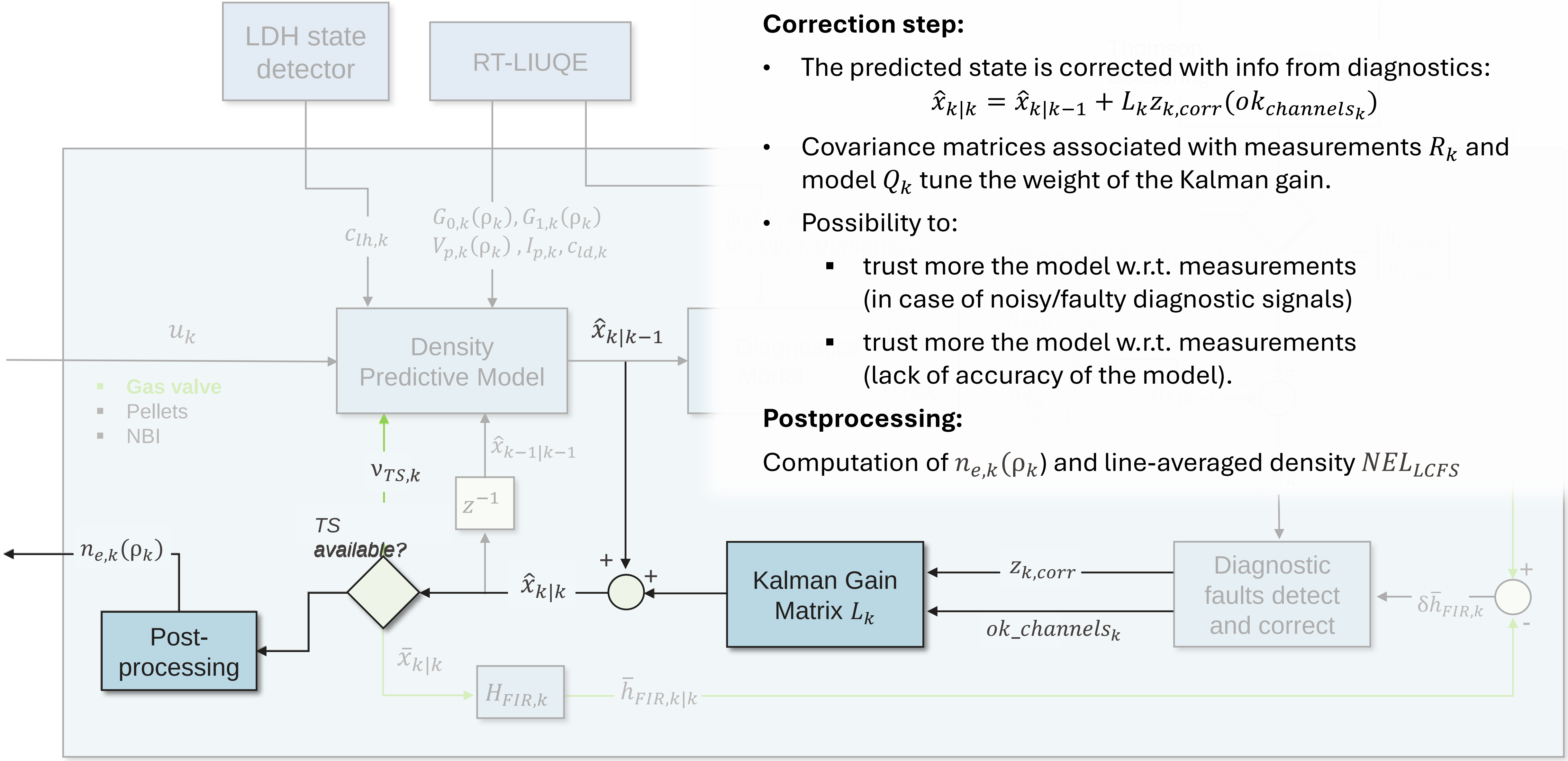

Correction step:

- The predicted state is corrected with info from diagnostics:

$$\hat{x}_{k|k} = \hat{x}_{k|k-1} + L_k z_{k,corr}(ok_{channels_k})$$

- Covariance matrices associated with measurements R_k and model Q_k tune the weight of the Kalman gain.
- Possibility to:
  - trust more the model w.r.t. measurements (in case of noisy/faulty diagnostic signals)
  - trust more the model w.r.t. measurements (lack of accuracy of the model).

Postprocessing:

Computation of $n_{e,k}(\rho_k)$ and line-averaged density NEL_{LCFS}

RAPDENS observer scheme

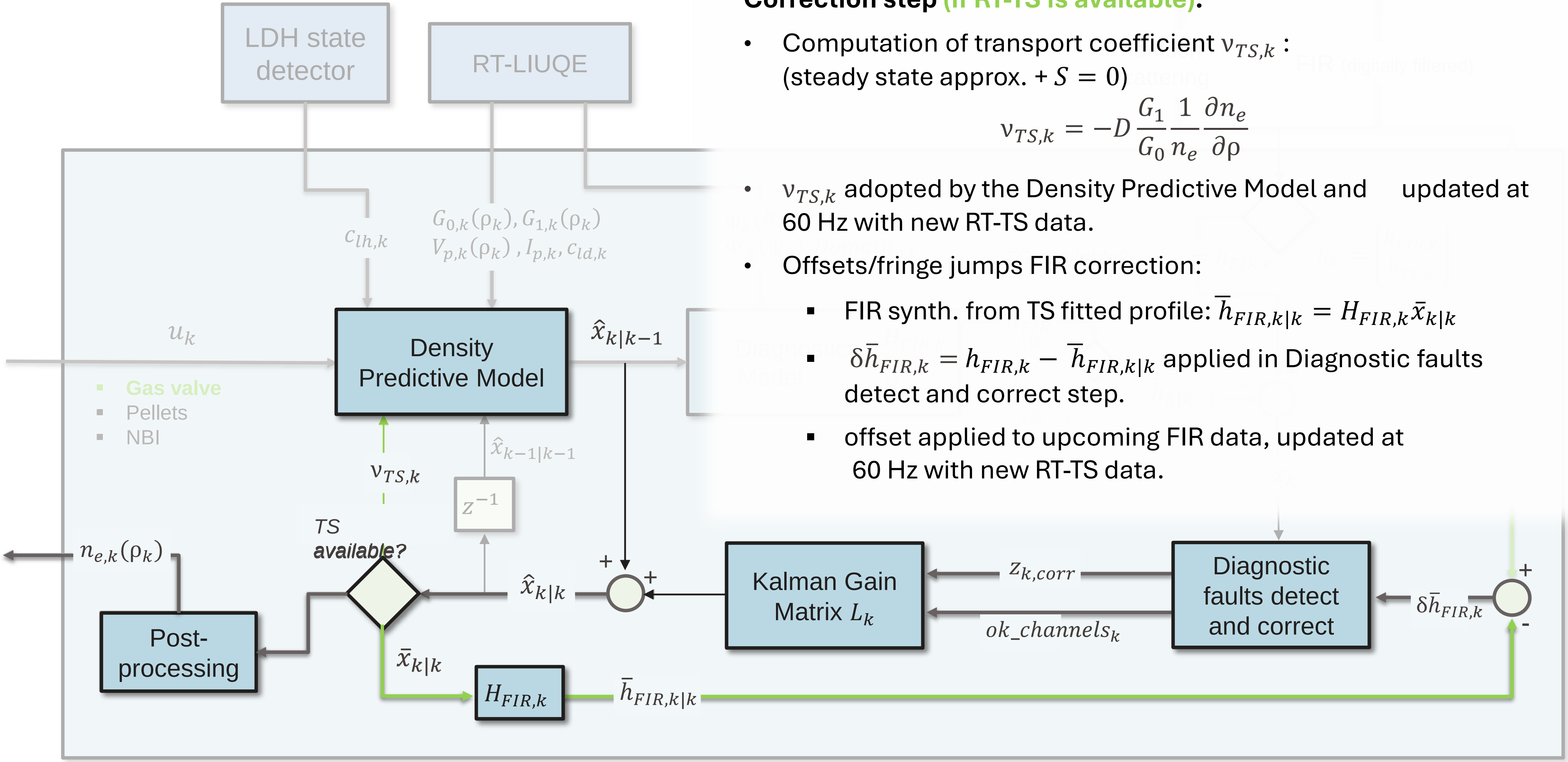

Correction step **(if RT-TS is available)**:

- Computation of transport coefficient $\nu_{TS,k}$: (steady state approx. + $S = 0$)

$$\nu_{TS,k} = -D\frac{G_1}{G_0}\frac{1}{n_e}\frac{\partial n_e}{\partial \rho}$$

- $\nu_{TS,k}$ adopted by the Density Predictive Model and updated at 60 Hz with new RT-TS data.
- Offsets/fringe jumps FIR correction:
  - FIR synth. from TS fitted profile: $\bar{h}_{FIR,k|k} = H_{FIR,k}\bar{x}_{k|k}$
  - $\delta\bar{h}_{FIR,k} = h_{FIR,k} - \bar{h}_{FIR,k|k}$ applied in Diagnostic faults detect and correct step.
  - offset applied to upcoming FIR data, updated at 60 Hz with new RT-TS data.

Tokamak à configuration variable - TCV

- Medium-sized tokamak, $R = 0.88\,m$, $B_t \leq 1.54\,T$, $a \approx 0.25\,m$.
- Unique shaping capabilities with 16 independent poloidal field coils+ highly elongated vacuum vessel.
- Exploration of different magnetic configurations for:
  - Alternative divertor concepts
  - Negative triangularity plasmas
  - Double nulls, doublets...

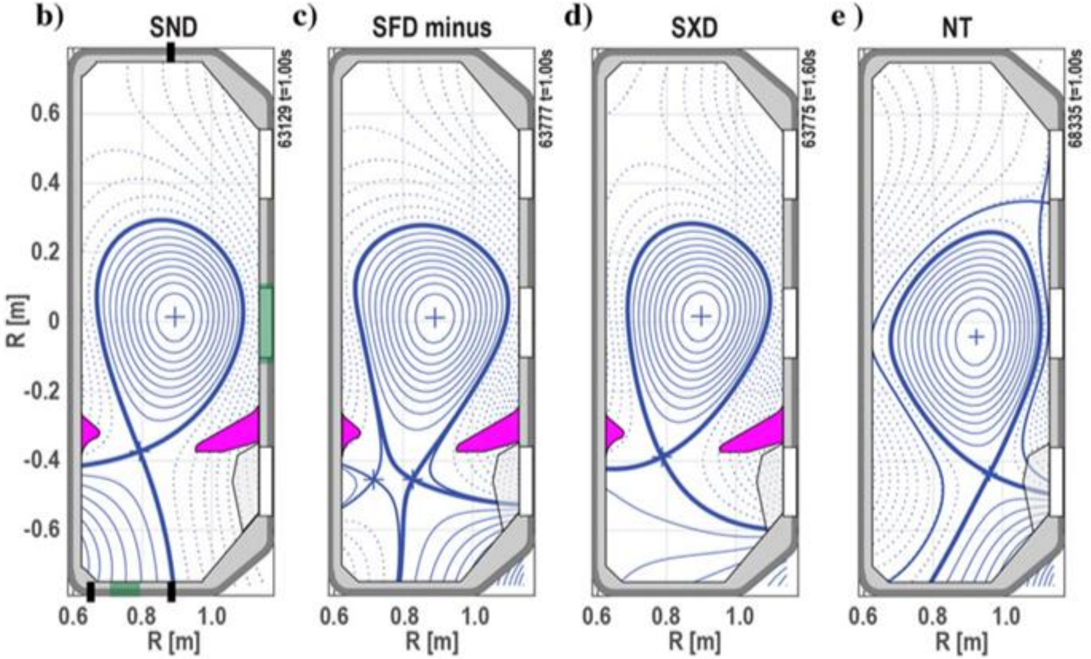

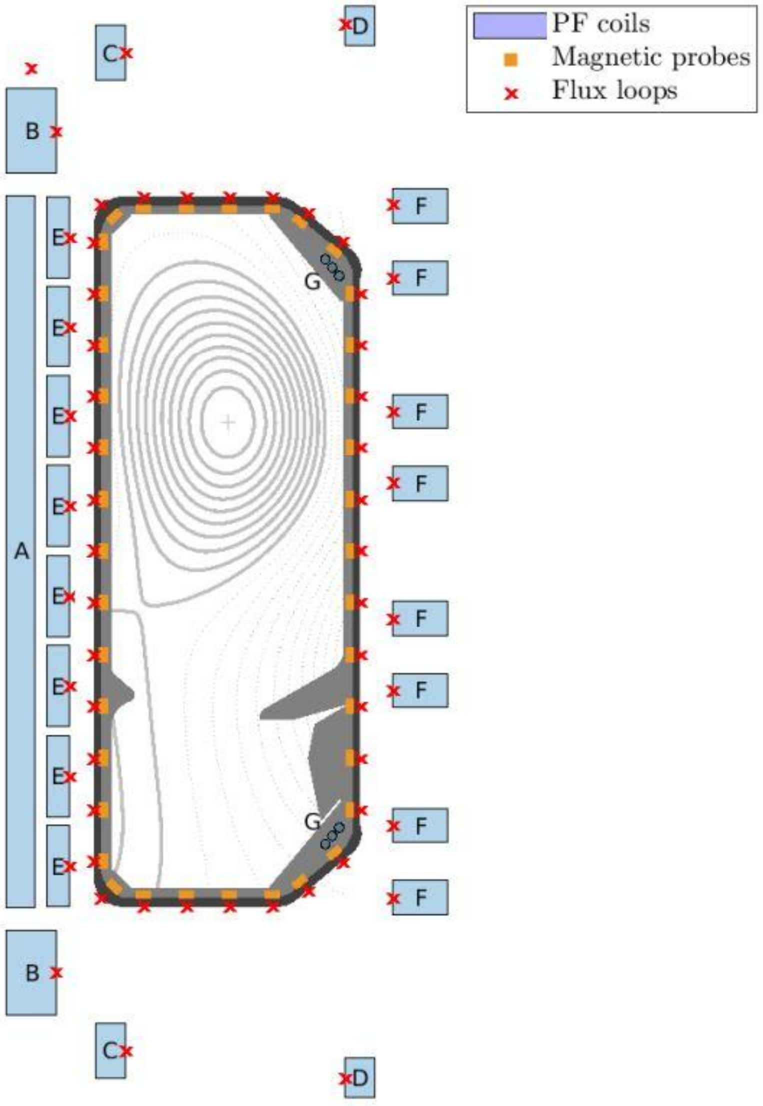

F. Pesamosca "Model-based optimization of magnetic control in the TCV tokamak: design and experiments." PhD thesis at EPFL Lausanne, Apr. 2021, p. 29

TCV heating system - NBI

- Possibility to heat the plasma with two NBI systems:
  - Opposite directions to control plasma rotation.
  - NBI-1: $P_{max} = 1.32\ MW,$ 28 keV in deuterium.
  - NBI-2: $P_{max} = 1.12\ MW,$ 50 keV in deuterium.
  - **Feedback controlled for e.g. beta control**

- DNBI to provide with CXRS system:
  - Carbon temperature & density
  - Plasma rotation

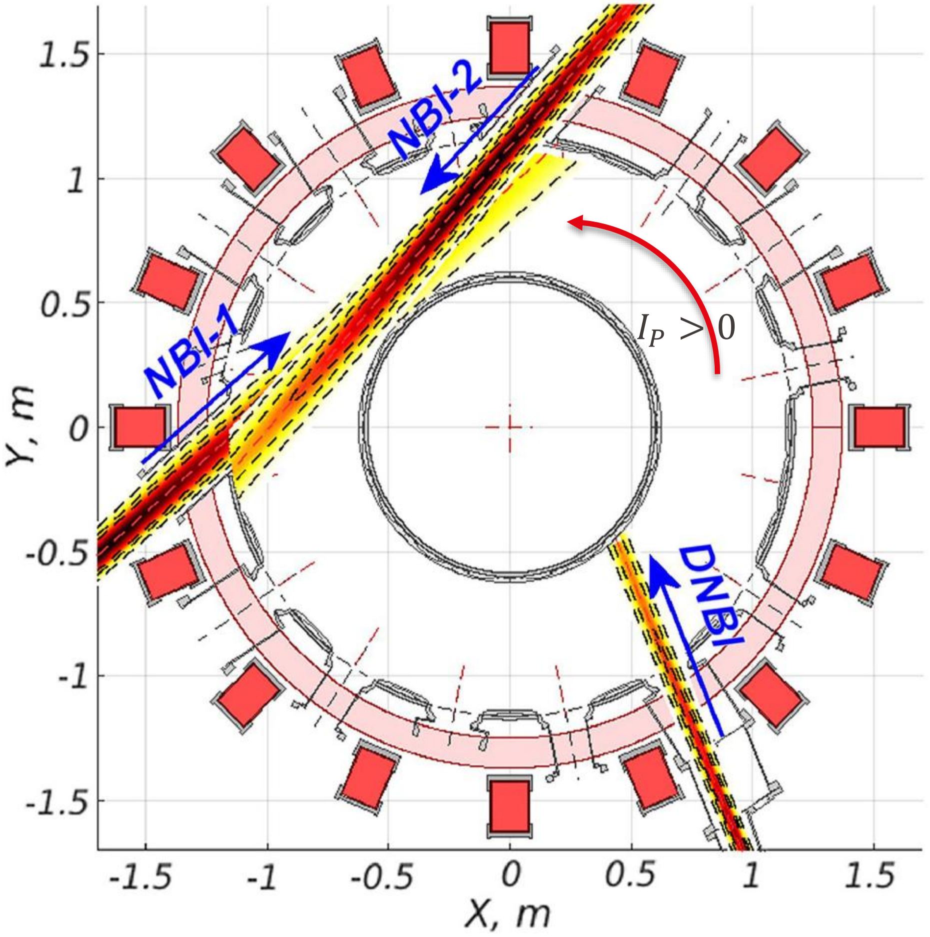

A. Karpushov et al., "Upgrade of the neutral beam heating system on the TCV tokamak – second high energy neutral beam ." FED, 187 (2023) 113384
doi: https://doi.org/10.1016/j.fusengdes.2022.113384

TCV heating system – ECH & ECCD

- Microwave heating for ECRH and ECCD with:
  - 1 Gyrotron in X2 (82.7 GHz), $P_{max} = 600\ kW$.
  - 2 Gyrotrons in X3 (126 GHz), $P_{max} = 900\ kW$.
  - 2 Gyrotrons dual X2-X3 (82.7 GHz -118 GHz) , $P_{max} = 1800\ kW$.
  - Upper and equatorial launchers for X2, **RT compatible steering mirrors (preemption & suppression of NTMs).**
  - Vertical launcher for X3.

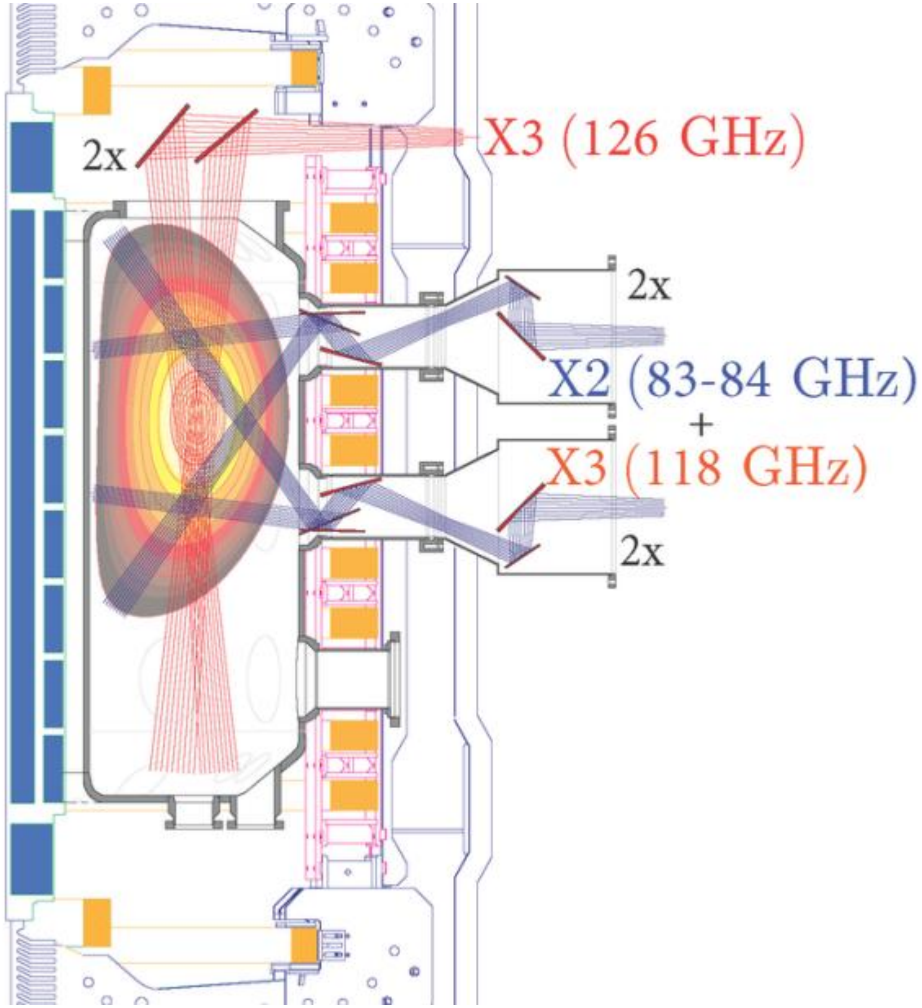

F. Pesamosca "Model-based optimization of magnetic control in the TCV tokamak: design and experiments." PhD thesis at EPFL Lausanne, Apr. 2021, p. 29

Local density control for ECH + NBIs discharges

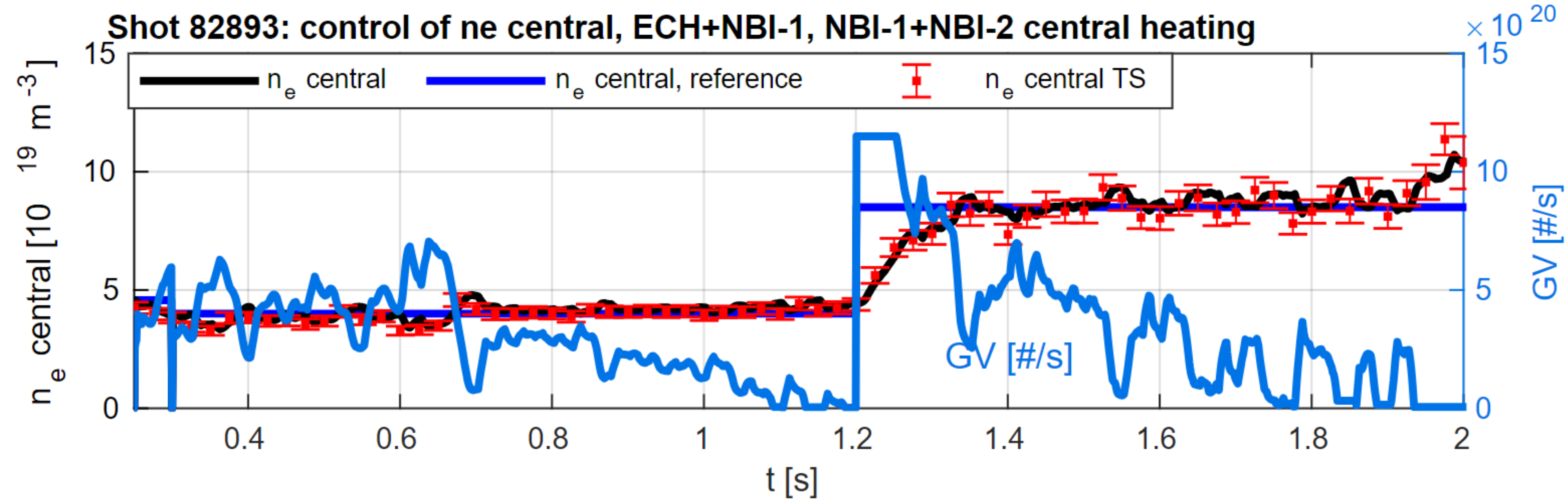

Shot 82893: control of ne central, ECH+NBI-1, NBI-1+NBI-2 central heating

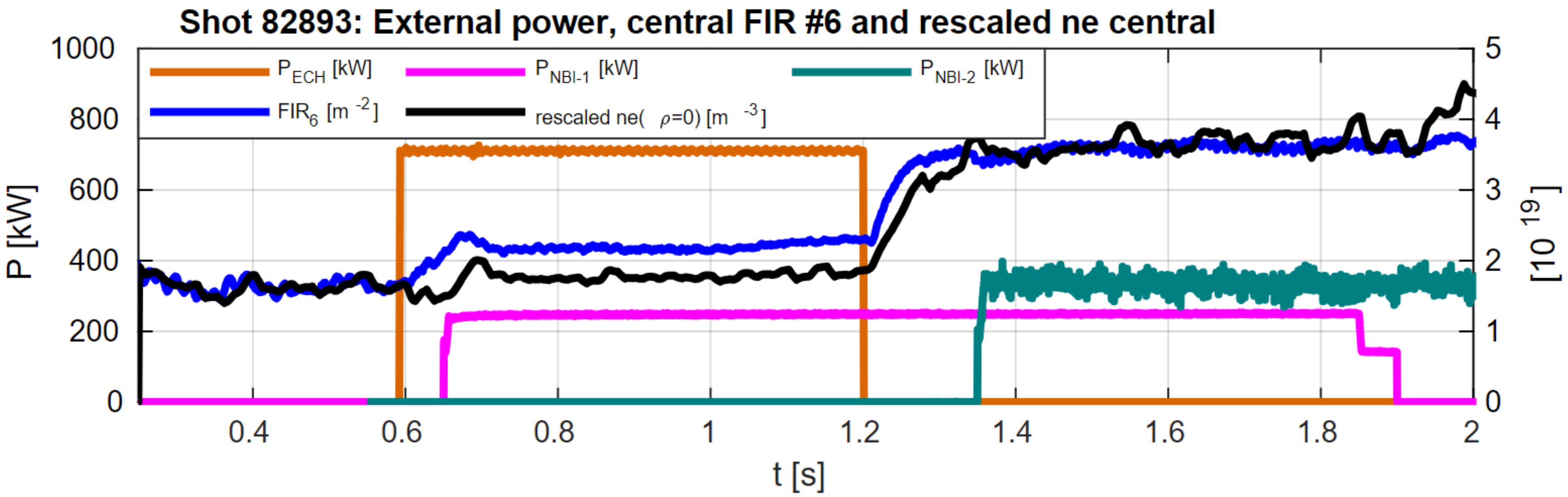

Shot 82893: External power, central FIR #6 and rescaled ne central

Local density control for ECH + NBIs discharges

- RAPDENS time-averaged profiles on different phases of the discharges 82913 and 82893

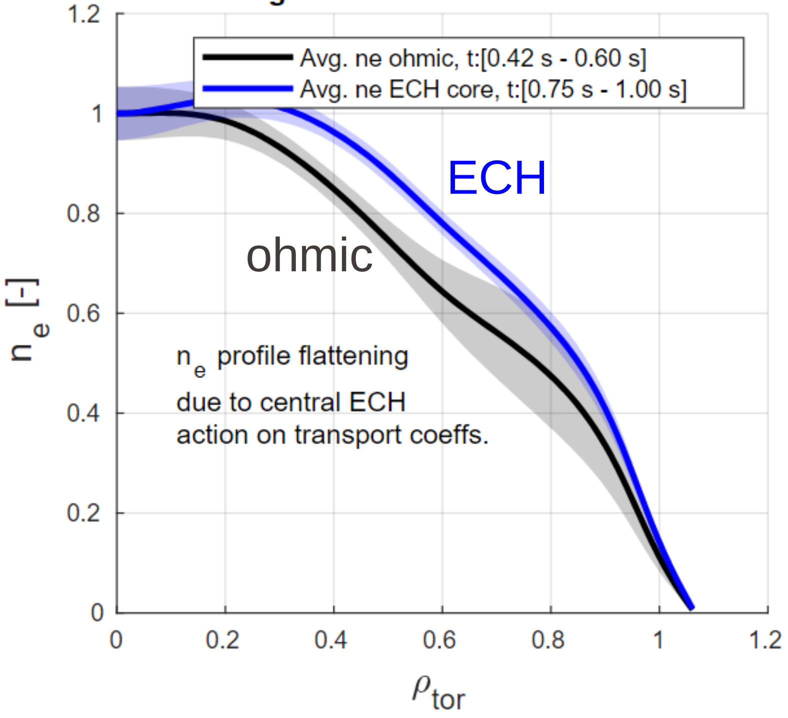

Shot 82913: avg. norm. ohmic vs central ECH

n_e profile flattening due to central ECH action on transport coeffs.

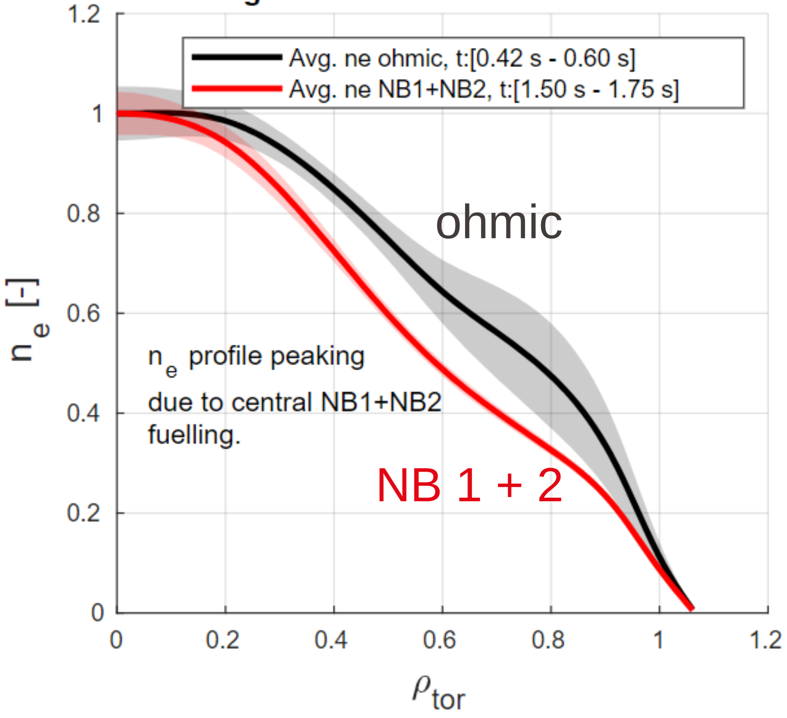

Shot 82893: avg. norm. ohmic vs core NB1+NB2

n_e profile peaking due to central NB1+NB2 fuelling.

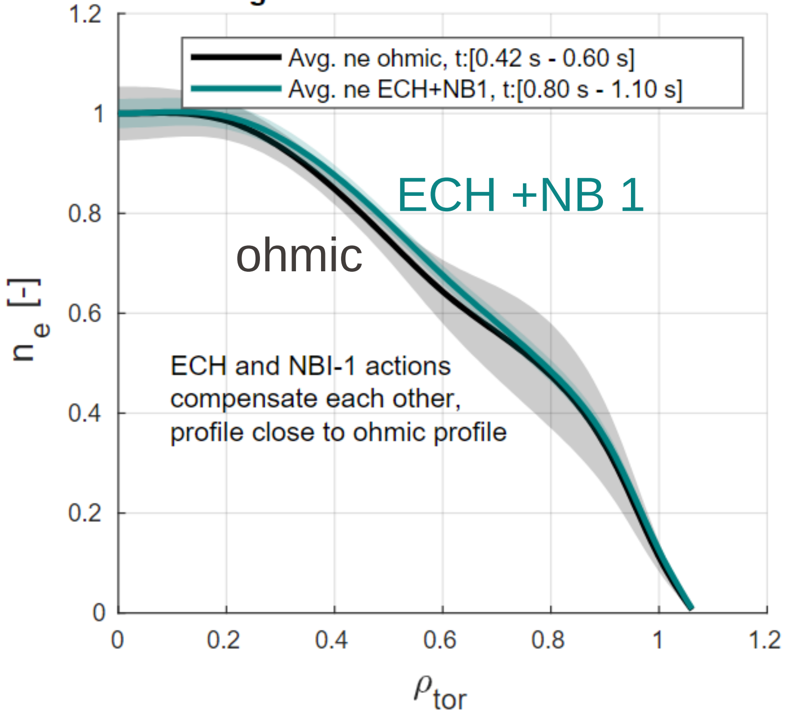

Shot 82893: avg. norm. ohmic vs core ECH+NBI

ECH and NBI-1 actions compensate each other, profile close to ohmic profile